universität wien

DISSERTATION

Titel der Dissertation

Cell fate regulation in the *Arabidopsis thaliana* stem: analysis of interfascicular cambium formation and development of a method for tissue-specific transcriptome analysis

Verfasser

Mag. Pablo Sánchez

angestrebter akademischer Grad

Doktor der Naturwissenschaften (Dr.rer.nat.)

Wien, 2013

Studienkennzahl lt. Studienblatt:	A 091 490
Dissertationsgebiet lt. Studienblatt:	Dr.-Studium der Naturwissenschaften Molekulare Biologie
Betreuer:	Dr. Thomas Greb

A mis padres

Zusammenfassung

Organe multizellulärer Organismen sind komplexe Strukturen, die sich in einem außerordentlichen Maß aus unterschiedlichen Zelltypen mit verschiedensten Funktionen zusammensetzen können. Diese verschiedenen Zelltypen entstammen wenigen pluripotenten Stammzellen, die in bestimmten Entwicklungsstadien oder Positionen innerhalb des Orgamismus aktiv sind. In Pflanzen bleiben diese Stammzellpopulationen, auch Meristeme genannt, auch im adulten Organismus erhalten und ermöglichen diesem dadurch ein theoretisch unbegrenztes Wachstum. Apikalmeristeme an Spross- und Wurzelspitze sind verantwortlich für das longitudinale Wachstum des Pflanzenkörpers, während in den meisten Gymnospermen und Dikotyledonen das Kambium, ein laterales Meristem, zusätzliches Dickenwachstum ermöglicht. Das Kambium ist in einer zylindrischen Domäne an der Peripherie der Sprossachse lokalisiert. Es besteht aus meristematischen Zellen, die durch perikline Teilungen nach außen gerichtet Phloem- und nach innen gerichtet Xylemgewebe bilden. Dieser Prozess ist der Ursprung der Holzbildung, aufgrund dessen er entscheidend zur Immobilisierung atmosphärischen Kohlendioxids beiträgt. Das ringförmig geschlossene vaskuläre Kambium wird postembryonal in der Sprossachse angelegt, indem zwischen den Primärbündeln lokalisierte Zellen Kambiumidentität erlangen. Dadurch werden die Prokambiumbereiche der einzelnen Bündel verbunden. Die postembryonale Bildung eines Meristems ist ein interessanter Entwicklungsprozess, da hier sowohl Dedifferenzierung als auch eine Wiedererlangung des ursprünglichen Meristemcharakters stattfinden kann. Trotz seiner biologischen und ökonomischen Bedeutung ist die Entstehung des Kambiums und der Sekundärvaskulatur relativ wenig erforscht. Deshalb habe ich mich im ersten Teil der vorliegenden Arbeit darauf konzentriert, weiteren Aufschluss über den Prozess der Kambiumbildung zu erlangen. Molekulare Marker, die die Aktivität von an der vaskulären Entwicklung beteiligten Genen sichtbar machen, hier PXY, WOX4 und APL, wurden verwendet um deren Aktivität im Laufe der Stammentwicklung in der Modellpflanze *Arabidopsis thaliana* zu verfolgen. Diesbezüglich war vor allem die Bildung des interfaszikulären Kambiums (IK) von Interesse. Die Beteiligung der Stärkescheide am Prozess der IK-Bildung wurde, unter Verwendung eines induzierbaren Reporters, durch die Verfolung der aus dieser durch Teilung hervorgegandenen Tochterzellen aufgeklärt. Durch die Untersuchung der PXY Aktivität konnte zudem gezeigt werden, dass interessanterweise nur eine einzelne, in der Stärkescheide stattfindende asymmetrische Zellteilung die IK-Bildung initiiert. Dabei wiedererlangen bereits ausdifferenzierte

Zellen meristematische Identität. Die Bildung des IK stellt dadurch ein geeignetes Modell dar, um sowohl Fragen zur Erlangung von Gewebespezifität, als auch zur Regulation lateralen Pflanzenwachstums zu beantworten.

Das Transkriptom, die Gesamtheit aller Transkripte in einer Zelle, ist eine unverwechselbare, die Identität einer Zelle reflektierende Signatur. Die Aufklärung gewebespezifischer Transkriptionsprofile ist entscheidend, um Verständnis über die Erlangung von Gewebespezifität und die Regulierung von Wachstum generell zu gewinnen. Der zweite Teil der vorliegenden Arbeit widmete sich der Methodenetablierung zur Bestimmung spezifischer Transkriptome von Geweben der Sprossachse von *Arabidopsis thaliana*. Hierfür wurden gewebespezifische Promotoren zunächst validiert, und im Anschluss verwendet, um die Expression des kernlokalisierten, grünfluoreszierenden Proteins (GFP) in bestimmten Sprossachsengeweben hervorzurufen. Mithilfe dieser transgenen Linien konnten unter Anwendung der sogenannten FANS-Technologie (Fluorescence-based Nucleus Sorting) Zellkerne der einzelnen Gewebe isoliert werden. Um die Methodik zur Bestimmung gewebespezifischer Transkriptome von Sprossachsengeweben zu validieren, wurde durch „Deep Sequencing“ von poy(A)-RNA zunächst das Transkriptom des Phloems ermittelt. Langfristig wird diese Methode die Basis für ein Langzeitprojekt bilden, dessen Ziel die Erstellung einer zahlreiche Gewebetypen einschließenden transkriptionellen Landkarte ist.

Detaillierte Informationen über bestimmte Gene, die in einzelnen Sprossachsengeweben in *Arabidopsis thaliana* aktiv sind, kombiniert mit der Erforschung spezifischer Entwicklungsprozesse wie z.B. der Bildung des IK, werden die Bedeutung der Sprossachse als Modell zur Analyse der Erlangung von Gewebespezifität und Wachstumsregulation vorantreiben.

Abstract

Organs of multicellular organisms are complex structures, which can accommodate an extraordinary range of different cell types with very diverse functions. These different cell types are established from groups of pluripotent stem cells active at distinct phases during development or at different sites within the organism. In plants, different stem cell populations, the so called meristems, are maintained in the adult organism, allowing indeterminate growth. The shoot and root apical meristems are responsible for longitudinal growth of the plant body. In most gymnosperms and dicotyledonous species the activity of a lateral meristem, the vascular cambium, additionally allows lateral growth of the stem. This lateral meristem is located in a cylindrical domain at the periphery of growth axes and consists of meristematic cells that divide periclinally to produce phloem towards the outside and xylem towards the center of the stem. This process is the origin of wood, one of the main sinks for stable immobilization of atmospheric CO_2. The vascular cambium is established post-embryonically in the shoot when cambium identity is established between primary vascular bundles in the interfascicular areas, thereby connecting the procambium from the individual vascular bundles. The post-embryonic formation of a meristem is an interesting developmental process since it may involve processes of de-differentiation and re-establishment of stem cell characters. Despite its biological and economic relevance the formation of the vascular cambium and secondary vasculature is hardly understood. Therefore, in the first part of this work, I aimed to shed light on the process of interfascicular cambium formation. Molecular markers visualizing the activity of genes regulating vascular development, in this case PXY, WOX4, and APL, were used to track gene activity domains during stem development in the model plant *Arabidopsis thaliana* and in particular during interfascicular cambium (IC) formation. The contribution of starch sheath cells to the process of IC formation was clarified by tracking the progeny of these cells using an inducible molecular marker. Interestingly, based on the analysis of PXY activity, IC identity is established during a single asymmetric cell division of starch sheath cells. These analyses showed that this process involves re-acquisition of meristematic identity in already differentiated cells. Therefore, the process of IC formation represents an instructive model for addressing questions regarding cell fate acquisition and the regulation of lateral plant growth.

The transcriptome, the totality of all transcripts present at one stage in a cell, is one signature that reflects the cell's distinct identity. Unraveling the tissue-specific transcriptional profiles is crucial for exploring cell fate acquisition and the regulation of growth dynamics. The second part of this

study aimed at establishing a pipeline for elucidating the tissue-specific transcriptomes of the stem in *Arabidopsis thaliana*. To this end, tissue-specific promoters were validated and used to drive the expression of a nucleus-targeted green fluorescent protein (GFP) in different stem tissues. These transgenic lines allowed the isolation of nuclei from tissues of interest using fluorescence-based nucleus sorting (FANS). As a proof-of-principle, deep sequencing of phloem-derived poly(A)-RNA provided the transcriptional profile of the stem phloem, thereby validating the pipeline established for elucidating tissue-specific stem transcriptomes. This method will be the basis for a long term project aiming at the establishment of a transcriptional map of a comprehensive set of stem tissues.

Detailed information about the genes active in individual *Arabidopsis* stem tissues, in combination with detailed information about developmental processes such as IC formation, will promote the role of the stem as a model for addressing questions regarding cell fate acquisition and plant growth.

Table of contents

1 - Introduction

1.1 Different cells specialized in specific tasks

Functional specialization of cells is a feature of multicellularity that has allowed greater efficiency and represents a very important step in the course of evolution (Grosberg and Strathmann, 2007). According to fossils of filamentous microbes discovered in Australia the first multicellular entities appeared around 3.5 billion years ago (Schopf, 1993). However, the first cell specialization within these entities only appeared 2.5 billion years ago once filamentous cyanobacteria specialized cells for nitrogen fixation (Tomitani et al., 2006). The enormous time gap between these steps may reflect the complexity of the regulation of cell specialization, which needs a tight control balancing selfish tendencies and the integrity of the organism (Buss, 1982; Michod, 1996). The complexity of growth control and body structures increased in parallel during the evolution of higher organisms whose development is controlled by extremely intricate gene networks.

1.2 Cell fate and plasticity

The development of a whole organism from a single cell requires complex regulatory networks and cell-to-cell communication to integrate internal and external cues (Artavanis-Tsakonas et al., 1999; Wagers et al., 2002). One of the processes that is tightly regulated is cell differentiation. Stem cells can give rise to a broad range of cell types or, like zygotes, to a whole organism (Costa and Shaw, 2007). The processes of differentiation are normally unidirectional and once a cell has differentiated it cannot return to an undifferentiated state. However, there are examples of cell fate changes in animals such as liver regeneration (Taub, 2004) or the paradigmatic cases of organ regeneration in amphibians (Makanae and Satoh, 2012). Cases of cell fate plasticity are more common in plants which can regenerate from single cells. One of the most extreme cases is somatic embryogenesis, in which a whole embryo is established from a somatic cell (Su and Zhang, 2009). Cell fate plasticity during animal embryogenesis is quite high; one extreme example of that is the two-cell-embryo. If it is divided, each cell can produce a whole individual (Mitalipov et al., 2002). That capacity decays during embryogenesis and the post-embryonic development is mostly an extension of the structures and organs produced during embryogenesis (Albert and Peters, 2009). In plants, due to their sessile life style, most development is post-embryonic. During embryogenesis a basic body plan is established. However, the final architecture of the plant is determined by the activity of groups of stems cells called meristems, which are maintained or established in different parts of the plant, allowing a more flexible development (Jurgens, 2001). In the aerial parts, meristems are responsible for producing repetitive elements called phytomers that

form the plant shoot (McSteen and Leyser, 2005). Each phytomer is composed of a piece of stem, a node, a leaf, and an axillary meristem (Sussex, 1989). The modulation of that unit is responsible for a huge variety of plant architectures within the plant kingdom.

1.3 Meristems

The meristems are groups of plant cells that can be defined as stem cells since they are self-perpetuating and give rise to a large repertoire of cell types (Laux, 2003). These groups of stem cells are responsible for the indeterminate growth of plants. The shoot apical meristem (SAM) and the root apical meristem (RAM) are respectively located in the shoot and the root tip, and they are responsible for the longitudinal growth of the plant (primary growth), while lateral meristems (phellogen and vascular cambium) are responsible for the thickening of shoot and root axes (secondary growth).

1.4 Origin and importance of the plant stem

Derived from the SAM, the stem is a central organ of the plant responsible for mechanical support and transport of substances between different parts of the plant. Although it is adapted to aerial conditions it shares some properties with the root. Both organs have anatomical similarities such as the single-layered epidermis, the endodermis or, despite their different distribution, the vascular tissues (Sanchez et al., 2012). The similarities between root and stem might be due to the fact that both structures have derived evolutionarily from telomes, cylindrical structures containing a vascular tissue organized as a protostele, with the xylem restricted to the central part of the stem surrounded by phloem (Friedman et al., 2004). Such structures have evolved in two different directions, specializing for either underground or aerial life. The original vascular distribution has also evolved to different conformations that differ between roots and stems and among species. In gymnosperms and dicots the stem vasculature is organized as a eustele in which individual vascular bundles are distributed around the central pith (Figure 1). That primary conformation of the stem gives rise to a secondary conformation by the activity of the interfascicular cambium which produces a complete cylinder of vasculature allowing coordinated lateral growth (Figure 1). The cambium-based lateral growth appeared around 400 million years ago and provided an advantage for water transport, as well as greater flexibility in stem growth (Gerrienne et al., 2011; Rowe and Speck, 2005; Spicer and Groover, 2010). Plants containing that advantage, gymnosperms and dicotyledons, are present in most biotopes of the planet. Such broad distribution is translated into the accumulation of a huge amount of biomass around the planet. Importantly, the

activity of the cambium producing xylem represents one of the main sinks for stable atmospheric carbon immobilization (Ciais et al., 1995). Therefore, from an ecological point of view, cambium activity is crucial. The produced biomass in form of xylem is the origin of wood, whose production in 2011 was 3,435 million cubic meters, representing an international trade of around

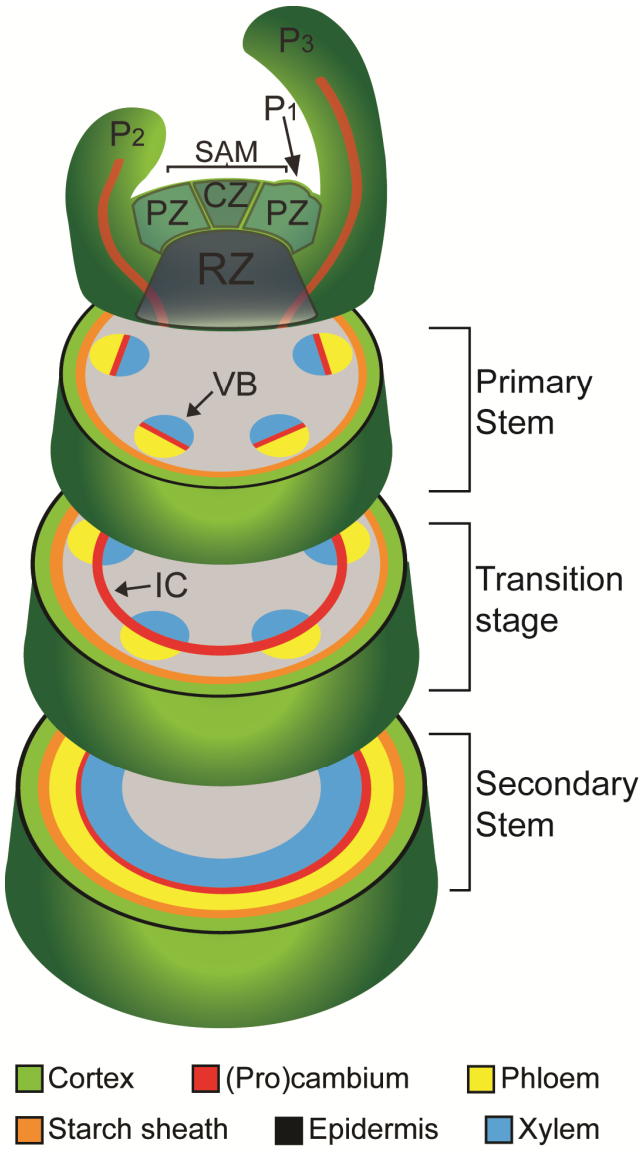

Figure 1: Schematic representation of the stem of dicotyledonous plants. The SAM establishes the primary stem carrying individual vascular bundles. IC formation gives rise to the secondary stem conformation in which the complete cylinder of the vascular cambium allows lateral growth. SAM: Shoot apical meristem. Px: Leaf primordia. CZ: Central zone. PZ: Peripheral zone. RZ: Rib zone. VB: Vascular bundle. IC: Interfascicular cambium. Adapted from (Sanchez et al., 2012).

200 billion dollars (www.fao.org). Despite its importance, the developmental processes allowing the transition from the primary to the secondary stem are not completely understood (Miyashima et al., 2012; Sanchez et al., 2012). Interestingly, the herbaceous model plant *Arabidopsis thaliana* displays both conformations of the stem (Figure 2), representing a suitable model for analyzing the developmental processes related with secondary growth including the transition from the primary to the secondary stem (Agusti et al., 2011a; Agusti et al., 2011b; Altamura et al., 2001; Busse and Evert, 1999; Chaffey et al., 2002; Dolan et al., 1993; Hirakawa et al., 2010; Ko and Han, 2004; Ko et al., 2004; Melzer et al., 2008; Suer et al., 2011; Ye et al., 2002).

1.5 Primary growth

Primary (longitudinal) plant growth is the result of the activities of apical meristems. In the case of the aerial part, the SAM is established during embryogenesis (Aida et al., 1999). The complex regulation of the establishment and maintenance of the SAM is just one example for the complex networks of genes controlling cell fate acquisition that is behind any developmental process. Many genes have been associated with the genetic control of the SAM. One example is the CLV-WUS pathway that is fundamental for maintaining a balance between cell differentiation and maintenance of the SAM. *WUSCHEL (WUS)* is one of the first genes active during the formation of SAM in the embryogenesis. It is expressed just below the central zone (CZ) and is non-cell-autonomously responsible for stem cell niche maintenance in the CZ (Laux et al., 1996; Mayer et al., 1998). A gradient of cytokinins from the epidermis (Jacqmard et al., 2002) may control the *WUS* expression domain, which overlaps with the expression domain of the cytokinin receptor *ARABIDOPSIS HISTIDINE KINASE 4 (AHK4)* (Gordon et al., 2009). *CLAVATA3 (CLV3)* is a signaling peptide which is secreted into the apoplast from the stem cells and down-regulates *WUS* expression in the cells around the central zone of the SAM (Lenhard and Laux, 2003) through *CLAVATA1* (*CLV1*). *CLV1* is a leucine-rich repeat receptor-like serine/threonine kinase (LRR RLK) that is directly activated by the *CLV3* peptide leading to a down-regulation of *WUS* expression (Clark et al., 1997; Ogawa et al., 2008). The LRR receptor like protein *CLV2* and the serine/threonine protein kinase *CORYNE* (*CRN*) are also involved in the perception of the *CLV3* signal and the *WUS* control (Jeong et al., 1999; Müller et al., 2008). Strikingly, in the root apical meristem a similar control mechanism is present. *WUSCHEL-RELATED HOMEOBOX 5 (WOX5)* is an homologue of *WUS*, expressed in the quiescent center of the RAM, which non-cell-autonomously maintains the stem cell identity of the surrounding cells (Sarkar et al., 2007). The signaling peptide *CLE40* is secreted from the columella cells and downregulates *WOX5* expression

around the quiescent center allowing cell differentiation. *CLE40* controls *WOX5* expression through the receptor-like kinase *ACR4* (Stahl et al., 2009). Both systems in the root and the stem are crucial for maintaining the correct ratio between stem cell division and cell differentiation.

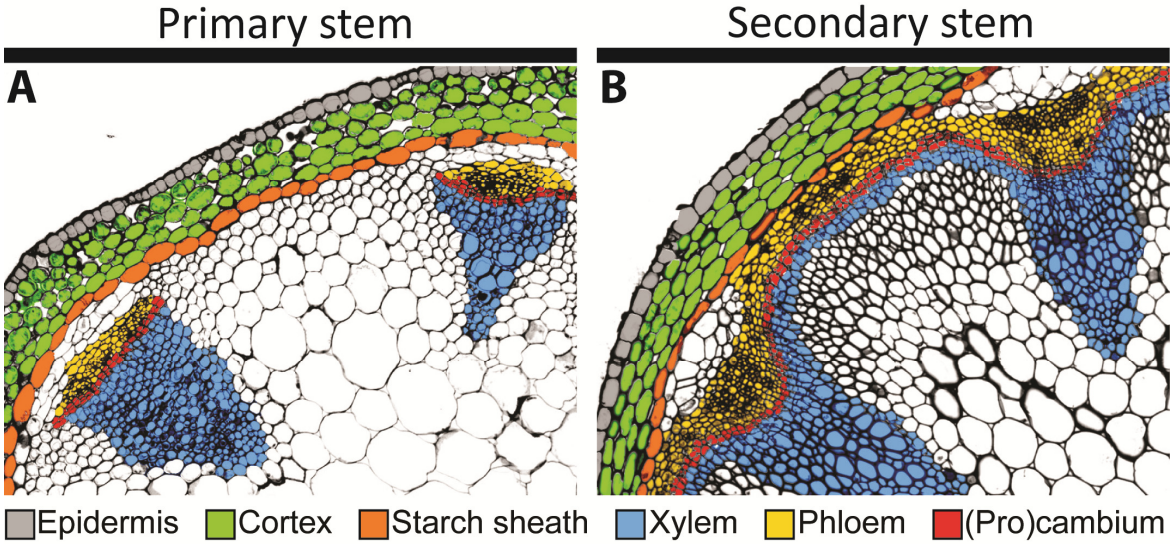

Figure 2: Comparison of stem conformations. Cross sections of the Arabidopsis primary stem (A) and secondary stem (B) (Agusti et al., 2011b; Sanchez et al., 2012).

The SAM is responsible for the formation of the primary stem and its longitudinal growth (Figure 1). Just below the SAM, in the rib zone, the different tissues of the primary stem are established (Ruonala et al., 2008). Difficulties in accessing that zone by microscopic approaches has meant that these processes were rarely investigated (Sanchez et al., 2012). The interaction between the transcription factors *SCARECROW (SCR)* and *SHORTROOT (SHR)* is fundamental for endodermis formation, which is the innermost cell layer of the cortex, in the root (Nakajima et al., 2001; Wysocka-Diller et al., 2000); although their relation during the formation of the primary stem in the rib zone was not described, *scr* and *shr* mutants lack endodermis, also called starch sheath (SS), in the stem (Fukaki et al., 1998), indicating that they are crucial for SS establishment during stem formation. In contrast with the first vascular plants that had the vascular tissues in the center of the stem, in dicots like Arabidopsis the center of the stem is occupied by the pith. The transcription factor *WRKY2* plays a role in keeping the parenchymatous nature of the pith cells by repressing *NAC SECONDARY WALL THICKENING PROMOTING FACTOR2* (*NST2*) (Zhong et al., 2010) which is involved in secondary cell wall formation. In fact, wrky2 mutants have a lignified pith, probably resembling the original conformation that had xylem in the central part of the stem (Wang et al., 2010). The primary stem in dicotyledonous plants and gymnosperms is

characterized by vascular tissues distributed in individual vascular bundles (Figure 1, Figure 2) arranged around the pith.

Each vascular bundle is produced by the activity of the procambium, a meristem which gives rise to the formation of xylem centripetally and phloem centrifugally. The procambium is established already in the Arabidopsis embryo and appears early during the formation of different organs (Turner and Sieburth, 2003). In the stem it is produced from the apical meristem. The distribution of the vascular strands is determined in the rib zone. It is not clear how that distribution is established but computational models suggest that it might be determined by the establishment of auxin maxima (Ibanes et al., 2009).

1.6 Transition from primary to secondary stem

Plant stems must be robust enough to support the aerial part of the plant. Stem thickening through secondary growth is the strategy for most dicotyledonous species and gymnosperms to achieve that robustness. Stems displaying secondary growth are called secondary stems (Figure 1). The main developmental change allowing secondary growth is related to the conformation of the vascular system. While in primary stems the vasculature is distributed in discrete vascular bundles, in secondary stems there is a complete cylinder of vasculature derived from the vascular cambium (Figure 2). The transition from the primary to the secondary stem is a developmental process related to the initiation of cambial activity in the interfascicular areas of the stem. The interfascicular cambium (IC) connects the cambium from adjacent vascular bundles, resulting in a closed cylinder of meristematic activity, the vascular cambium. IC formation shows some similarities with the process of lateral root formation: both processes are induced by auxins (Blakely et al., 1988; Little et al., 2002; Snow, 1935; Torrey, 1950); and a cylindrical cell layer (the starch sheath or the pericycle) seems to be the origin of the new tissue or organ (Dubrovsky et al., 2000; Sehr et al., 2010). The SS, according to histological analysis (Altamura et al., 2001), has been proposed as the founding tissue of the interfascicular cambium. This is very interesting since it would represent a *de novo* formation of a plant meristem out of a differentiated tissue. However, mutants that do not establish the starch sheath, such as *scr* or *shr* (Fukaki et al., 1998), are still able to develop secondary growth (Sehr, 2010). Processes considered to be dedifferentiation processes based in histological approaches have become controversial (Sugimoto et al., 2011). For example, lateral root formation which is often considered to be based on the dedifferentiation of pericycle cells seems to involve reactivation of existing meristematic cells present in this tissue (Dastidar et

al., 2012). In the case of the IC, only basic histological investigations addressed the relation between the tissues present in the interfascicular area and the formation of that meristem.

Interestingly, a control mechanism similar to the *CLV-WUS* regulatory loop present in the apical meristem has been described for the cambium (Hirakawa et al., 2010). The mechanism consists of the *CLE41-PXY-WOX4* pathway. The *CLE41* peptide produced in the phloem activates the LRR RLK *PHLOEM INTERCALATED WITH XYLEM* (*PXY*) in the cambium promoting the activity of that meristem (Fisher and Turner, 2007). pxy mutants display vascular bundles in which phloem is mixed with xylem, probably due to defects in the orientation of cambial cell divisions; this would indicate a role of this signaling module not only in promoting cell activity but also controlling the orientation of the cell divisions. *WOX4* is a transcription factor activated by *PXY* that promotes cambium proliferation (Hirakawa et al., 2010; Suer et al., 2011). CLE41 treatments produce *PXY*-dependent increase in the *WOX4* mRNA levels and promote cambium activity. Auxin accumulation induces cambium activity and also an increase in *WOX4* mRNA levels but in a *PXY*-independent manner (Suer et al., 2011). Therefore, it seems that *WOX4* integrates different pathways related with cambium activity. The formation of cambium cell identities in the interfascicular area is impaired or absent in *wox4* and *pxy* mutants respectively (Fisher and Turner, 2007; Suer et al., 2011).

1.7 Cell identity and transcriptomes

Usually, all cell types present in an organism share the same genome, but they present differences in morphology, physiology and function. Different cell properties are based on a differential gene expression and each cell type activates a different set of genes (Morozova et al., 2009). The characterization of the transcriptome of a specific cell type or developmental stage may provide information about the genes that play a role in such a cell type or process. Transcriptome profiling has been used to acquire information about developmental processes like cancer (Rhodes et al., 2004), aging (McCarroll et al., 2004) or cell differentiation (Brandenberger et al., 2004). In plants, the most complete transcriptional profiling approach has been done in the root, where the transcriptomes of most tissues have been elucidated at different developmental stages (Birnbaum et al., 2003; Brady et al., 2007). For the aerial part of the plant nothing similar has been done. In the case of the stem only the transcriptomes of a few tissues have been analyzed, such as those from the cambium and the cambium-derived tissues of poplar (Schrader et al., 2004), the Arabidopsis epidermis (Suh et al., 2005), or the transcriptome remodeling during interfascicular cambium formation (Agusti et al., 2011b).

Tools for analyzing transcriptomes have evolved tremendously in the last decades starting from single gene approaches going to next-generation sequencing (Morozova et al., 2009). The use of comprehensive probe sets plotted on microarrays (Schena et al., 1995) allowed the first nearly genome-wide analyses of transcriptomes. However, the advent of RNA-sequencing technologies allows a deeper analysis of the gene expression levels because it is not restricted to the genes plotted to the array and allows quantification of gene activity based on direct reads and not based on extrapolation of signal intensities (Wang et al., 2009).

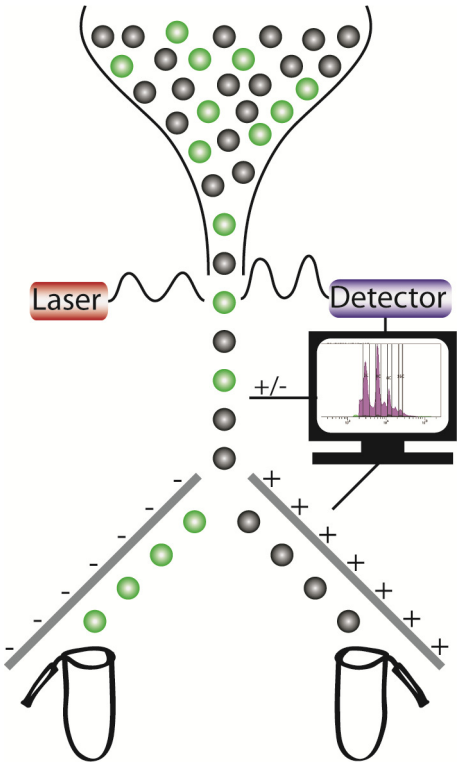

Figure 3: Scheme of cell sorter. Cells or nuclei can be separated according to their fluorescence properties.

1.8 Separation of tissues

Transcriptome analysis of a specific cell type is based on separating that tissue from the rest of the organism. A number of technical approaches exist for separating different plant tissues. The most obvious are based on the dissection of the tissues of interest; an example is the analysis of the cambium and cambium-derived tissues from sections of poplar stems produced by a cryo-microtome (Schrader et al., 2004) or the Arabidopsis epidermis obtained by pealing the stem (Suh et al., 2005). Beyond that, the method of laser capture microdissection (LCM) employs a laser for the isolation of cellular material (Espina et al., 2007); a recent example in plants is the analysis of

the maize shoot apical meristem (Takacs et al., 2012). In all these cases, the criteria for selection are the morphology of the cs or tissues, which can be identified directly or by the assistance of a microscope. A second group of methods for isolating cells exists based on the presence of molecular markers. The use of promoters for labeling a specific group of cells by a fluorescent protein is the basis of the technique Fluorescence Activated Cell Sorting (FACS), which was used in the transcriptional analysis performed in the root (Birnbaum et al., 2003; Brady et al., 2007). For FACS it is necessary to produce protoplasts that are later separated according to the presence of the fluorescence marker using a cell sorter (Figure 3). A variation of that method, which additionally relies on a molecular marker, is the isolation of nuclei only from the cells of interest. Currently two methods are available to achieve this: the fluorescence activated nucleus sorting (FANS), which is a variation of FACS; and the INTACT method. In both cases, nuclei from a specific tissue are labeled by a fluorescent protein or by a tag fused to a protein in the nuclear envelope, respectively. The labeled nuclei can be separated by flow cytometry (Haenni et al., 2012) or immunoprecipitation (Deal and Henikoff, 2010), respectively. Separation by immunoprecipitation can be performed without the assistance of a cell sorter, allowing thorough washing of the nuclei. On the other hand, the use of flow cytometry can easily produce more information about the nuclei, such as ploidy levels. In both cases the separated nuclei can be used for following different experimental approaches such as the analysis of the nuclear transcriptome or chromatin properties.

Individual analysis of the tissue transcriptomes provides information about the gene activity of a specific group of cells. In the context of the whole organism, the genes which are specifically active in a tissue are good candidates for playing a role in the formation or regulation of such tissue. The comparison between different tissues in the context of the whole organism can reveal networks of genes important for determining certain aspects of plant development such as cell fate acquisition or cell-to-cell signaling.

1.9 Aims of the study

This study was divided in two parts, both addressing specific aspects of cell identity regulation in the stem of the model plant *Arabidopsis thaliana*.

The aim of the first part was to clarify the formation of the IC in the transition from the primary to the secondary conformations of the stem. The interfascicular cambium is a meristematic tissue that is established post-embryonically in the interfascicular areas allowing secondary growth in

gymnosperms and dicots. Its formation had been addressed only by basic histological approaches. In this study the acquisition of vascular cell identities was tracked molecularly employing various informative molecular markers. The intention of the approach was to elucidate the contribution of the SS in the process of IC formation. To check parallelisms with the process of lateral root formation. And determine how different vascular identities interact in the stem. Clarifying whether interfascicular cambium formation involves a process of dedifferentiation or if it is just differentiation of pre-existing meristematic cells in that area is fundamental, since it could represent a fascinating model for addressing questions of cell fate acquisition during postembryonic development.

The aim of the second part of this study was to develop a technical pipeline allowing the elucidation of tissue-specific transcriptomes of the Arabidopsis stem as one of the cell identity signatures. The genes that are active in the cells of a specific tissue can offer crucial information about the biological processes present in those tissues and about the control mechanism establishing such cells. The established technical pipeline was based on fluorescence activated nucleus sorting for isolating the respective plant material in a tissue-specific manner and the use of RNA-sequencing for quantifying transcript levels in a genome-wide manner. The established pipeline was validated using one of the tissues of the stem, the phloem.

A better understanding of the developmental processes taking place in the stem, the formation of the IC for instance, in combination with new tools allowing the elucidation of tissue-specific transcriptional profiles puts the stem in a good position to serve as a model for addressing key biological questions regarding regulation of plant growth forms or postembryonic growth processes in plants.

2 - Materials and Methods

2.1 Materials

2.1.1 Plant material

Arabidopsis thaliana (L.) Heynh. plants of the accession Columbia were used for all experiments. Wild type plants and the mutants detailed in Table 1 were used in this study.

Genotype	Mutation/Construct (NASC ID)	Reference
alf4-1	12bp deletion	(DiDonato et al., 2004)
pxy-4	SALK_009542 (N800038)	(Fisher and Turner, 2007)
wox4-1	Gabi_462g01 (N376572)	(Hirakawa et al., 2010)

Table 1: Mutant plants used in this study.

2.1.2 Bacterial strains

For plasmid cloning the *Escherichia coli* strain DH5α was used. *Agrobacterium tumefaciens* strain C58C1 containing the helper plasmid *pSoup* (Hellens et al., 2000) was used for plant transformation.

2.1.3 Restriction enzymes

All restriction enzymes used in this study were produced by *Fermentas*, Canada or *New England Biolabs* (*NEB*), United Kingdom. They were used according to the instructions of the manufacturer.

2.1.4 Buffers and solutions

Toluidine blue staining solution

500 mg/l	Toluidine blue (Applichem)

50x TAE

242 g	Tris (pH 7.5)
100 ml	0.5 M EDTA
57.1 ml	Acetic acid
To 1 l	water
	pH 7.6

YEB medium

0.5%	Meat extract
0.5%	Peptone
0.1%	Yeast extract
0.5%	NaCl
0.5%	Sucrose
2 mM	MgSO4
1%	Bacto agar (only in solid medium)
	Autoclave

LB medium

1%	NaCl
1%	Peptone
0.5%	Yeast extract
1.5%	Bacto agar (only in solid medium)
	Autoclave

Isolation buffer

15 mM	Tris (pH 7.5)
2 mM	EDTA
0.5 mM	Spermidine
20 mM	NaCl
80 mM	KCl
15 mM	ß-mercaptoethanol
0.1%	Triton
	pH 7.5

10x TE buffer

100 mM	Tris (pH 8)
10 mM	EDTA (pH 8)

CTAB buffer

140 mM	Sorbitol
220 mM	Tris-HCl (pH 8)
22 mM	EDTA (pH 8)
800 mM	NaCl
1%	Sarkosyl
0.8%	Cetyltrimethylammonium bromide (CTAB)
	pH 8 with HCl, Autoclave

DNA isolation buffer

200 mM	Tris (pH 7.5)
250 mM	NaCl
0.5%	SDS
25 mM	EDTA

Denaturation buffer

1.5 M	NaCl
0.5 M	NaOH

Neutralization buffer

1.5 M	NaCl
0.5 M	Tris
	pH 7 with HCl, Autoclave

20x SSC

175.3 g/l	NaCl
88.2 g/l	Sodium citrate
	pH 7, Autoclave

Hybridization buffer

35 ml	20% SDS
50 ml	1M Na/PO_4(pH 7.2)
1 g	BSA
200 µl	0.5 EDTA

Loading dye

0.25%	Xylene cyanole
0.25%	Bromophenol blue
50%	Glycerol
10 mM	Tris (pH 8)
1 mM	EDTA (pH 8)

Propidium iodide solution

1:5000	Propidium iodide (Calbiochem 25mg/ml) Protected from light

NPA stock solution

5 mM	N-(1-naphthyl) phthalamic acid (Duchefa) Dissolved in DMSO

2.1.5 Primers

In this study the primers detailed in Table 2 were used. The primers in which a restriction site was needed at the beginning of the primer include the sequence ACTA to facilitate the activity of the restriction enzymes.

PRIMER NAME	SEQUENCE	USAGE
ERfor1	ACTAaagcttccaccatgaataagactaatcttttct	ER amplification HindIII site
ERrev3	actaGAATTCttagagttcgtcgtgcttgtacagctcgtccatgc	ER cloning with EcoRI
GFPrev1	actagaattctcaCTCTTGTACAGCTCGTCCATG	cloning primer EcoRI site
YFP/CFPfor4	actaCCATGGATaataagactaatcttttc	YFP/CFP amplification with NcoI site
YFP/CFPrev1	actaCTGCAGttagagttcgtcgtgcttgt	YFP/CFP for cloning with PstI site
YFP/CFPrev2	actaCCATGGttagagttcgtcgtgcttgt	YFP/CFP for cloning with NcoI site
APLfor1	actagagctcagctcttagtttgcttcaacaac	amplification of APL promoter, + SacI site
APLrev1	gtcgaccagacgtcacccatggtaatcgtctttggggtcgc	amplification of APL promoter, + NcoI, AatII, SalI site
APLfor5	ccatggatctgcagcagtcgacgtgatacaatttattaatttttatctatgagtg	amplification of APL promoter, + NcoI, PstI, SalI site
APLrev7	actaggtaccggcaaactgtcaaatatgaaaatcg	amplification of APL promoter, + KpnI site
PXYfor1	ACTAGAGCTCCTGCATGTTGAATTTGTGGTGG	PXY promoter cloning, + SacI site
PXYrev1	ACTACCCGGGATCCATGGTAGCTTTTAGAAAGAAATTAAAGT GAAG	PXY promoter cloning, + NcoI and XmaI site
PXYfor2	ACTACTGCAGTGTCAAAGGATTGGGGTGTGAT	PXY promoter cloning, + PstI site
PXYrev2	ACTAGGTACCGATTTCCACCAAGTGACCATAG	PXY promoter cloning, + KpnI site
WOX4for1	actaGGTACCTTTGGTTCATTTGGTTTTGGGA	WOX4 promoter, KpnI site
WOX4rev1	GCATGGATCCTACCATGGCTATATGTTAAAACTAGCAAATG	WOX4 promoter, NcoI, BamHI site
WOX4for2	GGTAGGATCCATGCTAGCGAAGTCATGAAGGTGAGGCAGAA A	WOX4 promoter, NheI, BamHI site
WOX4rev2	actaGAGCTCTTGAAAGATTCTTCTTGTTATCATCTCAT	WOX4 promoter, SacI site
YFP/CFPrev3	actaCCCGGGttagagttcgtcgtgcttgt	YFP/CFP for cloning with Cfr9I site
YFP/CFPfor2	actaCCCGGGccaccatgaataagactaat	YFP/CFP for cloning with Cfr9I (XmaI) site
SCRprom1	actagcggccgcCGACCACCACCGTCAACAAT	amplification and cloning of SCR 5' promoter, NotI site
SCR_Prom_R	actaggatccagatgcatggagattgaagggttgttggtc	Cloning of 5´SCR promoter, BamHI/NsiI
SCR_Prom3´_F	actacccgggcagcttggacgcctcgttcttag	Cloning of 3´SCR promoter, XmaI
SCR_Prom3´_R	AGAAATGAATTCAGAGCTCCACGGTGGTGG	Cloning of 3´SCR promoter, EcoRI
XIP1prom-for1	ACTAcccgggTTCAGAGAAAGATCAAAAGTAACCTAG	XIP1 promoter amplification with Cfr9I
XIP1prom-rev1	ACTAtctagaTCGTCAGAGAGTGTCATAATAGCA	XIP1 promoter amplification with XbaI
XIP1 3'prom-for1	actaCTGCAGtcatgctttcttggtgaagag	XIP1 3'promoter amplification with PstI
XIP1 3'prom-rev1	actaCTCGAGagagcttgtgaattataatgattcatt	XIP1 3'promoter amplification with XhoI
H4GFP-APLfor	actaACatgtcgggtcgtggaaaggga	cloning of H4-GFP into ptom4 and ptom49 PciI
H4GFP-APLrev	actaCTGCAGttatttgtatagttcatccatgc	cloning of H4-GFP into ptom4 PstI
H4GFP-WOX4rev	actaGGATCCttatttgtatagttcatccatgc	cloning of H4-GFP into ptom49, BamHI site
H4GFP-SCRfor	actaGGATCCttcgggtcgtggaaaggga	cloning of H4-GFP into psh4, BamHI site

Table 2 (part one): Primers used in this study.

H4GFP-SCRrev	actaCCCGGGttatttgtatagttcatccatgc	cloning of H4-GFP into psh4 and 35sprom XmaI
H4GFP-35Sfor	actaaagcttatgtcgggtcgtggaaaggga	cloning of H4-GFP into 35sprom HindIII
H4GFPfor2	actaACTAGTttcgggtcgtggaaaggga	cloning of H4-GFP, SpeI site
H4GFPfor3	actaGGATCCtcgggtcgtggaaaggga	cloning of H4-GFP, BamHI site
H4GFPrev2	actaGTCGACttatttgtatagttcatccatgc	cloning of H4-GFP, SalI site
H4GFPfor4	actaACATGTCTtcgggtcgtggaaaggga	cloning of H4-GFP, PciI site,
H4GFPfor-PstI	actaCTGCAGatgtcgggtcgtggaaaggga	cloning of H4-GFP PstI site
H4GFP-PXYfor	actaGCGGCCGCatgtcgggtcgtggaaaggga	cloning of H4-GFP into pPS24 NotI
H4GFPrev3	actaTCTAGAttatttgtatagttcatccatgc	cloning of H4-GFP, XbaI site
LTP1pGreenfor	actaGCGGCCGCgaccaaaatgattaac	cloning of LTP1prom in pGreen0229
LTP1pGreenrev	actaGGATCCatccatggattgatctcttaggtagt	cloning of LTP1prom in pGreen0229
LTP1prom3'for	actacccgggTGAGCTAGCAACGGTGAGATGATG	amplification of LTP1 3'prom. Cfr9I site
LTP1prom3'rev	actaggtaccCTTTTGTGGAAATAGAAACTTGGAGTTA	amplification of LTP1 3'prom. KpnI site
LTP1rev2	actacccgggATTGATCTCTTAGGTAGTGTTTTATGT	amplification of LTP1 promoter,Cfr9I site
LTP1rev3	actaggatccATTGATCTCTTAGGTAGTGTTTTATGT	amplification of LTP1 promoter, BamHI site
PXYfor7	TTTCCCTCGACCTCTCTCAC	Genotyping of pxy-4
PXYrev7	CCGTTCTCTTTGTTTTTTCCCC	Genotyping of pxy-4
SALK_LBa1	TGGTTCACGTAGTGGGCCATCG	Genotyping Left border T-DNA
Gabi_462G01_LP	TTTTTAGCGTGGTTCATGTCC	Genotyping of wox4-1
Gabi_462G01_RP	CATTTTTCCCTTCGATTTTCC	Genotyping of wox4-1
GABI-Kat	tctccatattgaccatcatactcatt	primer for detecting GABI-Kat insert
WOX4_rev14	CAGTGGTCGTGAAGCTGC	Genotyping of wox4-1

Table 2 (continuation): Primers used in this study.

2.1.6 Plasmids

A number of plasmids were used in this study (Table 3). pML988 and pML1054 were donated by Michael Lenhard (University of Potsdam). The rest were produced in the lab during the research process.

Plasmids produced for this study were based on the vectors pGreen0229 and pGreen0029 (Hellens et al., 2000). pGreen0229 contains the sequence of the neomycin phosphotransferase (NPTI) gene, encoding for an enzyme that confers kanamycin resistance. It also contains the sequence of the bacterial balophos resistance gene (nos-bar) which confers resistance to glufosinate ammonium (BASTA®) through the enzyme phosphinotricin aceltyl transferase (PAT). pGreen0029 contains NPTI and a nos-kan cassette that confers kanamycin resistance in plants.

In this study green fluorescence protein (GFP) and enhanced yellow fluorescence protein (YFP) and Cyan fluorescence protein (CFP) (Miyawaki et al., 1997; Shah et al., 2001) were used as

markers for identifying promoter activity in the stem. Their peaks of emission are different enough to allow the separation of their signals (Figure 4). To avoid diffusion of the fluorescent proteins, they were targeted to the endoplasmatic reticulum (ER) by fusing them to the correspondent sequence motifs ER and HDEL (Boevink et al., 1998; Haseloff et al., 1997).

Name	Construct	5´promoter length (bp)	3´ promoter length (bp)	Based on
pPS10	*APL:CFP*	2945	521	pGreen 0229
pPS11	*WOX4:YFP*	2943	645	pGreen 0229
pPS18	*PXY:CFP*	3102	771	pGreen 0029
pPS19	*PXY:YFP*	3102	771	pGreen 0029
pPS23	*SCR:YFP*	2517	554	pGreen 0229
pTOM36	*SCR:AlcR*	2517	554	pGreen 0129
pML988	*AlcA:CRE*	-	-	-
pML1054	*35S/nos-GUS/YFP*	-	-	-
pPS02	*APL:H4-GFP*	2945	521	pGreen0229
pPS20	*SCR:H4-GFP*	2517	554	pGreen 0229
pPS04	*WOX4:H4-GFP*	2943	645	pGreen 0229
pPS05	*35S:H4-GFP*	-	-	pGreen 0229
pPS16	*LTP1:H4-GFP*	3097	445	pGreen 0229
pMS59	*NST3:H4-GFP*	3028	523	pGreen 0229
pPS24	*PXY:H4-GFP*	3012	771	pGreen 0229
pPS31	*NST3:CFP*	3028	523	pGreen 0229

Table 3: Plasmids used in this study. The columns contain name of the plasmid, construct that contain the plasmid, the selected 5´promoter as bp upstream of the gene start codon, the selected 3´promoter as bp downstream of the gene stop codon and the pGreen plasmid in which it is based.

The plasmids pGreen0029 and pGreen0229 were used for producing plasmids in which a promoter drove the expression of YFP, CFP or H4-GFP in specific tissues (Figure 5). Promoters were amplified from genomic DNA with the indicated promoters (Table 2) taking a fragment of around 2 kb upstream of the start codon of the gene. The 3´part was amplified taking around 500 bp downstream from the gene stop codon. Primers for fragment amplification contained restriction sequences allowing their insertion in the vector of interest. The sequence of the fluorescent protein or the H4-GFP reporter was amplified with the indicated primers and included in the plasmids with the promoters.

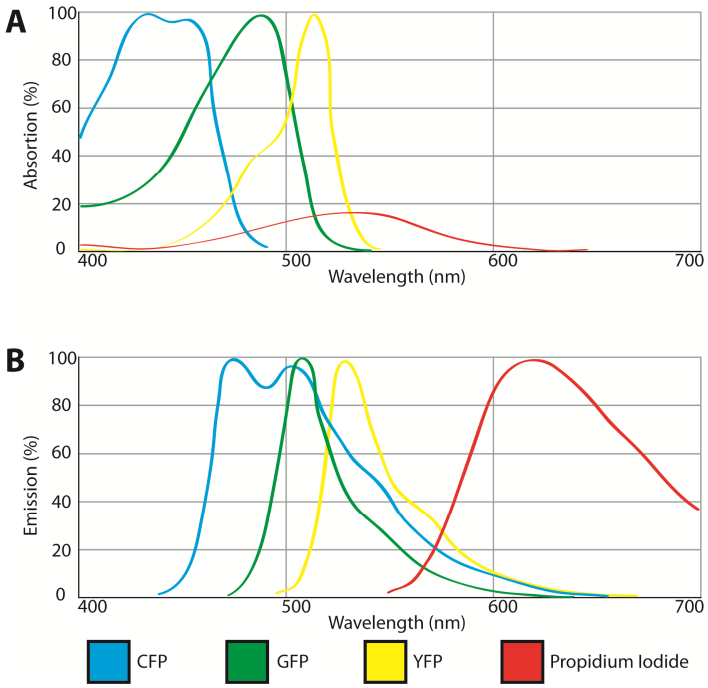

Figure 4: Wavelength of absorption (A) and emission (B) of YFP, CFP, GFP and the propidium iodide counterstaining.

2.2 Methods

2.2.1 Seed sterilization

All Arabidopsis seeds were sterilized before sowing them on soil or plates. They were placed in open 1.5 ml microcentrifuge tubes in a closed container containing a beaker with 100 ml bleach and 3 ml HCl. Seeds were sterilize by chlorine fumes for one hour.

2.2.2 Growing conditions

Short day conditions (SD): 8 h light, 16 h dark with constant temperature (21°C) and humidity (60%). Long day conditions (LD): 16 h light at 21°C and 8 h dark at 16°C. Humidity 60%.

Between 3-5 seeds were placed in individual pots (6 x 6 cm) filled with a 3:1 soil-perlite mixture (Einheitserde Special ED 63 T, Profi Substrat, Werkverband E.V.; premium perlite 2-6 mm, Gramoflor GmbH, Germany). Seeds were stratified for 3 days (4°C, darkness) and then transferred to SD conditions. After three weeks all but one plant from one pot were removed and plants were transferred to LD conditions.

2.2.3 Watering

Pots were soaked with water just before seed sowing. Later, plants were automatically watered twice a week by immersion for 10 min.

2.2.4 Pest control

Plants were treated occasionally against mildew with 2.5 g/l sulphur (spray). After pot preparation and every second week, plants were sprayed with a nematode solution (Steinernema feltiae, ENTONEM, Koppert) against the larvae of black flies (Sciaridae).

2.2.5 Ethanol treatments

Ethanol inducible plants were placed in a 40 dm^3 closed chamber containing two petri dishes with 10 ml 10% EtOH. The treatment was performed overnight and repeated during two consecutive days. 5 cm tall plants were induced and three weeks after the induction, rough hand sections from the base (0, 4 and 6 mm above the rosette) and the upper part of the first internode from the base were collected. Samples were incubated in propidium iodide for 5 minutes to stain tissues that produce autofluorescence. Samples were mounted on slides and analyzed by a LSM 710 Zeiss spectral confocal microscope (Carl Zeiss).

2.2.6 NPA treatments

The NPA stock solution was mixed with lanolin paste (Sigma Aldrich) to reach a 100 µM concentration. Lanolin was previously liquefied by heating and it was cooled down to around 40°C before mixing it with the NPA solution.

The NPA-containing lanolin was applied in a 5 mm ring around the middle part of the second internodes of ethanol-induced 10 cm tall plants. After 3 weeks, hand sections of the treated area were analyzed under the confocal microscope.

2.2.7 Histology

Fixation

Plant material was collected in microcentrifuge tubes containing 70% EtOH and vacuum infiltrated on ice for 15 minutes. After infiltration tubes were stored at 4°C.

Embedding

After fixation, plant material was introduced into embedding cassettes (Sanowa, Germany). Cassettes were introduced into a tissue processing machine (Tissue-Tek VIP, Sakura, The Netherlands) and infiltration by paraffin was performed automatically overnight. Samples were manually embedded (paraffin molding station) into molds with paraffin. After solidification, blocks were stored at 4°C.

Sectioning

Paraffin blocks were prepared removing the excess of wax around the specimen. Samples were mounted on the microtome (Microm HM325, Zeiss, Germany) and cut into sections of 10 µm. Sections were placed on slides (Superfrost, Menzel, Germany) covered with distilled water. Slides dried on a heating bank (OTS40, Meditel, Germany) at 42°C overnight.

Dewaxing and staining

Samples were dewaxed and stained by toluidine blue after the following protocol:

Histoclear	10 min
Histoclear	10 min
EtOH Absolute	1 min
EtOH Absolute	1 min
96% EtOH	1 min
85% EtOH	1 min
50% EtOH	1 min
30% EtOH	1 min
dH2O	1 min
dH2O	1 min
Toluidine Blue (0.5mg/ml)	4 min
dH2O	1 min
dH2O	1 min
dH2O	30 s
96% EtOH	30 s
EtOH Absolute	30 s
EtOH Absolute	30 s

The slides were air dried for 10 minutes. Cover slides were mounted and sealed by Entellan (Merck, Germany).

2.2.8 Stem hand sections

To analyze the stem under the confocal microscope hand sections of fresh material were produced. The stem fragments for analysis were cut by a scissor and introduced into a polystyrene cube. Fine sections were produced using a razor blade (Classic Wilkinson, Germany). The stem cross sections were mounted in a propidium iodide solution (1:5000) on a slide, and the cover slip was fixed by liquid glue. The samples were analyzed under the confocal microscope within a time frame that never exceeded 4 hours.

2.2.9 Vector Generation

Fragment amplification

The fragments of interest were amplified by PCR using the appropriate primers using as a template genomic DNA or other plasmids. The amplification of DNA fragments for cloning was performed ussing Phusion High Fidelity DNA polymerase (New England Biolabs, United Kingdom) or Pfu DNA polymerase (Fermentas, Canada) according to the manufacturer's instructions. The fragments were purified using a commercial kit (QIAquick PCR purification, QIAGEN, Netherlands) according to the manufacturer's instructions.

Enzymatic digestion

The fragment of interest and the host vector were digested by specific restriction enzymes according to the manufacturer´s protocol producing compatible overhangs that allowed insertion of the fragment of interest into the plasmid. After digestion the DNA was purified with commercial separation columns (QIAquick PCR purification kit, QIAGEN, The Netherlands).

Ligation

After digestion, the fragment and the vector were combined and ligated in a 20 µl reaction mix by using the T4 ligase (Fermentas, Canada) or T4 fast ligase (Fermentas, Canada) according to the manufacturer's instructions.

E. coli transformation

An aliquot of *E. coli* cells (200 µl) were thawed on ice and 10 µl from the ligation reaction were added. After 20 min incubation on ice the cells were incubated 75 s at 42°C. Subsequently, cells were cooled down on ice for 2 min and 800 µl LB medium were added. The cell suspension was

incubated at 37°C on a shaker for 2 hours. 100 µl of the suspension were plated onto plates containing selective medium. The plates were incubated at 37°C overnight.

Colony PCR

Individual colonies from the plates were tested by PCR to confirm the presence of the correct vector. Primers from the fragment and the vector were used to confirm the correct incorporation of the fragment. The positive colonies were used for inoculating 4 ml of liquid LB medium containing the respective antibiotic. The culture was incubated overnight at 37°C on a shaker. Next, the bacteria were precipitated by centrifugation and the plasmids isolated using a commercial kit (QIAprep, QIAGEN, The Netherlands) according to the manufacturer's instructions. The DNA concentration was determined using a Spectrophotometer (NanoDrop ND-1000). Samples were stored at -20°C.

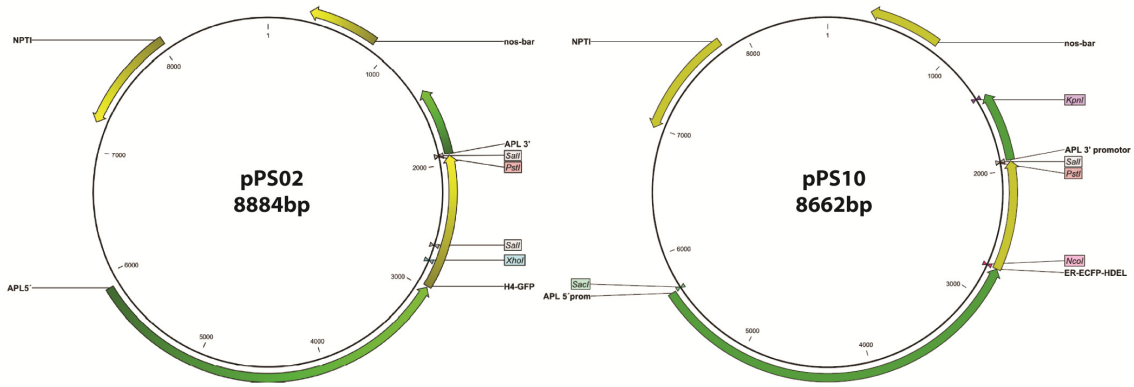

Figure 5: Schematic representation of the plasmids APL:H4-GFP (pPS02) and APL:ER-ECFP-HDEL (pPS10) as examples of the produced plasmids for checking promoter activity domains and for sorting.

Plasmid sequencing

To confirm the correct insertion of the PCR-derived fragments the inserts were fully sequenced, including the junctions to the vector. The samples were sequenced in the Vienna Biocenter facilities and the obtained sequences analyzed using the software CLC Main Workbench (CLC bio).

2.2.10 Transformation of Arabidopsis thaliana

Agrobacterium transformation

For introducing a plasmid into *Agrobacterium tumefaciens* cells, the freeze-thaw method was used (Hofgen and Willmitzer, 1988). An aliquot (200 µl) of the *Agrobacterium* stock was thawed on ice. 500 ng of the plasmid of interest were added to the cell suspension and incubated on ice for 5 min. After 5 min in liquid nitrogen the tube was incubated at 37°C for another 5 min. 800 µl of YEB medium were added to the tube followed by incubation at 28°C in agitation (180 rpm) for 3 h. After incubation, 100 µl of the suspension were plated on selective medium (YEB), containing 50 µg/ml rifampicin (selects for Agrobacterium itself), 5 µg/ml tetracycline (selects for the helper plasmid pSoup) and 50 µg/ml kanamycin (specific antibiotic for the plasmids used in this study). Plates were incubated at 28°C until colonies had a diameter of 2 mm (2-3 days).

Arabidopsis plant transformation: floral dip

Arabidopsis thaliana plants were transformed using the floral dip method (Clough and Bent, 1998). A colony of transformed *Agrobacterium* was used to inoculate 4 ml of selective medium (YEB and selective antibiotics as described before). After 24 h shaking at 28°C (180 rpm), the culture was used to inoculate 400 ml of selective medium in a big Erlenmeyer (2 l). The culture was incubated at 28°C in agitation (180 rpm) for another 24 h, and then the culture was transferred into 500 ml plastic tubes and centrifuged at 5000 rpm for 15 min at 20°C. The supernatant was removed and the pellet was rinsed and resuspended in 500 ml of 5% sucrose containing 0.02% Silwet L-77 (Lehle Seeds, Round Rock, TX, USA). Inflorescences of Arabidopsis (16 plants per pot, 5 pots per construct) were dipped into the bacterial solution for 5 min. The dipped plants were placed in trays with water and covered with plastic lids for keeping the humidity. The day after, lids were removed and the plants transferred to the growing chamber (LD conditions) until they produced seeds (T1).

Selection of transformed plants

For isolating kanamycin-resistant plants, seeds from transformed plants were laid out on plates containing ½ MS-medium and 50 mg/l kanamycin. Plates were sealed and placed into the plant culture room after incubation for 3 days in darkness at 4°C. Healthy plantlets were transferred to soil and used for further analysis. Plants transformed with plasmids conferring BASTA resistance were laid out directly on soil, stratified for 3 days in darkness at 4°C and transferred to LD

conditions. Plantlets were selected by spraying them with BASTA (40 mg/l BASTA/tap water) every third day. Surviving plants were transferred to individual pots and used for further analysis.

2.2.11 Southern blots

To check the number of transgenes in the plant genome, Southern blots (Southern, 1975) were performed in the first generation after transformation. It was performed according to the upward capillary transfer of DNA (Sambrook and Russell, 2006).

2.2.12 Nucleus extraction

Second internodes from the base (2 g) were collected into a 85 mm plastic petri dish resting on ice and transferred to the fume hood. 1 ml of isolation buffer was added to the petri dish and the plant material was chopped for 10 min using a razor blade (Classic, Wilkinson, Germany). The liquid was collected using a 1 ml pipette and transferred to a 2 ml microcentrifuge tube through a 50 µm filter (CellTrics, Partec, Germany). 1 ml of isolation buffer was added to the petri dish, the plant material resuspended and the liquid was again collected and added to the same tube through the filter. The tube was centrifuged at 2800 g at 4°C for 10 min. The supernatant was removed and the pellet gently resuspended in 500 µl of isolation buffer. The cleaning step was repeated two times and finally the pellet was smoothly resuspended in 300 µl isolation buffer. It was transferred to a new tube through a 50 µm filter (CellTrics, Partec, Germany) and 100 µl of DAPI staining buffer (CyStain UV Precise P, Partec) were added. Tubes were kept on ice and protected from light. Just before the sorting procedure, the buffer was filtered again with a 50 µm filter (CellTrics, Partec, Germany) to avoid presence of particle aggregates.

2.2.13 Nucleus Sorting

The sorting of the nucleus populations was performed by a cell sorter “FACSAria III” (BD Bioscience, USA). The machine takes particles in suspension and produces a thin flow allowing only single particles (events) to pass through a laser. Fluorescence properties are detected by detector. The intensity for GFP and DAPI fluorescence for each event is plotted in a two-dimension histogram. Areas of that plots can be selected as “gates”, meaning that the events in those areas will be collected. The gates were established according to event distribution using GFP negative and positive control samples. The negative control sample was a nucleus preparation from wild type plants. The positive control sample was a nucleus preparation from 35S:H4-GFP transgenic plants. All nuclei were sorted according to established gates. Nuclei for analysis under the microscope were collected directly into 1.5 ml microcentrifuge tubes kept at 4°C. Nuclei for

RNA extraction were collected into 1.5 ml tubes containing 400 µl of lysis/binding buffer from the RNA extraction kit (Dynabeads, Invitrogen). That buffer contains detergents at a high concentration that break the nucleus membranes releasing their content. The presence of LiDS (lithium dodecyl sulfate) in the buffer inhibits RNase activity.

2.2.14 Total RNA extraction

Second internodes were frozen in liquid nitrogen and ground in a mortar. Around 300 µl of frozen powder were transferred into a microcentrifuge tube. 1 ml Trizol (Invitrogen, Carlsbad, California, USA) was added, mixed and incubated at room temperature for 5 min. The tube was centrifuged at 14000 g for 5 min at 4°C. The supernatant was transferred to a fresh tube containing 200 µl of chloroform. The suspension was gently mixed and incubated at room temperature for 5 min. The tube was centrifuged at 14000 g for 15 min at 4°C. The aqueous phase was transferred to fresh tubes containing 500 µl isopropanol. Tubes were gently mixed and incubated at -20°C for at least 30 min. The tube was centrifuged at 14000 g for 10 min at 4°C. The supernatant was removed and the pellet dried after washing using 1 ml 70% EtOH. The dried pellet was dissolved in 50 µl H_2O. The RNA was purified using commercial columns (RNeasy MinElute Cleanup Kit, QIAGEN) according to manufacturer´s protocol. The RNA was quantified by a spectrophotometer (NanoDrop ND-1000).

2.2.15 mRNA extraction

PolyA RNA was extracted directly from sorted nuclei or from total RNA using polyT magnetic Beads (Dynabeads® mRNA DIRECT™ Kit, Invitrogen Dynal, Norway) according to manufacturer´s protocol. The amount and quality of the RNA was determined in a Bioanalyzer (Agilent) using a PicoChip (RNA 6000 pico kit, Agilent).

2.2.16 mRNA amplification

mRNA was amplified using the TargetAmp™ 2-Round Biotin-aRNA Amplification Kit 3.0 (Epicentre Biotechnologies, Madison, WI, USA) according to the manufacturer's protocol. It consists in the transcription of the RNA with T7-oligo(dT) primer to produce the first strand of the cDNA. The RNA was fragmented and those fragments primed the synthesis of the second cDNA strand. The T7 promoter integrated with the oligo(dT) allowed the transcription of antisense RNA. After this first round of amplification, the antisense RNA produced was used in a second round of amplification like the first one. RNA purification steps were performed using RNeasy MinElute Cleanup Kit (Qiagen). The volume was adjusted by speed vacuum centrifugation (Speed Vac).

2.2.17 High-throughput sequencing

Sequencing of the amplified mRNA was outsourced to BGI HONG KONG CO., LIMITED. mRNA samples were frozen and sent to Hong Kong by air mail with 4kg dry ice. Integrity of samples was checked upon arrival and a second control of quality performed. A 200 bp short-insert library was constructed. Sequencing was performed generating at least 20 Million 50 bp single end reads.

The bioinformatician Branislav Kusenda (GMI) checked the quality of the reads. The levels of 5' and 3' terminal bases were quantified in order to exclude (or detect) the presence of "T" barcodes, multiplexing indexes and other experimental artifacts. Illumina quality scores were used for discarding reads with low quality and removing terminal parts of reads with low quality of base calling. The reads were aligned to the reference TAIR10 (NC_003070.gb, NC_003071.gb, NC_003074.gb, NC_003075.gb, NC_003076.gb) with a maximum number of mismatches of 0 and a maximum number of hits of 1for a single read. Quantification of gene activity was performed using the CLC genomics workbench version 5.5.1 or the CLC server version 4.5 in accordance to the manufacturer's protocols. Secondary analysis, data-mining, and additional information from TAIR10 (gene ontologies, Locus symbols, aliases etc.) was performed using the MySQL relational database management system. Expression values were normalized by establishing RPKM values (Mortazavi et al., 2008).

2.2.18 Statistical analyses

Reads from APL+ and APL- samples were analyzed statistically using R, a language and environment for statistical computing (www.R-project.org). Data were analyzed with the package DESeq which was performed for analyzing differential gene expression in RNA-seq datasets (Anders and Huber, 2010). The analyses were based on a model which test for the negative binomial distribution. The p-value was adjusted according to the false discovery rate calculated according to the Benjamini-Hochberg method (Benjamini and Hochberg, 1995).

2.2.19 DNA extraction

Quick extraction

This method was performed for DNA extraction for genotyping. 1-3 leaves were collected into a 1.5 ml microcentrifuge tube containing 200 µl of DNA isolation buffer. The plant material was ground by a drill and additional 200 µl of the buffer were added. After inverting several times, the

tubes were centrifuged for 5 min at maximum speed (14000 rpm) at 20°C. 350 µl of the supernatant were transferred to a new 1.5 ml tube containing 350 µl isopropanol. After inverting several times, the tubes were incubated at RT for 10 minutes. Tubes were centrifuged at maximum speed for 5 min at RT. The supernatant was removed and the pellet washed by adding 300 µl of 70% EtOH and centrifuging again for 1 min at maximum speed. The supernatant was removed and the pellet dried. The dried pellet was resuspended in 50 µl 1x TE buffer by incubating it at 65°C for 10 min in a thermo mixer (Eppendorf). After spinning it down, 1 µl was used as template for PCR or stored at -20°C.

CTAB

Fresh plant material was harvested, frozen in liquid nitrogen and ground using a mortar and pestle avoiding thawing of the material. The frozen powder was put into a 1.5 ml microcentrifuge tube containing 1 ml CTAB buffer. The material was mixed with the CTAB buffer and incubated at 65°C for 15 min in a thermo mixer (Eppendorf) mixing occasionally. 400 µl of chloroform were added and mixed by inverting the tube several times. The tube was centrifuged for 10 min at maximum speed at RT and the aqueous phase was transferred to a new tube containing 700 µl of isopropanol. After inverting the tube several times, it was incubated at -20°C for 30 min. The tube was centrifuged at 4°C for 10 min at maximum speed and afterwards the supernatant was completely removed. The pellet was resuspended in 300 µl TE buffer by incubation at 65°C for 5 min. 2 µl RNaseA (DNase and protease-free, Fermentas) was added and incubated at 37°C for 20 min. 200 µl of phenol:chloroform (phenol:chloroform:isoamyl alcohol 25:24:1, AppliChem) were added and the tube was inverted several times and centrifuged for 10 min at maximum speed at RT. 200 µl of the upper phase were transferred to a fresh tube and 0.1 volumes of 3M NaAc (pH 5.5) and two volumes of absolute EtOH were added. After inverting the tube several times, it was incubated for 1 hour at -20°C. The tube was centrifuged for 10 min at 4°C and at maximum speed to pellet the DNA. The supernatant was removed and the pellet washed by adding 1 ml 70% EtOH and centrifuging again for 5 min. The supernatant was completely removed and the pellet resuspended in 50 µl TE by incubation at 65°C for 5 min. DNA concentration was determined using a NanoDrop Spectrophotometer ND-1000.

2.2.20 PCR

The PCR reactions were performed in a Biometra T3000 Thermocycler according to the following protocol:

2.5 µl	10 x Buffer (homemade)
0.25 µl	10 mM dNTPs (Fermentas)
1.5 µl	25 mM $MgCl_2$ (homemade)
0.5 µl	10 mM Forward primer
0.5 µl	10 mM Reverse primer
0.5 µl	Taq DNA polymerase (1:50, homemade)
100 ng gen. DNA 1 ng plasmid	template
Water	To 25 µl

1x	95°C	3 min
30x	95°C	30 s
	58°C	30s
	72°C	2 min
1x	72°C	7 min

2.2.21 Gel electrophoresis

The PCR fragments were mixed with 0.8 µl loading dye and loaded on a 1% agarose gel (Peqlab) in 1x TAE. A size marker was added to the gel (Gene Ruler 1kb, Fermentas). Electrophoresis was performed at 110 V 30 min. The gel was stained in an Ethidium bromide bath (1µg/ml in 1xTAE) for 30 min. The stained gels were analyzed using UV light (Gel Logic 2000 Imaging System, Kodak).

2.2.22 Crossing *Arabidopsis thaliana*

All siliques and flowers were removed from the stem of the mother plant. By the help of magnification lenses, all the floral buds were removed from the inflorescence except 3 mature but still closed ones. Flower buds were opened by forceps and all organs except gynoecia removed. Mature flowers from the father plant were used to pollinate the bare gynoecia. Siliques were collected in paper bags after ripening (Weigel and Glazebrook, 2002).

2.2.23 Imaging

Macroscopic photography

Macroscopic images were taken using a digital camera (Nikon D80) using an AF Nikkor 35 mm objective.

Light microscopy

Histological cuts stained by toluidine blue were analyzed using an Axio Imager M1 microscope (ZEISS). Pictures were taken using the microscope incorporated camera with the SPOT Advanced 4.6 software.

Fluorescence microscopy

Fluorescence microscopy was performed using a Zeiss Axio Imager M1 microscope (Carl Zeiss, Germany), employing a DAPI filtercube (365 nm excitation, 445/50 nm emission), a YFP filtercube (500/20 nm excitation, 535/30 nm emission) or a CFP filtercube (436/25 nm excitation, 480/40nm emission).

Confocal microscopy

A Spectral confocal LSM 710 or LSM 780 microscope (Zeiss, Germany) was used for analyzing the fluorescence marker lines. Produced images are the average of 8 frames of 8 bits. Signals from different fluorescence proteins were collected in different tracks. YFP was excited by an Argon laser (514 nm), a beam splitter MBS 458/514 and emission was collected between 522-542 nm. CFP was excited by an Argon laser (458 nm), a beam splitter MBS 458/514 and the signal emitted between 469-490 nm was collected. The propidium iodide-derived signal was collected in an independent track, excited by a 514 nm Argon laser using a beam splitter MBS 458/514 and emission was detected in the range from 620 to 670 nm.

Image processing

Images were processed using the software SPOT advanced 4.6, ZEN2010 and Adobe Illustrator (CS5).

3 - Results part one:

Establishment of the secondary stem

In this part of the project the transition from the primary (Figure 6-A) to the secondary (Figure 6-C) stem conformation in *Arabidopsis* was addressed, paying special attention to the processes occurring in the transition stage (Figure 6-B) in order to gain a better understanding of secondary growth initiation. The progeny of the starch sheath was tracked to elucidate its role in the formation of the interfascicular cambium (IC) during those developmental stages of the stem. The moment in which the vascular identity is acquired in the interfascicular areas was dissected using one of the cambium molecular markers, and the relation between lateral root formation and IC formation was briefly analyzed in the *alf4* mutant.

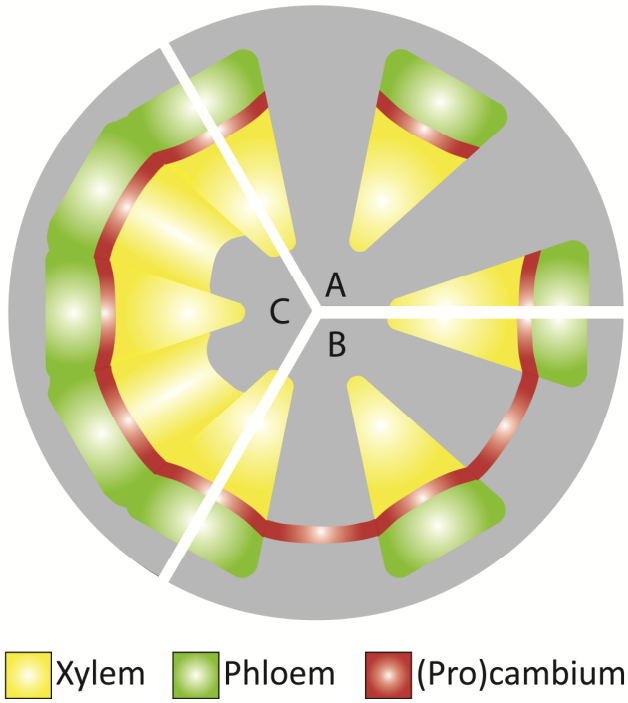

Figure 6: Different stages of the Arabidopsis stem. Simplified scheme of the A) primary stem with individual vascular bundles. B) Transition stage between the primary and the secondary stem conformation. The process of IC formation is initiated but not completed. C) Secondary stem. In this conformation, more prominent in trees, there is a complete ring of vasculature. Red: (pro) Cambium. Yellow: Xylem. Green: Phloem.

3.1 The contribution of starch sheath cells to IC formation

Histological analyses of the interfascicular region in the transition stage (Altamura et al., 2001; Sehr et al., 2010; Ye et al., 2002) suggested that cells from the starch sheath (SS), which is the innermost cell layer of the cortex, divide in the interfascicular area and contribute to the formation of the IC. However, when this study began no molecular data confirming this hypothesis were available. Histological observations can be misinterpreted due to the close interconnection

between tissues in the plant stem. In addition, mutants like *scr* or *shr,* which do not establish the SS in the stem (Fukaki et al., 1998), still retain the capacity to produce the IC (Sehr, 2010). To elucidate molecularly whether the SS indeed contributes to the process of IC formation, I took advantage of the promoter of *SCR*. *SCR* is specifically expressed in SS cells (Wysocka-Diller et al., 2000) and can be used as a marker for SS identity. The promoter was used to follow different experimental approaches that allowed me to visualize SS identity and track its progeny during IC formation.

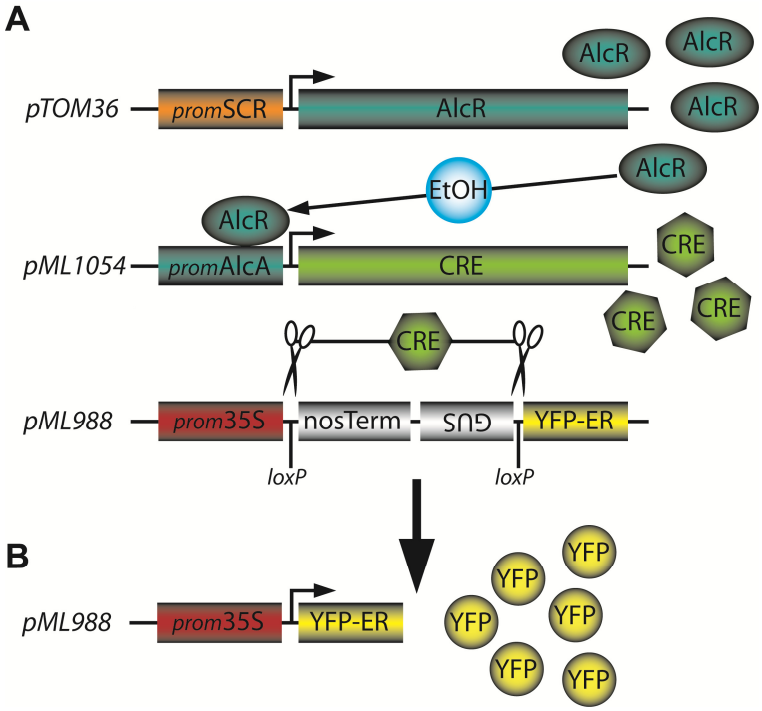

Figure 7: Ethanol-inducible three component system for tracking starch sheath cell progeny. A) Mode of action upon ethanol treatment. AlcR, which is present in SCR-expressing cells, binds the *AlcA* promoter, activating the CRE recombinase and eliminating the fragment between the loxP sites. B) Situation after ethanol induction. The *35S* promoter drives the expression of *ER-YFP* and it is therefore also active in all descendant cells.

3.2 SS cells can dedifferentiate and initiate IC identity

To visualize the progeny of the SS cells, I used plants containing a three component clonal analysis system (Figure 7-A). In this system the promoter of *SCR*, which is active in the SS, drove the expression of AlcR, a transcription factor that activates the *AlcA* promoter upon ethanol treatment (Roslan et al., 2001). The *AlcA* promoter controls the expression of the CRE recombinase that removes part of the third construct, resulting in the induced conformation of the system (Figure 7-B). In this conformation the *35S* promoter drives the expression of the YELLOW

FLUORESCENT PROTEIN (YFP) (Eriksson et al., 2010) fused to ER target sequences. In summary, after ethanol induction the system is activated in *SCR*-expressing cells and YFP expression is maintained in all daughter cells because the *YFP* gene is driven by the constitutive *35S* promoter. The system thus allows visualization of SS cells and all their progenies.

Plants containing the three transgenes were induced by ethanol treatment when they were 5 cm tall. 3 weeks later, hand sections of different parts of the stem (Figure 8-E) were stained by propidium iodide and analyzed under the confocal microscope. In the upper part of the first internode where IC formation does not take place (Figure 8-A), the YFP signal was restricted to a single cell layer on the proximal side of the cortex, which presumably represented the SS. The position 6 mm above the rosette corresponded to the transition stage, since the vascular cambium was not produced but some periclinal cell divisions were present in the interfascicular area (Figure 8-B). At this position cells proximal to the SS expressed *YFP* (arrows). They probably originated from a SS cell that divided periclinally. 4 mm above the rosette (Figure 8-C), propidium iodide staining showed organized columns of cells presumably originated from cambium cells, and at this position, therefore, the stem harbors a secondary conformation. At this position files of cells from the cortex to the xylem expressed YFP, indicating that they all originated from SS cells. At the base, just above the uppermost rosette leaf (Figure 8-D), cambium activity was again evident from the presence of columns of cells radially organized in the interfascicular areas. However, at this position the YFP signal was restricted to SS cells. This observation can be explained by the initiation of cambium activity before ethanol induction and SS labeling since 5 cm tall plants already establish secondary growth at this position (Sehr et al., 2010). This observation can also indicate that SS cells do not continue dividing and continuously producing IC, but that rather this is a single event and could also mean that not all IC cells derive from the SS.

3.3 The IC can derive from SS cells

NPA (α-naphtalenacetic acid) is widely used in pharmacological approaches to block PIN-dependent auxin transport in plants (Muday and DeLong, 2001; Rubery, 1990; Ruegger et al., 1997). Strikingly, it was shown that local NPA treatments on stems induce secondary growth in *Arabidopsis* (Agusti et al., 2011a; Little et al., 2002; Suer et al., 2011; Sundberg et al., 1994). NPA blocks the basipetal transport of auxin along the stem, leading to an accumulation of the hormone in and above the treated area. This, in turn, results in local lateral growth induction including the formation of the IC. To confirm my results obtained at the base of the stem where IC formation takes place naturally, the SS progeny was tracked during NPA-induced IC formation. Plants

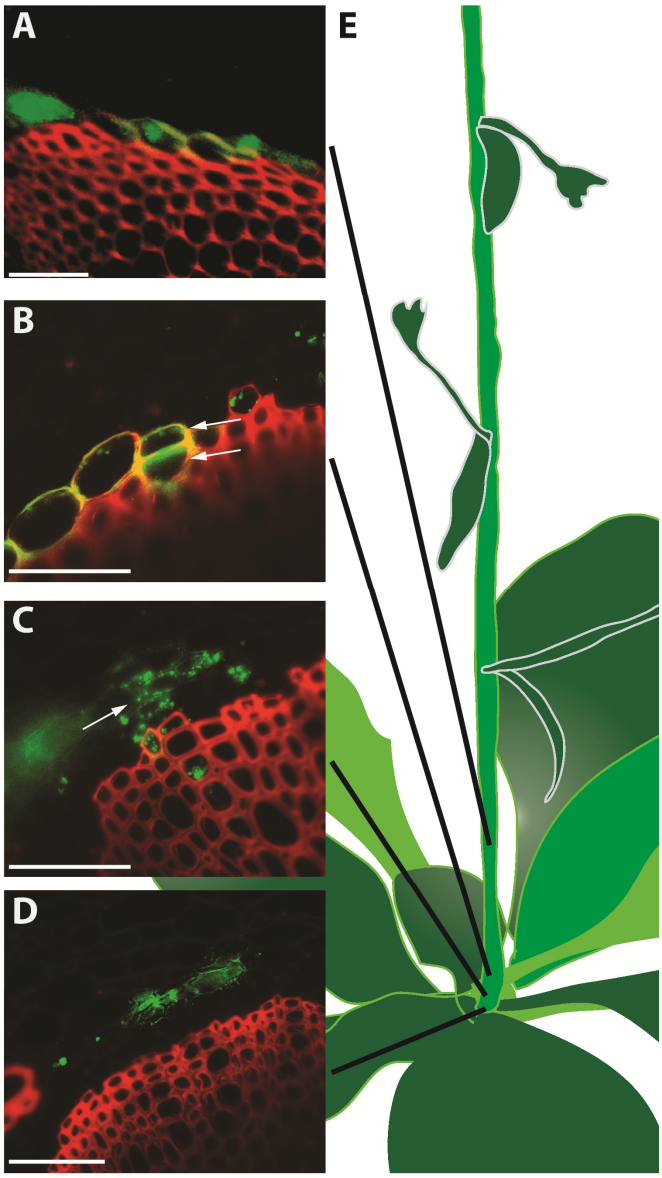

Figure 8: Starch Sheath progeny during IC formation at the base of the *Arabidopsis* stem. A) Presence of *YFP* activity was restricted to the starch sheath at positions where no IC was formed. B) *YFP* activity at positions where the starch sheath started dividing. C) Clones of SS-derived cells expressing *YFP*. D) At the base of the stem YFP was restricted to the starch sheath cells. E) Scheme of the plant showing the studied positions (0, 4, 6 and 30 mm above the base). Arrows: cells expressing *YFP*. Size bars: 50µm. Green channel: YFP-derived signal. Red channel: propidium iodide-derived signal.

containing the three transgenes (Figure 7) were grown on soil to a height of 10 cm. At that point, they were induced by ethanol and then rings of lanolin containing NPA or a mock solution were applied to the plant stem to induce IC formation (Figure 9). Three weeks later, hand sections of the treated area were produced, stained with propidium iodide, and the interfascicular areas were investigated under the confocal microscope.

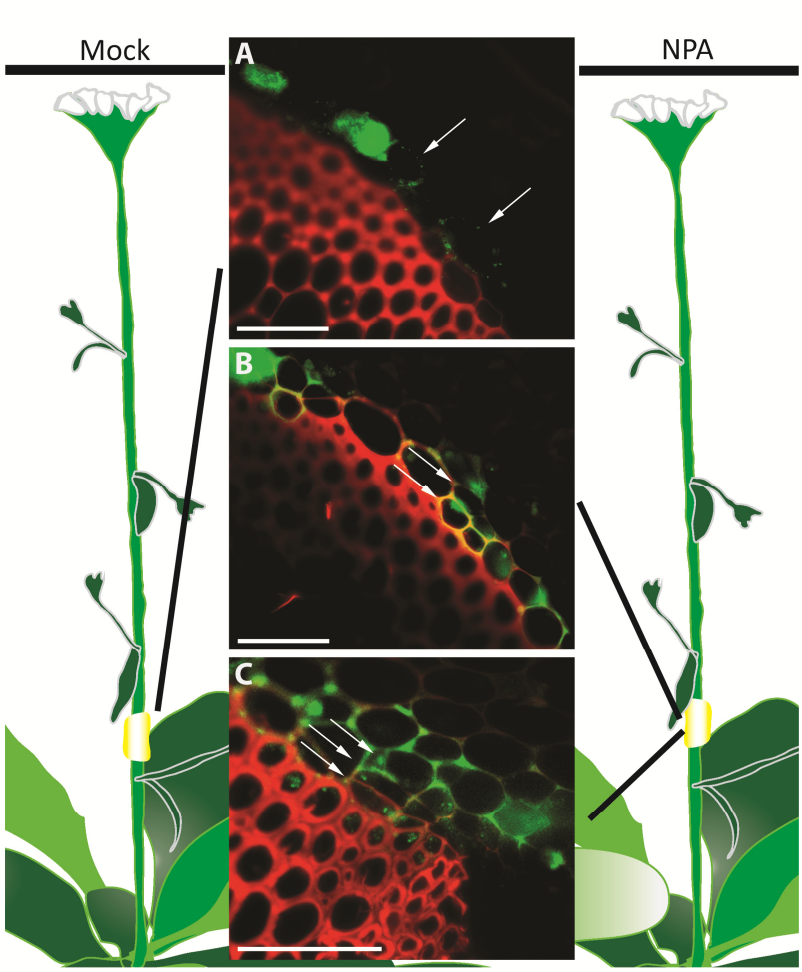

Figure 9: Starch sheath progeny during induced IC formation. A) Mock-treated plants showing the YFP signal restricted to the starch sheath. B) NPA-treated areas showing the first divisions in the starch sheath. C) NPA-treated areas showing a developed file of SS-derived cells. Arrows: *YFP*-expressing cells. Size bars: 50 µm. Green channel: YFP-derived signal. Red channel: propidium iodide-derived signal.

In the mock-treated plants (Figure 9-A), the cellular pattern indicated that cambium activity was not initiated. In all cases *YFP* expression was only detected in the SS, arguing that the transgenic system was activated but that SS cells had not divided. In contrast, just above the NPA-treated area (Figure 9-B, arrows) cells proximal to the SS expressed *YFP*, indicating that SS cells had divided similarly as in the transition zone during natural IC formation (Figure 8-B). In the NPA-treated area (Figure 9-C), files of *YFP*-expressing cells are present in the interfascicular region. They appear in radial columns in the typical conformation when produced by IC activity. This indicates that they were indeed derived from SS cells. In summary, these results confirm that SS cells can give rise to the IC.

3.4 Starch sheath identity is maintained during lateral growth initiation

To visualize the cells harboring SS identity during different phases of stem development, I produced the plasmid *pPS23* (*SCR:YFP*), a transcriptional marker in which the *SCR* promoter drives the expression of *YFP*, which was again targeted to the endoplasmic reticulum with the help of the appropriate target motifs (Boevink et al., 1998) to avoid passive diffusion. Plants containing the *SCR:YFP* transgene were grown on soil to a height of 20 cm. Hand sections of the second internode and base were produced and analyzed under the confocal microscope (Figure 10). In the second internode (Figure 10-A, B), *YFP* activity was restricted to the SS. The cellular pattern highlighted by propidium iodide-staining showed no radial columns of cells in interfascicular regions, indicating that no secondary growth had taken place at this position. In the secondary stem (Figure 10-C, D), the staining by propidium iodide revealed radial columns of cells derived from the IC. Interestingly, the YFP signal was restricted to a single cell layer located on the inner side of the cortex, indicating that SS identity is not lost during the transition from primary to secondary stem and that it remains as a single cell layer.

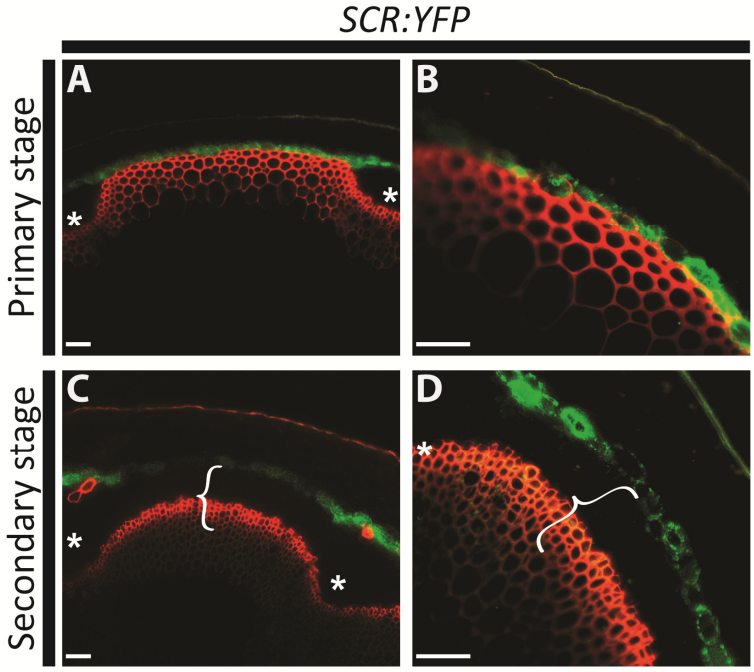

Figure 10: The dynamics of SS identity in the stem. *SCR* is expressed specifically in the SS and here SS identity was visualized with the marker *SCR:YFP*. A) Primary stem. B) Higher magnification of the primary stem. C) In the secondary stem *SCR:YFP* is still active and labels SS identity as in the primary stem. D) Higher magnifications of the secondary stem. Size bars: 50µm. Brackets: Secondary growth. Green channel: YFP. Red channel: propidium iodide. Asterisks: vascular bundles.

In summary, these experiments demonstrated that starch sheath cells can give rise to the IC in a discrete event and that, at the same time, SS cells retain their original identity. Therefore, IC formation seems to be a process of de-differentiation and *de novo* formation of cambium identity.

3.5 Dynamics of gene vascular domains during stem development

The transition from primary to secondary conformation of the stem represents mainly alterations in the vasculature, which changes from discrete entities, the vascular bundles, to a continuous cylindrical system in which the vascular cambium produces phloem and xylem towards the stem periphery and towards the center, respectively (Figure 6). For the control of the vascular meristem a regulatory loop consisting of *CLE41*, *WOX4*, and *PXY* had been described (Fisher and Turner, 2007; Hirakawa et al., 2010), which is similar to the *CLV3/CLV1/WUS* regulatory loop (Brand et al., 2000) in the shoot apical meristem and the *CLE40/ARC4/WOX5* loop in the root (De Smet et al., 2008; Sarkar et al., 2007; Stahl et al., 2009). The transcription factor *ALTERED PHLOEM DEVELOPMENT* (*APL*) is crucial for acquiring phloem identity (Bonke et al., 2003) and its activity reflects a differentiated state during vascular development. To observe how vascular identities are distributed in the primary and the secondary stem, the expression domains of *PXY, WOX4,* and *APL* were tracked at different developmental stages of the stem. To observe how these vascular genes influence each other, their expression domains were tracked in *pxy* and *wox4* mutants.

Plant lines carrying fluorescent markers visualizing *PXY* (*pPS18, 19*), *WOX4* (*pPS11*), and *APL* (*pPS10*) promoter activities were produced. The activity of these promoters should reflect the actual endogenous expression domain of these genes since complementation experiments taking advantage of the same promoter constructs were able to recover wild type phenotypes (Bonke et al., 2003; Fisher and Turner, 2007; Suer et al., 2011). Similarly to the *SCR:YFP* line, the fluorescent proteins were again ER-targeted (Figure 10). Plants containing the transgenes were grown on soil to a height of 20 cm, and hand sections stained with propidium iodide were produced and analyzed under the confocal microscope. At least 3 plants for each construct were examined. The expression domain of these promoters was analyzed in wild type and two mutant backgrounds, *pxy* and *wox4*, to see whether the absence of one of them affects the expression domain of the others. The analysis was performed in vascular bundles at different developmental stages (base, 1st, 2nd, and 3rd internodes).

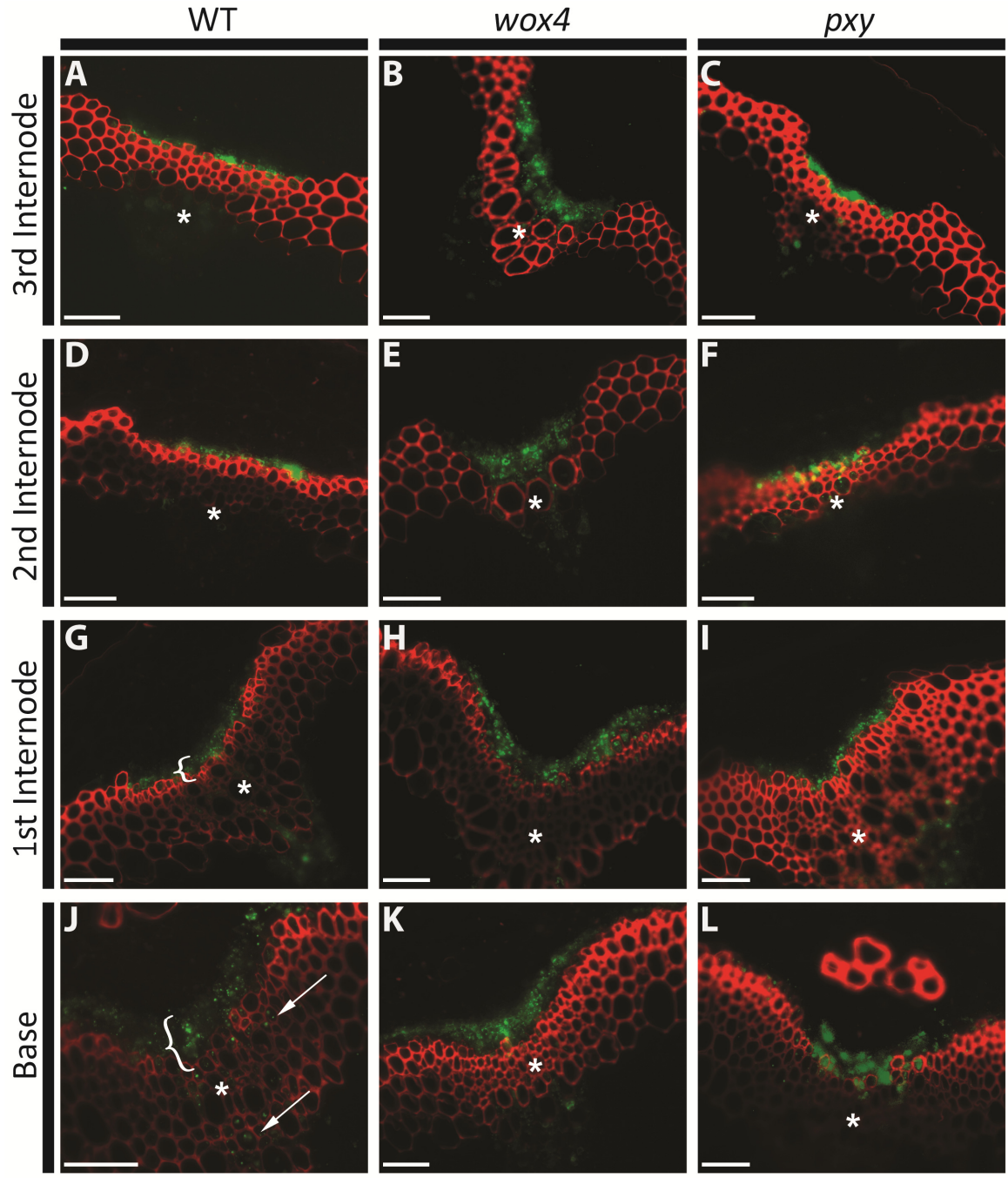

Figure 11: *PXY:YFP* activity in vascular bundles. Expression of *PXY* in the vascular bundles of the 3rd internode (A, B, C), 2nd internode (D, E, F), 1st internode (G, H, I), and the Base (J, K, L) in wild type, *wox4*, and *pxy* backgrounds. Size bars: 50 µm. Green channel: YFP-derived signal. Red channel: propidium iodide-derived signal. Asterisks: vascular bundles. Arrow: YFP signal in the xylem. Brackets: *PXY:YFP* domain.

3.6 Expression domains of vascular genes in vascular bundles

3.6.1 *PXY* expression domain in the vascular bundle

In wild type vascular bundles (Figure 11), the *PXY:YFP* signal was present in a narrow region distal to the propidium iodide-stained xylem and fiber cells. At the base some cells in the xylem area also displayed *YFP* activity (Figure 11-J arrows). There were no fundamental differences in the *PXY:YFP* expression domain comparing the third, second and first internode (Figure 11-A, D, G), indicating that there is no change in the *PXY* activity domain in the primary stem once the vascular bundles are established. At the base of the stem however (Figure 11-J), where secondary stem conformation was established, the region displaying *YFP* activity was broader due to distal extension (Figure 11-J, brackets). Strikingly, in comparison to wild type plants, *wox4* mutants generally displayed a broader *PXY:YFP* expression domain in both the primary and secondary stem (Figure 11-B, E, H, K). The signal was always restricted to the area distal to the xylem, and in this case no differences were observed between the internodes and the base. The *pxy* mutant displayed the *PXY:YFP*-derived signal in the vascular bundles similarly to wild type plants. The observation that mutants presented some alterations in the vascular bundle tissue pattern confirms the described defects in the vascular bundle anatomy of the *pxy* mutant (Fisher and Turner, 2007). In sum, the expression of *PXY* seems to be restricted to the area corresponding to the fascicular cambium in the vascular bundles, and this distribution does not change during the studied developmental stages in wild type including the primary and the secondary stem. The *PXY:YFP* domain in the vascular bundles is larger in *wox4* mutants, and in the case of *pxy* mutants it visualizes the described morphology alterations of the vascular bundle.

3.6.2 *WOX4* expression domain in the vascular bundle

In the analyzed sections of the wild type stem (Figure 12), *WOX4:YFP* was active in the vascular bundle in a narrow area distal to the propidium iodide-stained cells of the xylem and fibers in a domain of similar shape to that found for *PXY:YFP* activity. The signal was also present in cells of the primary xylem close to the pith (Figure 12-A arrow), indicating that those cells have cambium identity or, more likely, that the *WOX4:YFP* reporter is not exclusively marking (pro)cambium identity since *WOX4* activity was not observed in this area in several studies investigating the *WOX4* expression pattern (Hirakawa et al., 2010; Suer et al., 2011). There were no fundamental differences in the expression domains at the different positions along the stem analyzed in this approach (Figure 12). In *wox4* mutants (Figure 12-B, E, H, K) there were no obvious differences

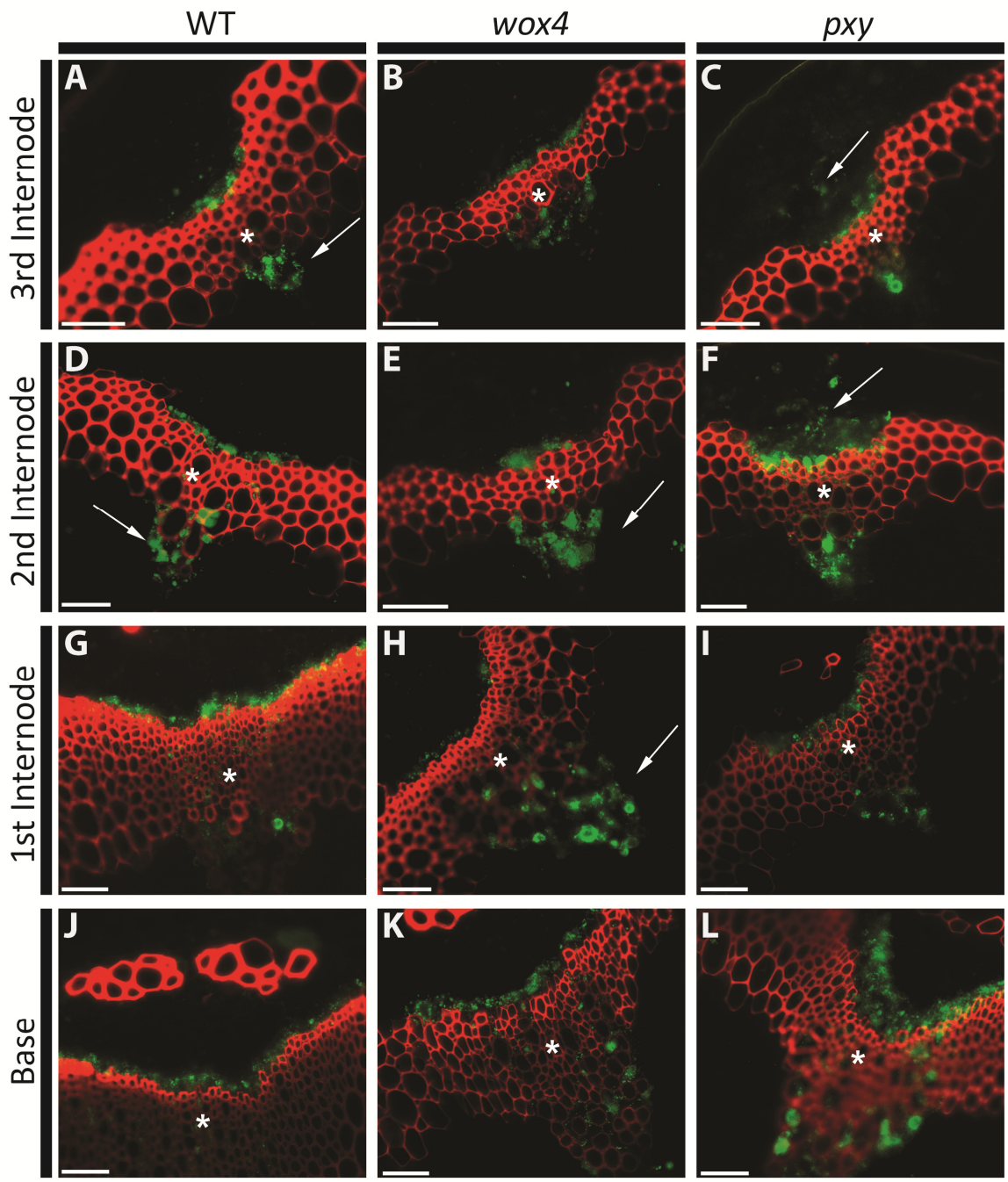

Figure 12: *WOX4:YFP* activity in vascular bundles. Expression of *WOX4:YFP* in the vascular bundles of the 3rd internode (A, B, C), 2nd internode (D, E, F), 1st internode (G, H, I), and the Base (J, K, L) in wild type, *wox4*, and *pxy*. Size bars: 50 µm. Green channel: YFP. Red channel: propidium iodide. Arrows: YFP presence in non-cambium areas. Asterisks: vascular bundles.

in the expression domain of *WOX4:YFP* in comparison to wild type plants. Strikingly, in *pxy* mutants a number of differences were observed in comparison to wild type. In the primary stem the YFP-signal was not restricted to the narrow domain distal to the xylem but extended into the

phloem area and sometimes even into the SS (Figure 12-C, F, arrows). However, in the 1st internode and at the base the signal was not present in the phloem area (Figure 12-I, L). In conclusion, the *WOX4:YFP* marker is expressed in two zones of the vascular bundle: one overlaps with the domain observed for *PXY:YFP*; and the other corresponds to the innermost area of the vascular bundles, in the area of the xylem with no lignified cell walls. The *wox4* mutant does not show differences in the pattern of expression in comparison with wild type plants. Interestingly, in the *pxy* mutant *YFP*-expressing cells are present in the phloem area and in the starch sheath in the upper region of the stem.

3.6.3 *APL* expression domain in the vascular bundle

In sections from wild type plants (Figure 13-A, D, G, J) *APL:CFP* expression was restricted to the phloem area. There was a narrow area between the *CFP*-expressing cells and the secondary walls of the xylem that potentially corresponded to the cells of the cambium and the primary xylem (Figure 13-A, arrow). Within the studied bundles the size of the area where *APL:CFP* was active gradually increased with the development of the bundles. In *wox4* vascular bundles (Figure 13-B, E, H, K) the *APL:CFP* domain was similar to wild type in the upper region of the stem. However, at the base the *APL* domain was narrower than in wild type plants. This might be due to the fact that the cambium is not maintained and therefore phloem production is reduced in this background. In *pxy* mutants the *APL:CFP* domain was similar to that in wild type, except for the base (Figure 13-L), where the expression domain was discontinuous and more disperse than in wild type. In conclusion, the *APL:CFP* domain increases progressively in more developed vascular bundles. However, this progression is affected in the studied mutants. The domain is reduced at the base of *wox4* and the distribution is disrupted at the base of *pxy* mutants, perhaps due to the presence of intercalated xylem cells.

3.7 The dynamics of vascular genes during IC formation

During the transition from the primary to the secondary conformation of the stem, vascular tissue is produced in the interfascicular areas, connecting vasculature from the vascular bundles. The markers for the vascular genes *PXY*, *WOX4*, and *APL* were analyzed in the interfascicular areas during this developmental transition to observe their progression during the establishment of the secondary conformation of the stem. To see how they affect each other the same markers were analyzed in the *pxy* and *wox4* backgrounds.

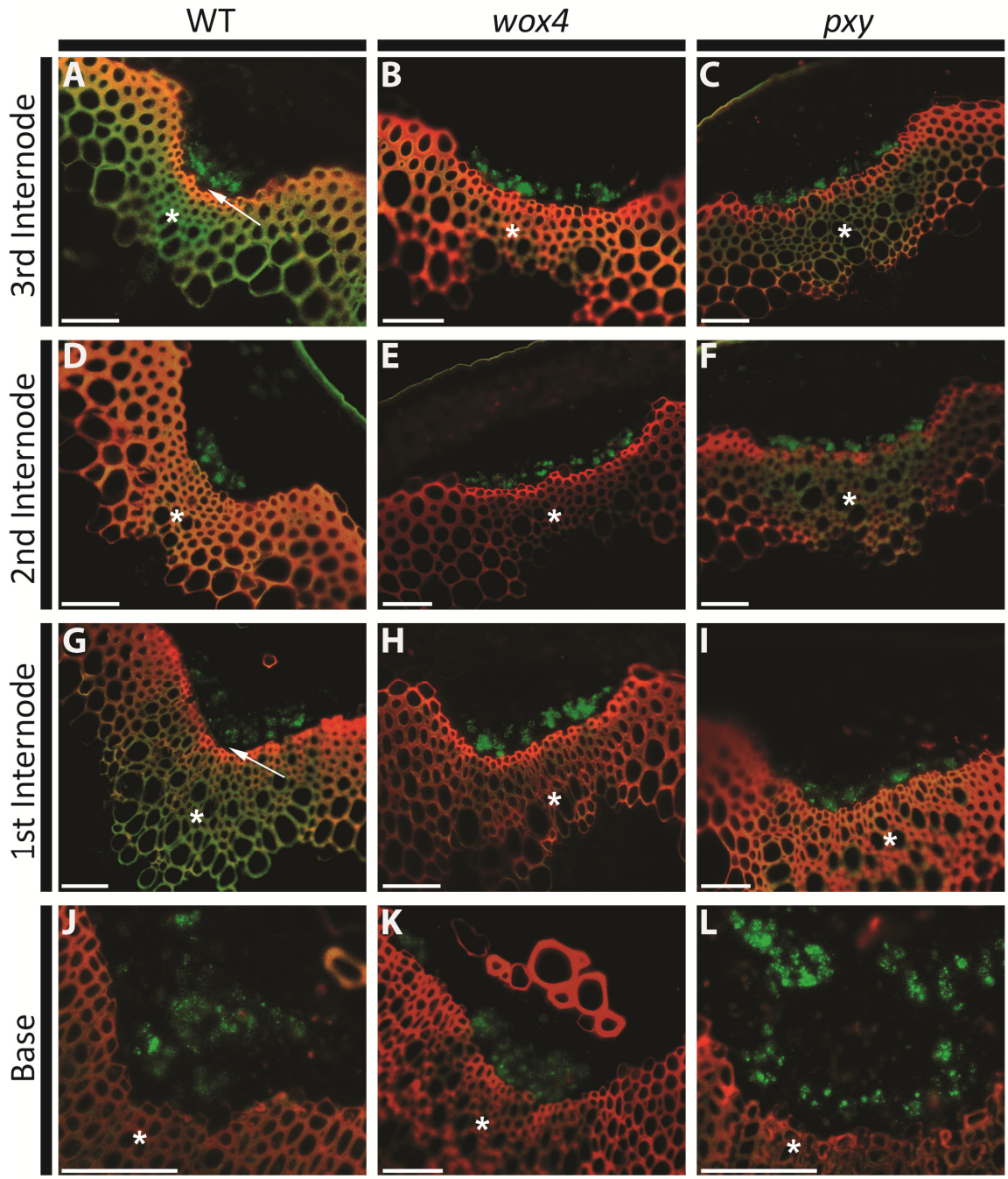

Figure 13: ***APL:CFP*** **expression in vascular bundles. Expression of** ***PXY*** **in the vascular bundles of the 3rd internode (A, B, C), 2nd internode (D, E, F), 1st internode (G, H, I), and base (J, K, L) in wild type,** ***wox4***, **and** ***pxy*****. Size bars: 50 µm. Green channel: YFP. Red channel: propidium iodide. Arrows: cambium area. Asterisks: vascular bundles.**

3.7.1 The *PXY* promoter activity during IC formation

In primary stem of wild type plants (Figure 14-A), the *PXY:YFP* derived fluorescent signal was restricted to vascular bundles, to an area that corresponds to the cambium since it is located just distally to the propidium iodide-stained cells of the xylem and fibers. The same distribution was observed in the *wox4* and *pxy* mutants (Figure 14-B, C). According to the propidium iodide staining, there were no differences in the histological cell distribution or morphology in the interfascicular area of the primary stem between wild type and the vascular mutants. No reporter gene activity was observed, indicating that vascular identity in the interfascicular areas of the primary stem is absent. In the transition zone, 6 mm above the rosette, the *PXY:YFP* activity domain was different between wild type, *wox4*, and *pxy*. In wild type plants (Figure 14-D) the domain extended from the vascular bundles into the interfascicular area in a thin layer externally to the area with secondary cell walls. Such a continuous domain of *PXY: YFP* activity was not present in *wox4* mutants (Figure 14-E). However, the *wox4* mutants showed a larger *YFP*-positive domain in the vascular bundle in comparison to wild type (Figure 14-E). In the *pxy* mutants the signal was restricted to the vascular bundles (Figure 14-F) and resembled the signal in the primary stem. At the base of the stem, wild type plants displayed secondary conformation, as indicated by the structure of propidium iodide-stained cells in the interfascicular area (Figure 14-G). In these plants the continuous domain of *PXY:YFP* activity was larger in the radial orientation than in the transition zone, indicating that there were more cells with cambium identity (Figure 14-D, G). In the *wox4* mutants cells expressing *PXY:YFP* in the interfascicular area were in a narrow domain, a situation that resembles the transition zone in wild type (Figure 14-H). In the *pxy* background there was never *PXY:YFP* expression in the interfascicular regions, and at all positions the stem displayed a primary conformation (Figure 14-I). In summary, the *PXY:YFP* activity, which should reflect cambium activity, appears in the interfascicular areas in parallel with the transition to a secondary conformation of the stem. In the case of the *wox4* and the *pxy* mutants *PXY:YFP* activation is delayed or altogether absent, respectively.

3.7.2 The *WOX4* promoter activity during IC formation

In interfascicular regions of primary stems the *WOX4* promoter activity visualized by the reporter construct *WOX4:YFP* (*pPS11*) did not show differences between wild type, *wox4*, and *pxy*. The signal was restricted to the vascular bundles, to an area distal to the propidium iodide-stained cells

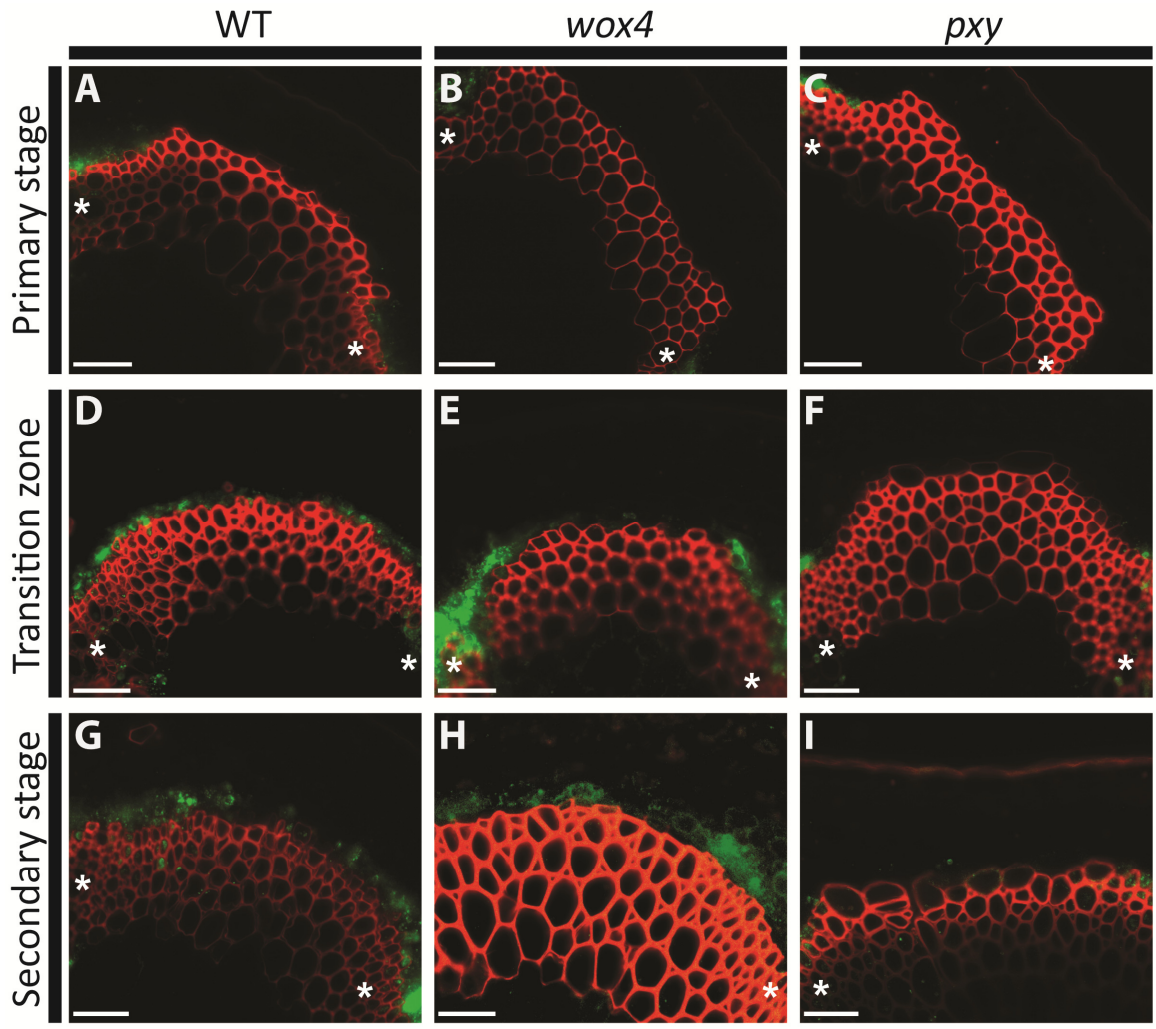

Figure 14: *PXY:YFP* expression during IC formation. Interfascicular area of the primary conformation of the stem (A,B,C), the transition zone (D,E,F), and the secondary conformation of the stem (G,H,I) in wild type, *wox4*, and *pxy*. Size bars: 50µm. Green channel: YFP-derived signal. Red channel: propidium iodide-derived signal. Asterisks: vascular bundles.

(Figure 15-A, B, C), thereby resembling the *PXY:YFP* domain. In the transition zone some cells in the interfascicular area displayed *WOX4:YFP* activity in wild type plants (Figure 15-D), but the signal was absent or very weak in the interfascicular area of *wox4* and *pxy* (Figure 15-E, F). At the base of wild type stems, radial files of propidium iodide-stained cells were detected and a continuous ring of *WOX4* expression was recognizable connecting the vascular bundles (Figure 15-G). At the base of *wox4* mutants the stem presents an impaired secondary growth according to the propidium iodide-stained cell walls; the *WOX4:YFP*-derived signal was present in the interfascicular area (Figure 15-H), thereby resembling the transition stage in wild type. In *pxy* mutants the signal was restricted to vascular bundles and no activity was detectable in the

interfascicular area (Figure 15-I). In summary, the activity of the *WOX4:YFP* reporter showed a similar pattern to the *PXY:YFP* reporter. Both markers are related to cambium identity and they appear in the interfascicular area associated with the establishment of the secondary conformation of the stem. The behavior of the markers in the *wox4* and *pxy* mutants indicates that the process is delayed or completely absent in these backgrounds, respectively, demonstrating that both genes are important for the establishment of a continuous cambial domain.

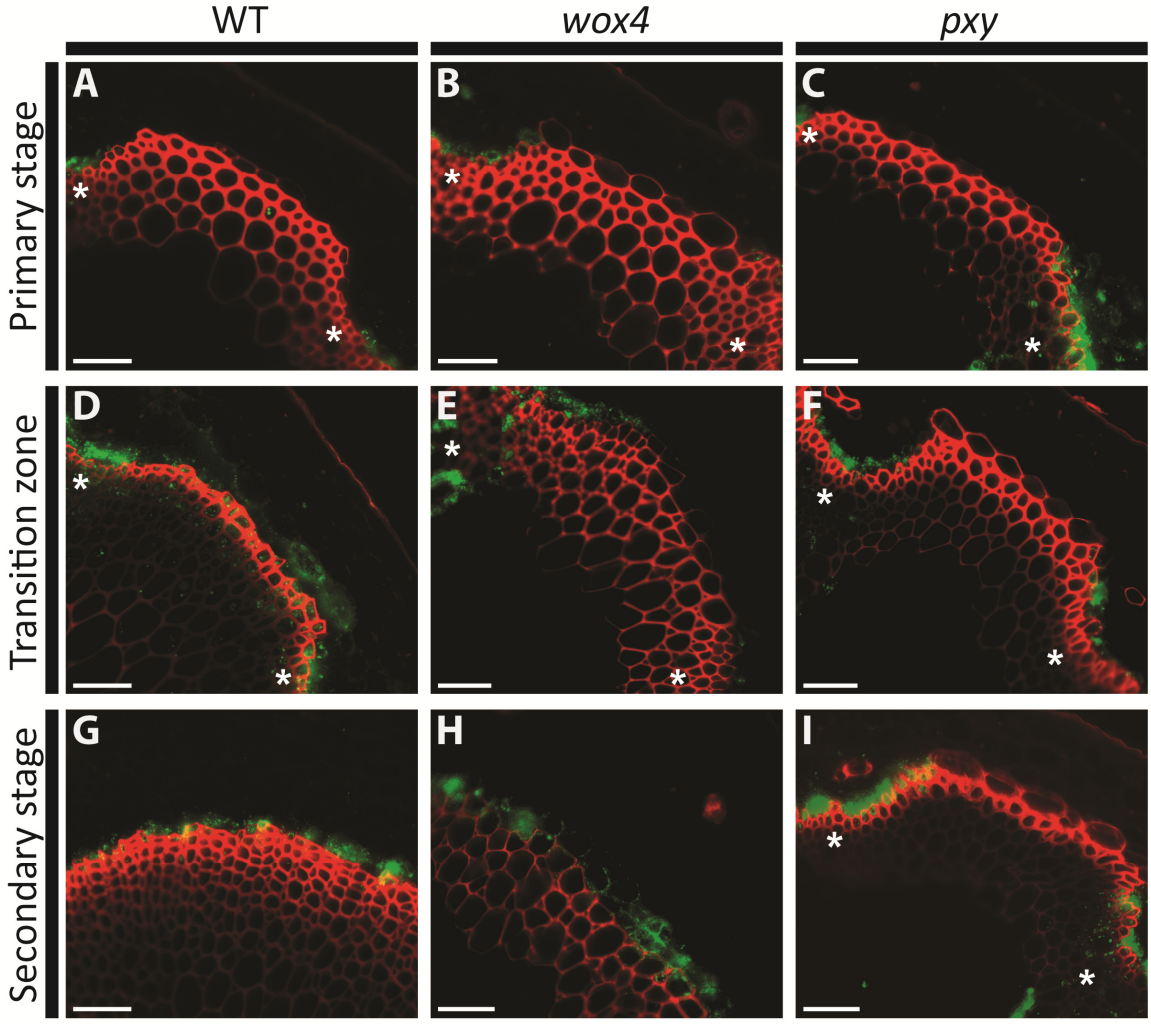

Figure 15: *WOX4:YFP* expression during IC formation. Interfascicular area of the primary internode (A, B, C), the transition zone (D, E, F), and the secondary internode (G, H, I) in wild type, *wox4*, and *pxy*. Size bars: 50 µm. Green channel: YFP-derived signal. Red channel: propidium iodide-derived signal. Asterisks: vascular bundles.

3.7.3 The *APL* expression dynamics during IC formation

The *APL* expression domain, visualized by the reporter construct *APL:CFP* (*pPS10*), appeared restricted to the vascular bundles in the primary stem. In the bundles it was active in the typical invagination of propidium iodide-stained cells that correspond to the phloem. The gap between the *CFP*-expressing area and the propidium iodide-stained cells would correspond to the cambium cells. The same signal distribution was observed in the primary stems of wild type, *wox4*, and *pxy* (Figure 16-A,B,C). The CFP signal was completely absent from the interfascicular area, as similarly observed for *PXY:YFP* and *WOX4:YFP* derived signals. In the transition zone I observed several differences between the *APL:CFP* signal in the different backgrounds. In wild type there were clusters of *APL:CFP* activity (Figure 16-D). In the *wox4* background (Figure 16-E) *APL:CFP* activity was less prominent in interfascicular regions with fewer *CFP*-positive clusters than in wild type plants. The *pxy* mutant did not show *APL:CFP* signal in the interfascicular area (Figure 16-F). At the base of wild type stems the clusters of cells expressing *APL:CFP* (Figure 16-G) were thicker than in the transition zone, indicating that more phloem had been produced. *wox4* mutants showed less and smaller phloem clusters at the base than wild type plants and resembled the transition zone in wild type plants. In *pxy* mutants (Figure 16-I) the fluorescent signal was completely absent from the interfascicular area, indicating that no secondary phloem was produced.

In conclusion, according to all markers tested there is no cambium identity in the interfascicular area of the primary stem. This observation confirms previous basic histological analyses. In all genetic backgrounds tested in this experiment, the promoter activity of the studied genes was restricted to the vascular bundles at this stage. In the transition zone and the secondary stem, the vascular genes were active in the interfascicular area and differences between mutants were visible. The vascular genes started to be active in the transition zone of wild type plants and showed a larger activity domain in the secondary stem. *pxy* mutants, which are not able to produce IC, always kept a primary stem conformation and did not show any sign of cambium activity in the interfascicular area. The *wox4* mutants displayed some cambium activity in the interfascicular area at the base, which resembled the wild type transition stage. It seems that IC formation in *wox4* is delayed but that plants are still able to produce the IC, which can also differentiate into phloem. The absence of cambium activity in the *pxy* background indicates that *PXY* is essential for IC formation. Because the *wox4* mutant was able to establish the IC to some extent, *WOX4* cannot be crucial for IC establishment or the *wox4* mutant must be a weak allele. At the positions where the

markers for *PXY* and *WOX4* were active in continuous domains, APL was present in clusters. There are zones in which *PXY* and *WOX4* are present but not *APL*; this might indicate that this gene is the last of the studied genes appearing in the interfascicular area during the formation of the secondary stem conformation.

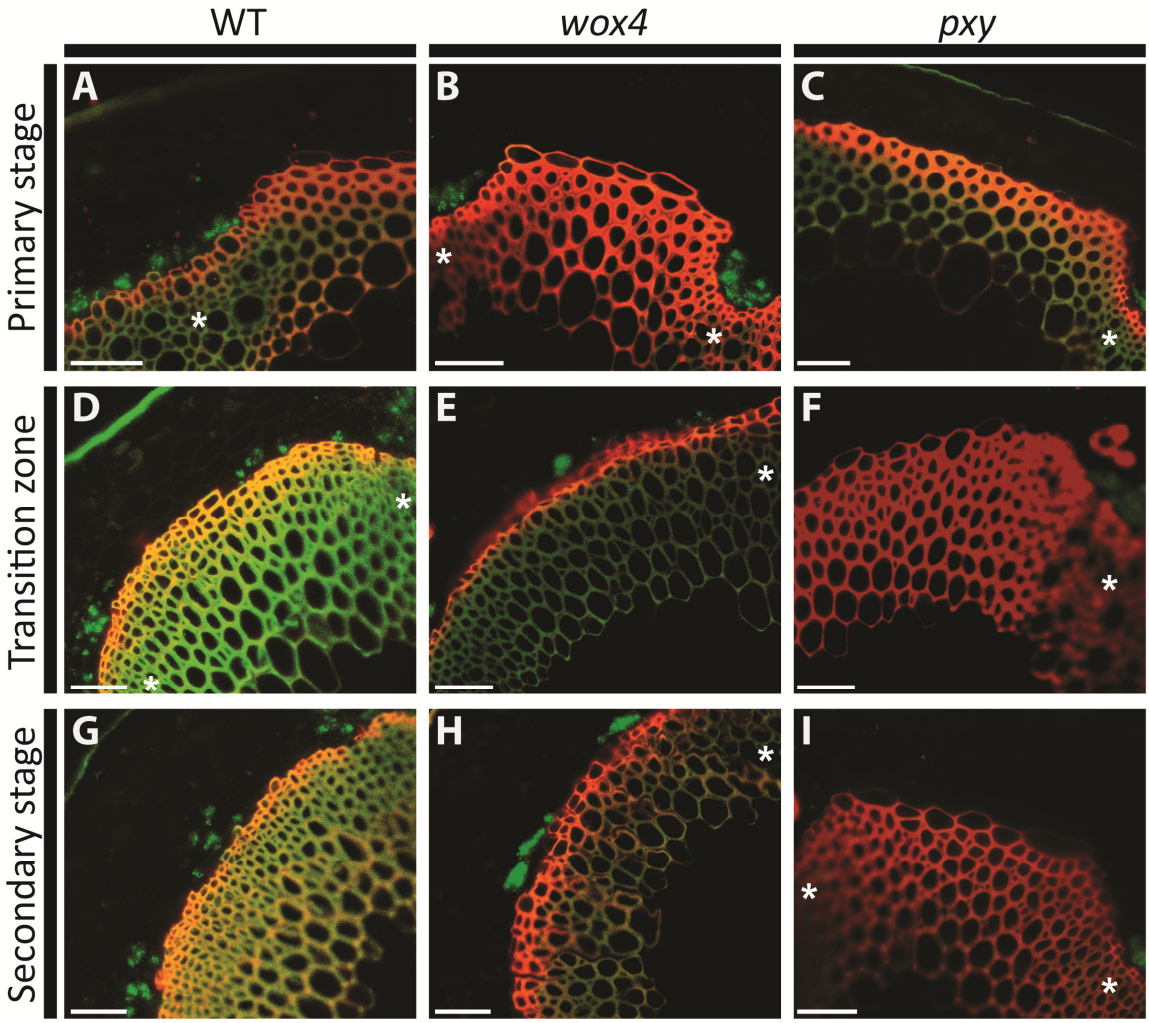

Figure 16: The *APL:YFP* activity during IC formation. The interfascicular area of the primary internode (A, B, C), the transition zone (D, E, F), and the secondary internode (G, H, I) in wild type, *wox4*, and *pxy*. Size bars: 50µm. Green channel: YFP-derived signal. Red channel: propidium iodide-derived signal. Asterisks: vascular bundles.

3.8 Spatial interaction between expression domains

The small size of the cells in the vascular bundles and the close vicinity of the involved tissues made it difficult to determine clear boundaries between the studied reporter gene domains. Thus, to establish spatial relationships of the studied expression domains, two markers were combined in

the same plant line. The use of different fluorescent proteins allowed the analysis of the individual fluorescent signals by selecting different wavelengths for excitation and collection of the emitted light, allowing the visualization of two reporter expression domains in one plant.

3.8.1 *PXY* and *WOX4* expression domains overlap in the cambium area

The presence of *PXY* and *WOX4* in the same pathway controlling vascular development (Hirakawa et al., 2010) makes it especially important to investigate in detail the spatial relationship of their expression domains in the vascular bundle. Plants containing both *pPS11* (*WOX4:YFP*) and *pPS18* (*PXY:CFP*) were analyzed when they were 20 cm tall (Figure 17-A, B, C). As expected, the expression domains of *PXY:CFP* and *WOX4:YFP* overlapped in the cambium area (Figure 17-A, B, C white arrows), indicating that both genes are active in the same cells. In the xylem area close to the pith only *WOX4:YFP* was active (Figure 17-C red arrow). Collectively, this suggests that the chosen promoters are active in the same domain in the cambium area but not in the proximal part of the bundle.

3.8.2 *APL* and *PXY* expression domains do not overlap in the vascular bundles

The expression domains of *APL:CFP* and *PXY:YFP* were clearly separated in the vascular bundle (Figure 17-D, E, F). In the studied developmental stages both domains were adjacent to each other but they did not overlap, indicating that there is no transition area with cells expressing both genes. Moreover, no gap was observed between both reporter activities, suggesting that phloem initiation starts immediately after cells have left the *PXY* expression domain.

3.9 Interfascicular cambium is established by an asymmetric cell division

It was shown above that SS cells give rise to the IC. It was further shown that vascular identity (cambium or phloem) is restricted to the vascular bundles in the primary conformation of the stem and appears later in the interfascicular areas, forming a continuous domain. A question that arose during this analysis regards the timing of the acquisition of vascular identity. To elucidate when vascular identity is established during IC formation I took advantage of the *PXY* marker line, which is very specific for the cambium (Figure 14). 20 cm tall plants containing the *PXY:YFP* transgene were analyzed carefully to visualize the first divisions during IC formation. The analysis was performed in wild type and *wox4* mutant plants (*pxy* mutants were excluded because they do not form the IC at all). Hand sections from the transition zone, 6 mm above the base in wild type

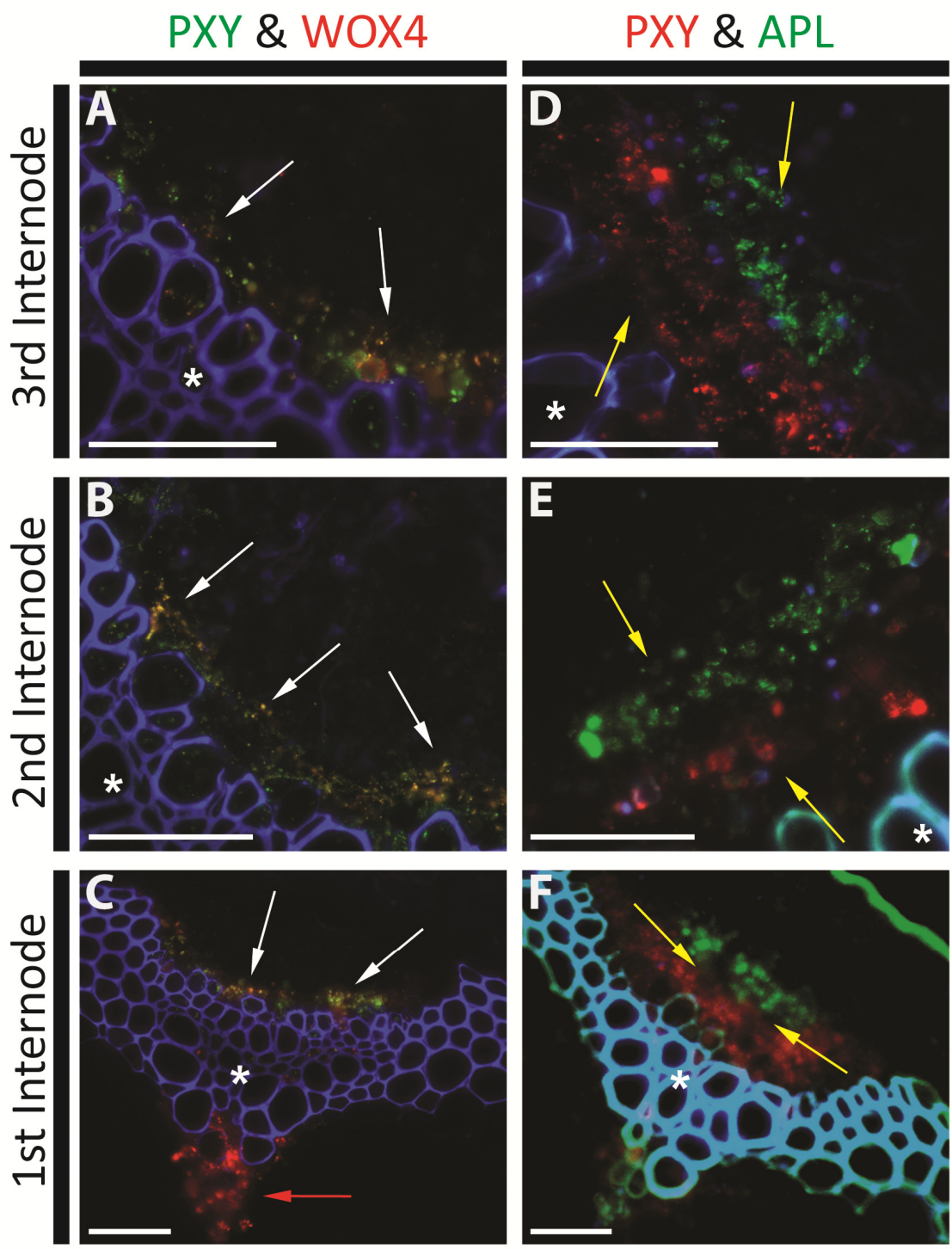

Figure 17: Expression domains comparison. Combined analysis of the activity of *PXY:YFP/CFP*, *WOX4:YFP* and *APL:CFP* reporters in vascular bundles in the 3rd internode (A, B), 2nd internode (C, D), and 1st internode (E, F) Size bars: 50 µm. Green channel: CFP. Red channel: YFP. Blue channel: propidium iodide. White arrows: coexpression of *WOX4:YFP* and *PXY:CFP* in the cambium area. Red arrow: *WOX:YFP* expression in a non-cambium area. Yellow arrows: different expression domains of *PXY:YFP* and *APL:CFP*. Asterisks: Vascular bundles.

and at the base in *wox4* mutants (IC formation is delayed in those mutants), were produced and analyzed under the confocal microscope. In the transition zone of wild type plants (Figure 18), I focused on the innermost cell layer of the cortex, which can be identified by its close vicinity to the propidium iodide-stained cells. These cells showed an oval shape that is characteristic for the SS. At the transition stage, (Figure 18-B, arrow) the SS cells had periclinally divided once. Interestingly, *YFP* activity was predominantly in the daughter cells adjacent to the propidium iodide-stained walls, indicating a differential expression of *PXY* in the progeny of the SS cells. At the base of the *wox4* mutant the same pattern appeared, with only the proximal daughter cells expressing *PXY*. These observations indicate that SS division is asymmetric in the sense that the proximal cells acquire vascular identity during or just after the division. Importantly, the establishment of this identity is independent from *WOX4* activity.

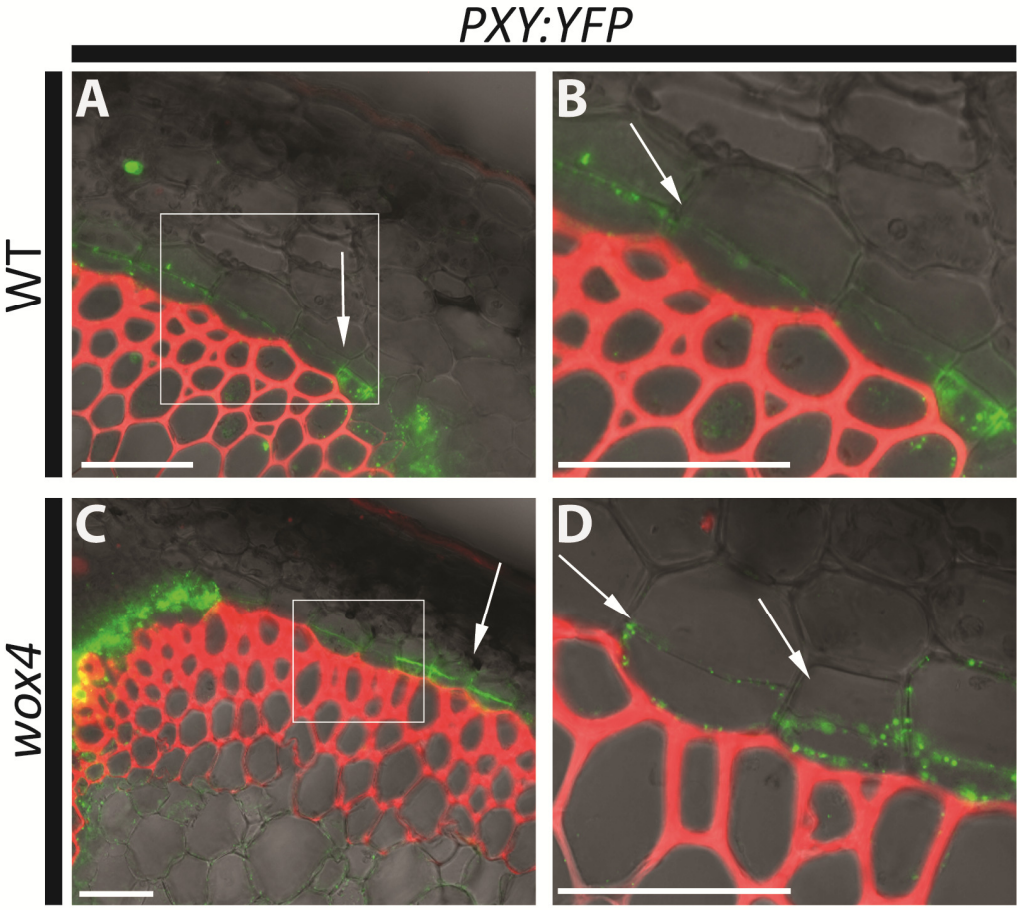

Figure 18: Vascular identity during IC formation. *PXY:YFP* activity in the dividing SS indicates different cell identities. The proximal cells expressing preferentially *YFP* indicates that vascular identity is established during the first division. In wild type transition zone (A, B) and *wox4* (C,D). B and D are magnifications of A and C, respectively. Size bars: 50 µm. Green channel: YFP. Red channel: propidium iodide. White squares indicate amplified areas in B and D. Arrows: points of special interest.

3.10 The processes of lateral root formation and IC initiation employ different regulatory mechanisms

The similarities in the processes of lateral root (LR) formation and IC initiation (see above) leads us to consider the possibility of common regulatory mechanisms for both processes. The gene *ABERRANT LATERAL ROOT FORMATION 4* (*ALF4*) plays a key role in creating the cellular plasticity that is necessary for LR development (DiDonato et al., 2004). The first division that gives rise to the lateral root primordium is already impaired in this mutant and it displays severe growth alterations (Figure 19-A), probably due to the severely reduced root system that does not generate lateral roots (Celenza et al., 1995; DiDonato et al., 2004). To see whether IC formation is controlled by the same mechanism, I checked the capacity of the *alf4* mutant to establish the IC. *alf4* and wild type plants were grown on soil and five stems of each were collected (when wild type controls were 20 cm tall) and analyzed histologically. The diameter of mutant stems (Figure 19-B) was much smaller than that of wild type stems (Figure 19-C), however there was no alteration in the general pattern of the stem tissues. The *alf4* plants displayed files of cells in the interfascicular regions, indicating IC formation. Such files of cells were smaller in the mutant (Figure 19-B, arrows) than in wild type plants. Thus, despite its severe overall growth alterations, *alf4* retains the capacity for IC formation; this points towards distinct mechanisms controlling lateral root and IC formation.

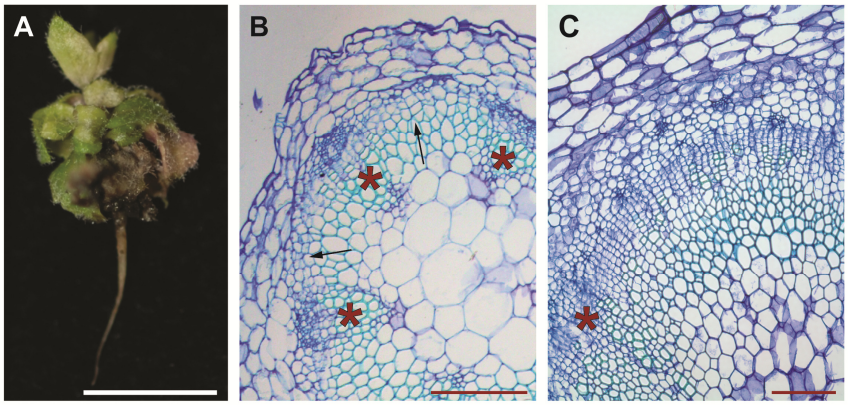

Figure 19: Secondary growth in *alf-4* mutants. Despite its severe growth alterations due to the absence of lateral roots (A), *alf4* mutants retain the capacity to initiate secondary growth in interfascicular regions (arrows) (B) in a similar manner as in wild type (C). Arrows: files of cells produced during SG. Asterisks: vascular bundles.

4 - Results part two:

A method for isolating tissue-specific transcriptomes in the *Arabidopsis* stem

The transcriptome is the complete set of transcripts in a cell and determines its particular function (Wang et al., 2009). Elucidating the specific transcriptomes of the different cell types of an organ yields essential information that can be the foundation for knowing the genes behind a specific cell identity or for deciphering the gene networks controlling cell fate. In plants, various tissue-specific transcriptomes have been described, in which respect the root is the best characterized organ (Brady et al., 2007). On the other hand, despite the importance of the aerial axis as a central part of the plant and its essential role in development, ecology, and economy, very few approaches targeting tissue-specific transcriptomes in the stem have been followed. Tissue-specific analyses include those targeting the epidermis, the cambium and its derived tissues, and the IC (Agusti et al., 2011b; Schrader et al., 2004; Suh et al., 2005). In this part of the project, I developed a technical pipeline for isolating individual stem tissues to elucidate their transcriptional profiles. The development of this pipeline to produce such information will open a wide range of opportunities for a deeper analysis of all the processes taking place in the plant stem.

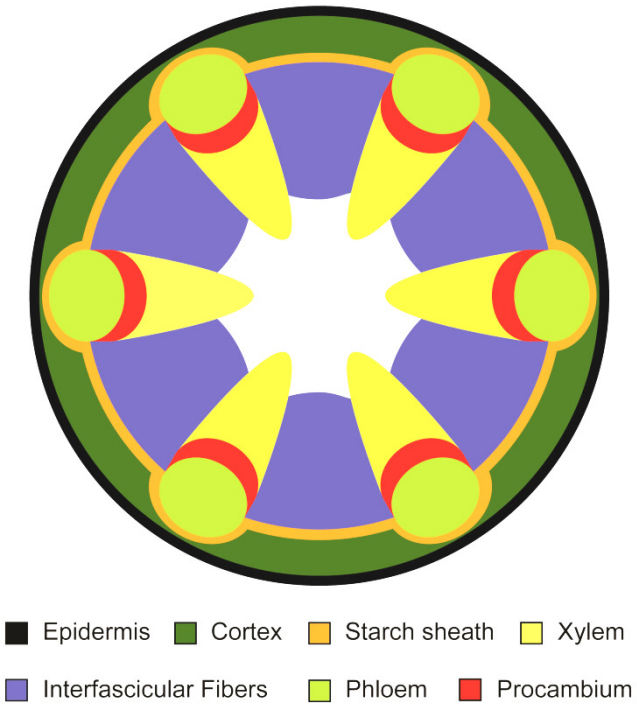

Figure 20: Tissues of the primary stem. Schematic representation of a cross section of the primary stem with the major tissues indicated with a color-code.

The extensive presence of secondary cell walls makes the isolation of protoplasts, as previously done for the root (Birnbaum et al., 2003), rather difficult. I therefore selected fluorescence activated nuclei sorting (FANS) as a method to gain access to specific tissues. The experimental design was based on the production of transgenic lines in which a tissue-specific promoter drove the expression of the green fluorescent protein (GFP) fused to the histone 4 (H4-GFP). This approach resulted in the presence of GFP in the nuclei of a specific stem tissue. Nuclei were extracted and sorted into GFP+ (nuclei in which GFP was present) and GFP- (nuclei in which GFP was absent) populations, which is to say, nuclei derived from a specific tissue were separated from nuclei from the remaining stem tissues. I validated my methodological pipeline by characterizing the transcriptional profile of the phloem. From a line expressing the H4-GFP protein specifically in the phloem tissue, the different populations were collected, and polyA RNA was extracted, amplified, and sequenced. The reads obtained from the sequencing were mapped to the Arabidopsis genome and the comparison between the GFP+ and GFP- samples provided lists of genes specifically active in the phloem. The developed tools now allow the generation of a global expression map of all stem tissues.

4.1 Validation of tissue-specific promoters

The use of FANS for isolating tissue-specific material from the stem strongly depended on the tissue-specific H4-GFP expression. For driving the expression of the marker in each one of the tissues of the stem it was thus crucial to identify promoters that are active exclusively in those areas (Figure 20). To this end, a number of candidate genes for tissue-specificity were selected from the literature. Between 2-3 kb upstream of the start codon and around 500 bp downstream of the stop codon of the respective genes were selected as the promoter regions. To confirm the specificity of the selected promoters, stably transformed marker lines in which the promoter drove a fluorescent protein were produced (Figure 21; Table 4). To have the fluorescent protein widely distributed throughout the cells and to avoid its diffusion, it was targeted to the endoplasmic reticulum (ER) by adding the appropriate target sequences (Boevink et al., 1998). The transcriptional marker lines were grown on soil to a height of 20 cm and hand sections from the second internode (counting from the base) were analyzed. The second internode displays a primary stem conformation and was the plant material later used for the sorting approach. The internode sections were stained by propidium iodide to identify structures producing autofluorescence and analyzed under the confocal microscope.

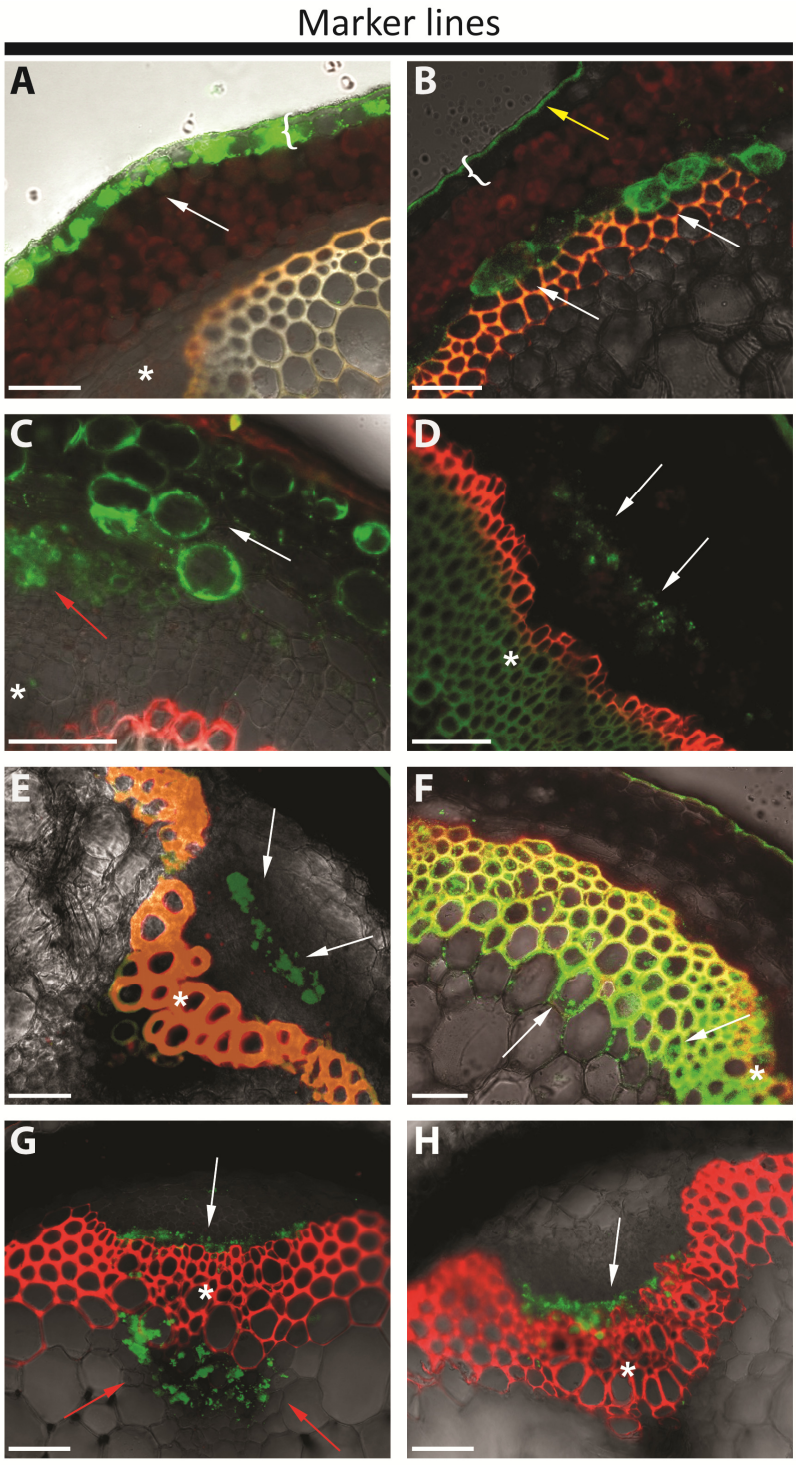

Figure 21: Tissue-specific promoter activity in the stem. Analysis of the transcriptional marker lines A) *LTP1:YFP*, B) *SCR:YFP*, C) *KNAT1:CFP*, D) *XIP1:CFP*, E) *APL:CFP*, F) *NST3:CFP*, G)*WOX4:YFP*, and H) *PXY:YFP*. Green color: YFP or CFP. Red color: propidium iodide. Size bars: 50 µm. White arrows: sites of expected expression. Red arrows in C and G: promoter activity in nonexpected regions. Yellow arrow in B: cuticle autofluorescence. Asterisks: vascular bundles. Brackets in A and B: comparison of cuticle autofluorescence and epidermis fluorescence.

The gene *LIPID TRANSFER PROTEIN 1* (*LTP1*) had been described as being specifically active in the epidermis of aerial plant parts (Benjamins et al., 2001; Thoma et al., 1994). The LTP1 promoter activity was tested using the transcriptional marker line *LTP1:YFP* (Figure 21-A). As expected, the YFP signal was restricted to the epidermis cells (arrow). It was important here to avoid confusion with the signal emitted by the cuticle, an extracellular protective matrix of the epidermis (Nawrath, 2006) composed, among others, of different fatty acids derivatives and cuticular waxes (Suh et al., 2005). The cuticle auto-fluoresced in a wide range of wavelengths, but was not stained by propidium iodide. However, it could easily be distinguished morphologically from the epidermis by its characteristic position and shape. (Figure 21-A, B, yellow arrow, brackets). The activity of the marker *LTP1:YFP* indicated that the selected promoter is ideal for targeting epidermis cells.

The *SCARECROW* (*SCR*) gene is essential for establishing starch sheath identity (Fukaki et al., 1998) and its expression in the primary stem had been reported as being specific for the starch sheath (Sehr, 2010; Wysocka-Diller et al., 2000). *SCR* promoter activity was analyzed using the transcriptional marker *SCR*:*YFP* (Figure 21-B, see above). Indeed, analysis of the YFP signal indicated that the *SCR* promoter activity in the primary stem is restricted to starch sheath cells (Figure 21-B, white arrows), rendering the *SCR* promoter the promoter of choice for targeting this tissue type.

The *KNOTTED*-like homeobox gene *KNAT1* was described before as being specifically active in the cortex (Douglas et al., 2002). Here the activity of the *KNAT1* promoter was investigated using the transcriptional marker *KNAT1*:*CFP*. However, the distribution of the CFP-derived signal (Figure 21-C) indicated that the selected promoter was active not only in the cortex (white arrow) but also in other tissues (red arrow). The activity indicated by the transcriptional marker suggested against using this promoter for accessing tissue-specific material from the cortex and underlined the importance of validating the promoter activity domains before using them in the FANS approach.

The activity of the leucine-rich repeat receptor-like kinase *XYLEM INTERMIXED WITH PHLOEM1* (*XIP1*) had been previously described as being vascular specific (Bryan et al., 2012); consequently, the *XIP1* promoter was one of my candidates for driving cambium-specific expression. I checked the activity domain of the promoter using the marker line *XIP1:CFP* (Figure 21-D). The fluorescence was restricted to the vascular bundles between the cortex and the lignified cells of the xylem, the region that corresponds to the phloem (white arrows). The observed

fluorescence derived from the marker *XIP1:CFP* indicates that this promoter would be a good marker for the phloem but not for the cambium.

The gene *ALTERED PHLOEM DEVELOPMENT* (*APL*) had been described as being specifically active in phloem tissue (Bonke et al., 2003; Ollram, 2011). Here, by checking the activity of the *APL:CFP* transcriptional marker, the phloem-specificity of the chosen promoter fragment was confirmed (Figure 21-E, white arrows) for the primary stem. This observation indicates that the *APL* promoter is a good choice for targeting the phloem.

The transcription factor *NAC SECONDARY WALL THICKENING PROMOTING FACTOR 3* (*NST3*) is involved in secondary cell wall formation and, in the stem, it is specifically active in cells with secondary cell walls (interfascicular fibers and secondary xylem) (Mitsuda et al., 2007). I therefore tested the activity of the *NST3:CFP* marker (Figure 21-F) for its fiber/xylem specificity. As expected, the CFP-derived signal was restricted to tissues with secondary walls (arrows), indicating that the *NST3* promoter is indeed valid for targeting these tissues.

The transcription factor *WUSCHEL-RELATED HOMEOBOX4* (*WOX4*) had been described as being cambium-specific (Hirakawa et al., 2010; Suer et al., 2011). Consequently, the transcriptional marker *WOX4:YFP* was analyzed (Figure 21-G). The YFP-derived signal was observed in the cambium area (white arrow), but expression in non-cambium areas was also observed (Figure 21-G, red arrows, see above). The non-specific activity of the chosen promoter observed here and in the previous chapter indicated that it is not an optimal choice for the FANS approach.

The leucine-rich receptor-like kinase *PHLOEM INTERMIXED WITH XYLEM* (*PXY*) plays a key role in controlling cambium activity and was described to be specifically active in the cambium (Fisher and Turner, 2007). Here I investigated its promoter activity, employing the transcriptional marker *PXY:YFP* (Figure 21-H). As expected, the YFP-derived signal was restricted to the cambium area (Figure 21-H, white arrow), indicating that it is a suitable tool for accessing cambium-specific nuclei.

In summary, the marker line analysis showed the importance of validating the activity domains of the selected promoters, because in some cases they showed non-expected activity domains, which reduces their potential for the subsequent transcriptional analysis. The study of the markers indicated that a cortex-specific promoter is still missing, but other promoters were validated such

as those for the epidermis (*LTP1*), the fibers (*NST3*), and the starch sheath (*SCR*) (Table 4). Among the candidates for cambium-specificity, the *PXY* promoter was chosen because it showed a specific cambium activity in contrast to the WOX4 and XIP1 promoters. Among the phloem-specific promoters, *APL* was selected because its specificity is well documented by other studies (Bonke et al., 2003; Ollram, 2011).

4.2 A collection of plant lines with nuclei labeled in a tissue-specific manner

The promoters that displayed tissue-specificity were used for producing DNA vectors in which they drove the expression of the H4-GFP protein. These vectors were used for transforming wild type Arabidopsis plants, thereby generating a collection of transgenic plants expressing H4-GFP specifically in different stem tissues. In addition, a *35S:H4-GFP* line was established. The 35S promoter is active in all the tissues (Odell et al., 1985) and it was used as a control for defining the sorting gates (Table 4).

Tissue	Promoter	Specific	Selected for *H4:GFP* line
Epidermis	*LTP1*	✓	✓
Cortex	*KNAT1*	×	×
Starch sheath	*SCR*	✓	✓
Phloem	*XIP1*	✓	×
	APL	✓	✓
Cambium	*WOX4*	×	✓
	PXY	✓	✓
Xylem fibers	*NST3*	✓	✓
Interfascicular fibers			
All	*35S*	N/A	✓

Table 4: Collection of studied promoters. ×: no; ✓: yes

4.3 A method for extracting nuclei from the stem

Depending on their composition, plant cell walls can be recalcitrant to enzymatic digestion. This is specially true for tissues with secondary walls or woody parts (Galbraith, 2007). However, the use of gentle chopping procedures has been demonstrated to be a feasible method for releasing plant nuclei (Galbraith et al., 1983). Here we isolated nuclei following a chopping procedure indicated in the methods section (Chapter 2.2.12, page 27), which is a modification for the *Arabidopsis* stem

of a previously described protocol (Galbraith et al., 1983). To reduce the developmental variability in the primary stem material, only second internodes were taken as starting material. The stem internodes were put on ice immediately after harvesting, and kept on ice or at 4°C during the entire extraction process. Keeping the plant material at low temperatures stops, or at least reduces, transcriptional activity and transcripts levels should thereby change only slightly during the process. The chopping procedure was standardized for 2 g of plant material, which in all cases produced at least 50,000 GFP+ nuclei that were used for RNA extraction. Chopping time was set to 10 minutes since this period generated sufficient nuclei in a reasonable time. The filtering step (50 µm pore size) after chopping (see methods, chapter 2.2.12) is crucial for removing large pieces of debris. The extra filtering steps added just before the sorting procedure to eliminate particle aggregates prevents blocking the flow, which can reduce the sorter performance. In addition, protection from light, especially after DAPI staining, is an important step to avoid strange behavior of the sorted particle population, probably due to DAPI degradation (data not shown). In sum, the procedure presented here for nucleus isolation is adapted to the particularities of the plant stem and resulted in good performance of the analyzed material.

4.4 Establishing sorting parameters

The accuracy of the description of the tissue-specific transcriptomes relies on a correct separation of the nucleus populations from other particles derived from the chopped plant material. In addition, avoiding cross contamination of the GFP+ and the GFP- nucleus fractions is crucial for the accuracy and sensitivity of the subsequent transcriptome analyses. To achieve those goals it is crucial to establish the proper selection criteria in the cell sorter. To distinguish between nuclei and pieces of debris derived from plant structures, the samples were DAPI (4',6-diamidino-2-phenylindole) stained. DAPI is a fluorescent dye that binds DNA, thereby allowing discrimination between nuclei and other particles in the flow cytometer; in addition, it allows the quantification of DNA content present in the nuclei (Coleman et al., 1981; Sgorbati et al., 1986) selected according to the GFP and DAPI derived signals. The GFP presence provided information about the origin of the nuclei and the DAPI fluorescence allowed discrimination between nuclei and debris particles. The GFP and DAPI intensity for each event were plotted in graphs (Figure 22), which were used for drawing the sorting gates. Appropriate sorting gates were determined by selecting zones of the diagram containing the events of interest to be separated. Once the gate is established, the sorter will collect the events plotted in that zone of the chart into a tube. The sorting gates were established using positive and negative controls, that is, populations in which all the nuclei were

GFP negative (obtained from wild type plants) or GFP positive (obtained from 35S:H4-GFP transgenic plants). Events derived from both controls were plotted (Figure 22-A, C)

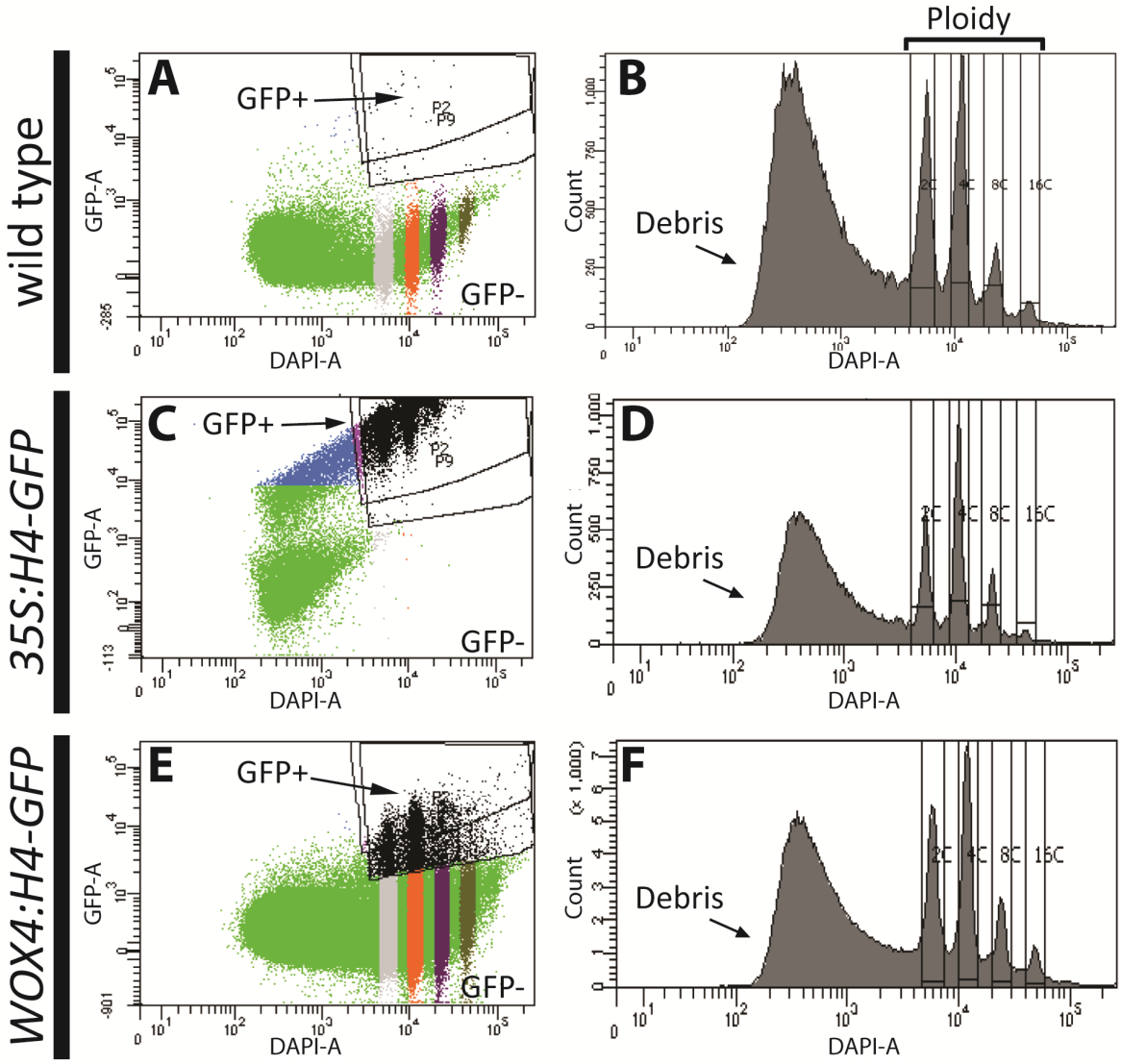

Figure 22: Establishment of sorting gates. Left column panels (A, C, E) plot of GFP versus DAPI intensity for each particle. Right column panels (B, D, F) plot of the number of particles versus DAPI intensity. The analysis of nuclei from the GFP negative control (wild type (arrow), A, B) and a GFP positive control (*35S:H4-GFP*, C (arrow), D) allowed the establishment of gates for isolating nuclei from a specific tissue (E (arrow), F). The separation was based on the ploidy level (B, D, F) that can be extrapolated from the level of the DAPI-derived signal and on the presence of GFP-derived fluorescence (A, C, E). The DAPI signal allowed discriminating between nuclei (highlighted according to ploidy levels in grey, orange, violet, and olive in E) and debris. The GFP signal allowed discriminating between nuclei containing GFP and nuclei that did not contain GFP. Wild type plants were used as negative control. *35S:H4-GFP* transgenic plants were used as positive control. *WOX4:H4-GFP* transgenic plants were used as an example for plants containing GFP in a fraction of the nuclei only.

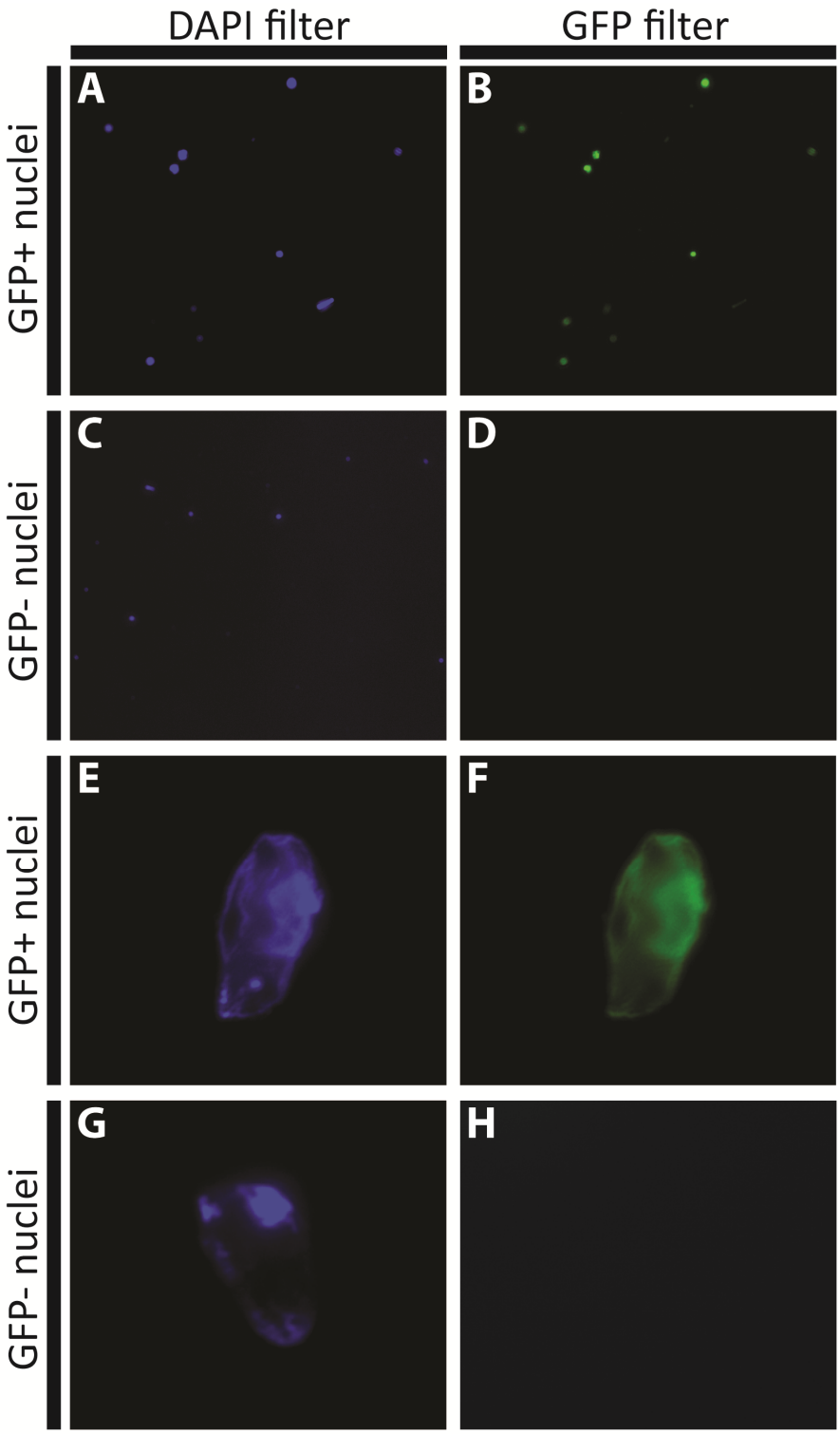

Figure 23: Validation of sorting. The sorted samples were analyzed under the microscope to validate successful separation. The DAPI filter (blue, A, C, E, G) indicates the presence of nuclei in both GFP+ and GFP- fraction. GFP filter (green, B, D, F, H) indicates the presence of GFP-containing nuclei only in the GFP+ fraction. A global view of the sample (A, B, C, D) and a detailed view of one individual nucleus (E, F, G, H) is presented.

The nuclei were separated using a FACSAriaIII cell sorter, which detects particles (events) and is able to separate them according to their fluorescence properties. In this study the particles were and gates for GFP positive nuclei were drawn according to the non-overlapping zones between both controls. To discriminate between nuclei and debris, gates were established in the histograms in which DAPI signal intensity versus the number of events were plotted (Figure 22-B, D, F). The debris is distributed among all DAPI intensities. However, nuclei contain a specific amount of DNA according to their ploidy level, which is reflected by prominent peaks in the graph. The areas where those peaks are present were selected as sorting gates, allowing discrimination between nuclei and debris. The events that were allocated to the set gates were collected into a tube. An example of a plant line expressing GFP in some nuclei only is WOX4:H4-GFP (Figure 22-E, F).

The specificity of the selected sorting gates was confirmed by analyzing the GFP+ and GFP- fractions under the fluorescence microscope using DAPI and GFP filters (Figure 23). Both the GFP+ and GFP- fractions from nuclei extracted from internodes of WOX4:H4-GFP transgenic plants were analyzed. Analysis using the DAPI filter showed that nuclei are present in both samples (Figure 23-A, C, E, G). Analysis using the GFP filter showed all nuclei containing GFP in the positive fraction (Figure 23-B, F), and an absence of false negatives in the negative fraction (Figure 23-D, H). This observation confirmed that the selected gates (Figure 22) were appropriate for separating nuclei fractions.

4.5 Nuclei from different tissues show different ploidy distribution

The nuclear DNA content in a cell is the result of the coordination between DNA replication and cell division (Kondorosi et al., 2000). The number of sets of chromosomes in a cell (ploidy) varies among organisms and, within an organism, between different cell types. The ploidy level can offer information about the developmental state of a cell and has been related with different developmental processes (Li et al., 2012; Rewers and Sliwinska, 2012). Knowing the ploidy level in different tissues of the stem can provide information about the developmental state of such tissues. To see whether the ploidy level varies among the different tissues of the stem, the ploidy levels were determined in the phloem, fibers, and cambium using the transgenic lines APL:H4-GFP (phloem), NST3:H4-GFP (fibers and secondary xylem), and WOX4:H4-GFP (cambium) as examples of meristematic and differentiated cell types in the stem. Second internodes from 20 cm tall plants were used for nucleus sorting. DAPI staining allowed visualization and determination of the ploidy level distribution. The percentages of the different ploidy levels were calculated according to the number of events present in each fraction in relation to the total number of events.

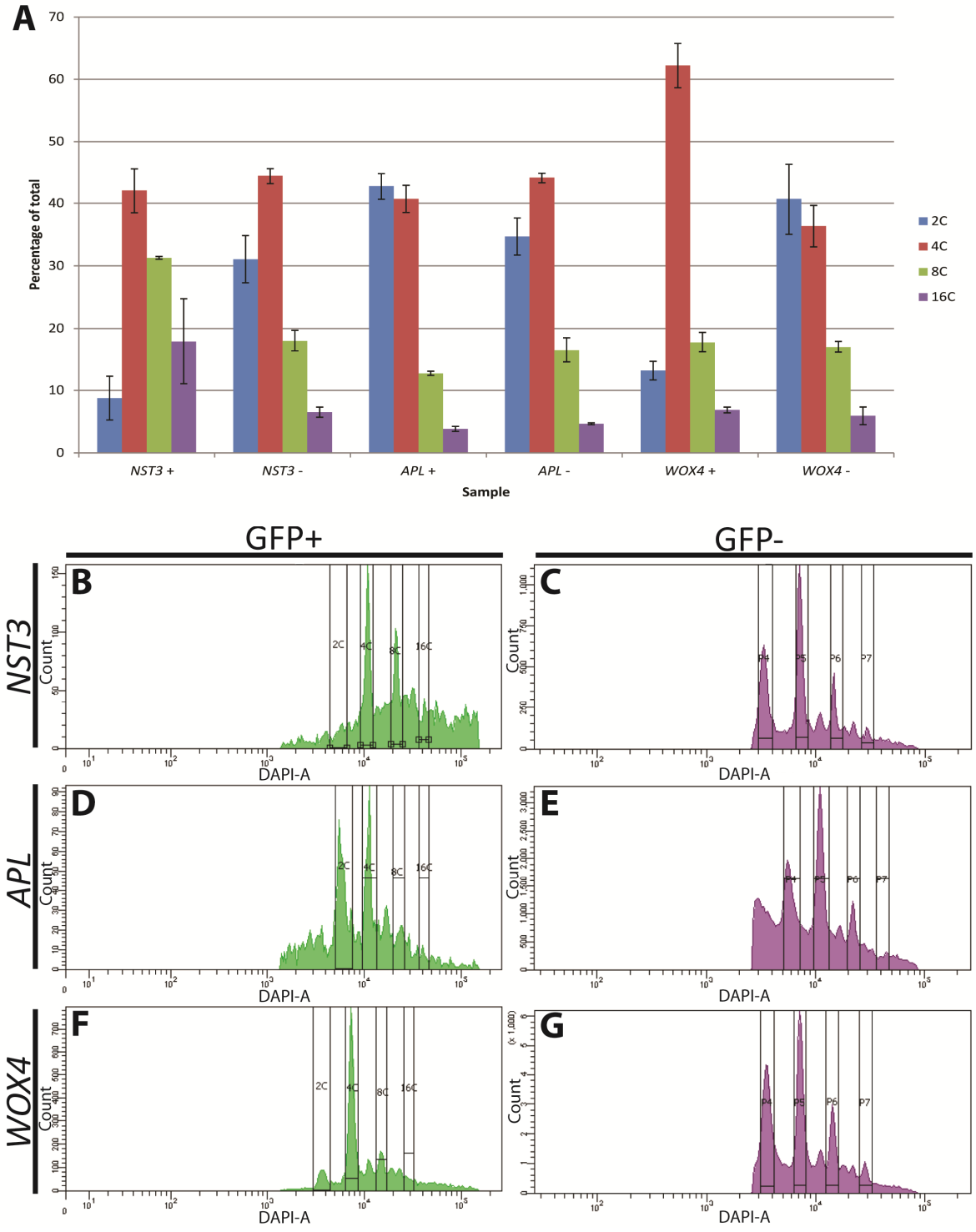

Figure 24: Different tissues show specific ploidy profiles. The quantification of the ploidy ratios (A) from different tissues indicates the presence of distinct ploidy profiles. The nuclei from NST3-expressing cells (B), APL-expressing cells (D), and WOX4-expressing cells (F) present different distributions of ploidy levels among them and in comparison with the stem average (C, E, G).

Interestingly, differences were detected in the ploidy level distribution between different tissues (Figure 24-A). The GFP-negative fraction of the samples (NST3-, APL-, and WOX4-) should represent the average ploidy levels in the second internode because they contain all the tissues except the sorted one. Indeed, relations between the different ploidy levels in the negative fractions were very similar. In the three cases most of the nuclei (between 75% and 79 %) were found to be in the 2C and 4C fractions. The rest of the nuclei were distributed between the 8C (16% to 18%) and 16C (5% to 7%) populations. The 2C and 4C fractions were comparable in the NST3- and APL- samples (31% to 35% of 2C and 44% of 4C). However, there was a clear shift in the case of the WOX4- fraction (41% of 2C and 36% of 4C). This shift could be due to the strong overrepresentation of 4C nuclei in the WOX4+ population. In the tissue-specific nucleus populations (NST3+, APL+, and WOX4+), there were bigger differences in the ploidy levels. NST3+ nuclei (Figure 24-A) displayed a shift to higher ploidy levels. The 2C fraction was underrepresented (9%) in comparison to the average of the whole stem (GFP-negative fraction). The underrepresentation of 2C nuclei was compensated by a higher percentage of 8C and 16C nuclei that together represented 49% of the total number of nuclei. Since high ploidy levels have been positively correlated with cell size (Kondorosi et al., 2000), the observed ploidy levels in NST3+ nuclei (from xylem and interfascicular fibers) could be due to the large size of these cells. In the APL+ samples (from the phloem), the percentage of 2C nuclei was higher than in the average negative fraction and the other ploidy levels were partially reduced in comparison to the negative fraction. The WOX4+ population showed a profile in which most nuclei belonged to the 4C fraction (62%), to the detriment of the 2C population (13%) and without effect on the 8C and 16C populations, which remained at similar levels to the negative fraction.

In conclusion, the use of the transgenic lines expressing H4-GFP in the phloem, cambium, and xylem/fibers allowed the description of ploidy distributions in tissues of the stem representing different degrees of cell differentiation. Such analyses indicated that the ploidy levels are not the same in different tissues, and this information could reflect different developmental states in different tissue types.

4.6 Nuclear mRNA reflects the transcriptional state of the cell

mRNA follows pathways of maturation in the cell during its transition from the nucleus to the cytoplasm where it is translated. One concern that can arise from the use of nuclear mRNA for transcriptional profiling is to what extent this RNA reflects the general state of the translated cell transcriptome. To clarify this aspect, an experiment was performed in which mRNA from sorted

nuclei was compared to whole mRNA with both populations extracted from plant internodes. Second internodes from 20 cm tall wild type plants were used for nuclei sorting or direct RNA extraction. Nuclei were DAPI stained and 50,000 events collected using the flow cytometer. mRNA was extracted directly from the sorted nuclei using magnetic poly-T beads (Dynabedads).

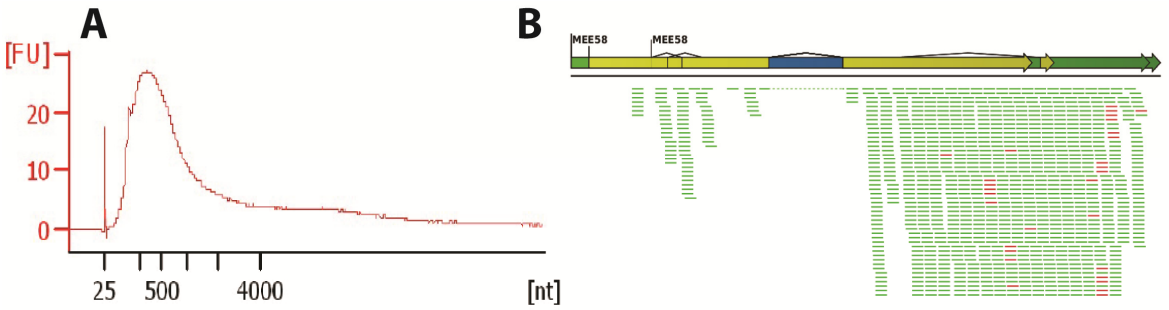

Figure 25: Effect of mRNA amplification. After two rounds of amplification there was a high number of small RNA molecules, around 500 nt in size (A). The read mapping indicated a 3´bias of the generated reads. Example of reads mapped to a gene (B).

The extraction of the poly A-RNA directly from sorted nuclei resulted in better results than the extraction of total RNA by TRIZOL or affinity columns (Qiagen). poly-T beads do not bind rRNA and therefore enzymatic steps for removing the rRNA are not necessary. The amount of mRNA extracted by the magnetic beads ranged from 0,3 – 1,3 nanograms. Therefore it was necessary to amplify the RNA in order to reach the 40 µg necessary for RNA sequencing. mRNA was amplified in two rounds of amplification using a commercial kit (Epicenter). As a first step, the RNA was primed by T7-oligo(dT) primers, so that only polyA RNA was amplified. As expected, the amplification does not always produce full length molecules of RNA. It gave rise to a higher abundance of RNA molecules of about 500 nt (Figure 25-A). Since the amplification started from the poly-A tail, generated fragments showed a bias towards the 3' end of the gene, as is evident from the distribution of mapped reads (Figure 25-B). As a typical result of the amplification process, this bias was expected; however, since it is the same for all genes and samples, it should not affect the final relative comparison of reads. The mRNA from two biological replicates for each sample was sequenced by BGI (Hong Kong), as indicated in the methods section.

The reads were mapped by Branislav Kusenda (GMI) to the *Arabidopsis* reference genome, no mismatches were allowed, and only reads with unique matches were considered. In all samples the majority of the reads mapped to exons (Figure 26). However, a small fraction mapped to introns or intron-exon junctions (total intron reads). The percentage of exon reads was 96.55% in the RNA

from DAPI-sorted nuclei (Figure 26-A) and 98.27% in the RNA from whole cells (Figure 26-B). The difference probably reflected different levels of maturity between the nuclear and cytoplasmic mRNA. This difference cannot be due to random variability because the phloem samples (see below) show a similar read distribution to the DAPI samples. Overall, the differences in the percentages of reads mapped to introns should not affect the global analysis of the reads since they represent only a small fraction of the total number of reads. In addition, the low number of intron reads in nuclear and whole organ preparations indicates that the degree of mRNA maturity is comparable.

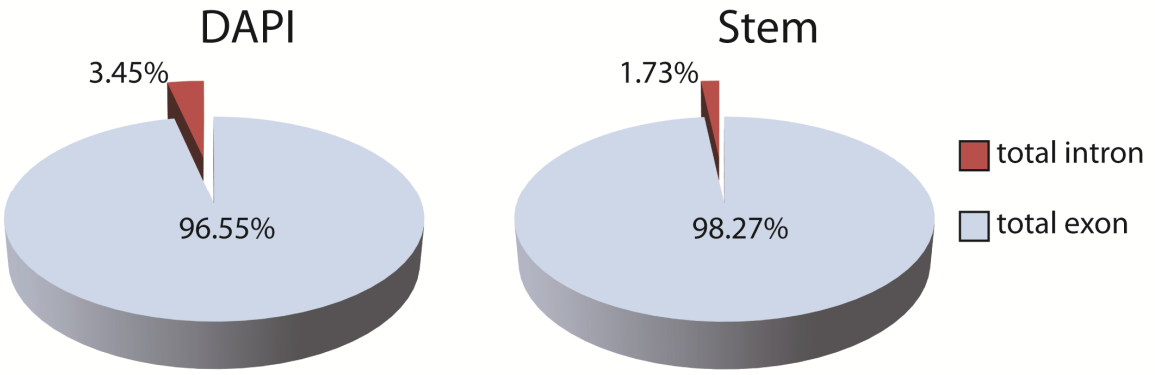

Figure 26: Read-distribution in the genome. Reads produced from mRNA-seq analyses of DAPI sorted samples and the whole stem were mapped to the genome. Most reads mapped to exons. The percentage of reads that mapped to introns is higher in the nuclear mRNA, indicating a slightly lower level of maturity. However, more than 96% of reads mapped to exons in both cases.

Expression values for individual genes were normalized by establishing the RPKM value (Reads per Kilobase of exon per Million mapped reads), which considers the length of the different genes and the total read number for the individual samples (Mortazavi et al., 2008). The correlation between the different samples was investigated by determining Pearson´s coefficient (Table 5). It revealed a similar correlation between DAPI replicates and DAPI – STEM samples. The high correlation between the two STEM samples could be due to the reduced number of steps in the sample processing, which does not include the procedure of nucleus sorting that might introduce variability in other samples.

In sum, the comparison of mRNA from nuclei and from whole cells showed that reads mapped to exons with similar percentages in both cases. Apart from the two stem samples whose correlation is much higher, the correlations between DAPI and STEM samples remain in similar ranges.

	DAPI1	STEM1	DAPI2	STEM2
DAPI1	1	0.64	0.67	0.64
STEM1		1	0.56	0.96
DAPI2			1	0.62
STEM2				1

Table 5: Pearson's coefficient comparing the different samples.

4.7 A case study: Elucidation of the phloem transcriptome from the primary stem

The aim of this project section was to establish a technique allowing the characterization of tissue-specific transcriptomes of the stem. The transcriptome of the stem phloem was characterized in a case study because it represents an internal stem tissue surrounded by other tissues with secondary cell walls and because it is connected to the cambium. In addition, the transcriptome of the phloem had been analyzed in the root (Brady et al., 2007; Zhang et al., 2008). The comparison of both transcriptomes can show the parallelism in the expression profile of this tissue in the two organs.

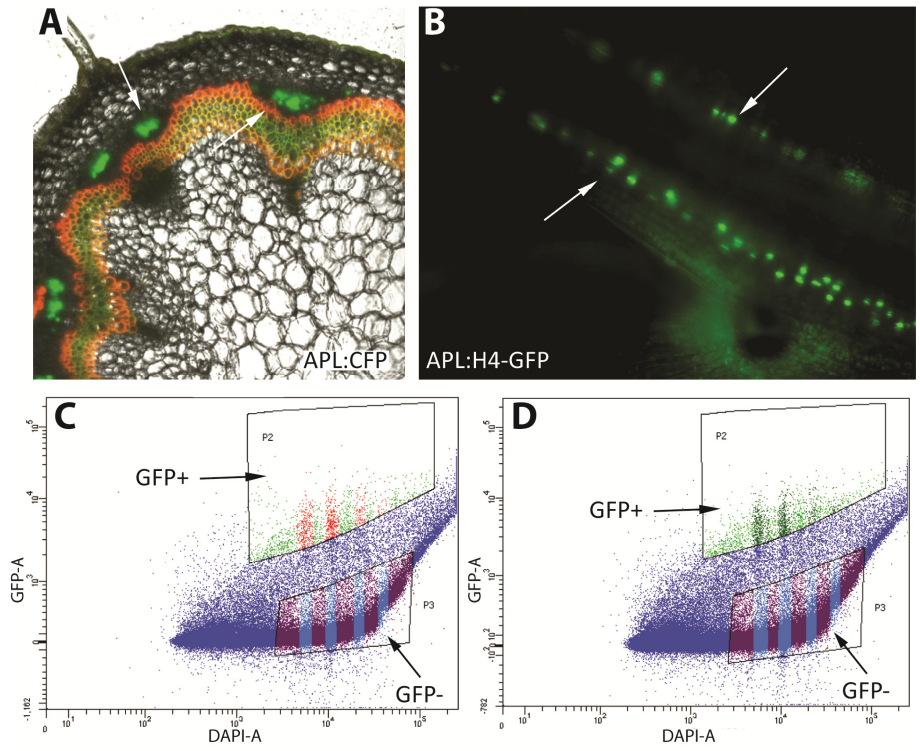

Figure 27: Phloem nucleus sorting. The sorting of nuclei from the phloem was based on the *APL* promoter, which is specifically active in the phloem, as can be seen in a cross section of the stem from the *APL:CFP* line (A, green). That specificity allowed producing an *APL:H4-GFP* whose GFP-labeled phloem nuclei were visualized in the hypocotyl (B). Transgenic plants containing *APL:H4-GFP* allowed the separation of nuclei based on GFP activity. Graph of the event distribution in two biological replicates (C, D) according to their fluorescence properties.

APL is a MYB-type transcription factor that is essential for establishing phloem identity. The *APL* promoter is specifically active in phloem cells (Bonke et al., 2003; Ollram, 2011) (Figure 21-E, Figure 27-A). For this reason, the *APL* promoter was used to drive the expression of *H4-GFP* in the phloem. A transgenic line containing the *APL:H4-GFP* transgene (Figure 27-B) was used for phloem nucleus isolation. To isolate the phloem nuclei of the primary stem in a comparable developmental stage, only second internodes from 20 cm tall transgenic plants were used for the analysis. The internodes (2 g) were collected in petri dishes on ice and nucleus extraction was performed as previously indicated. 50,000 GFP+ and GFP- particles were collected in microcentrifuge tubes. Two biological replicates were produced (Figure 27-C, D). mRNA was extracted and amplified as previously indicated.

4.7.1 Sequencing RNA from the phloem

The mRNA from the 4 samples (2x phloem and 2x non-phloem) was analyzed by sequencing as previously indicated. At least 20 million 50 bp single end reads were produced for each sample and mapped to the *Arabidopsis* genome, no mismatches were allowed, and only reads with unique matches were considered (Table 6). More than 50 million reads were mapped to the *Arabidopsis* reference genome, 21 million for both GFP+ samples (phloem) and 29 million for both GFP- samples (non-phloem tissues) (Table 6). Most reads mapped to exons or exon-exon junctions (Figure 28) and the fractions of intron reads were always below 5%. The percentage of reads mapping to introns was similar to that observed in the DAPI sorted nuclei (compare Figure 26 and Figure 28).

	APL1+	APL1-	APL2+	APL2-
Mapped	13,524,041	16,885,225	77,153,13	12,087,378
non-mapped	9,780,511	5,892,318	17,306,653	11,980,817
Total	23,304,552	22,777,543	25,0219,66	24,068,195

Table 6: Mapped reads. Number of produced and mapped reads for the phloem and non-phloem RNA.

To test reproducibility of the results, expression values were normalized by calculating RPKM values and each sample was compared with its replicate (Figure 29). Pearson´s coefficient was 0.89 comparing the two GFP+ samples and 0.81 for the two GFP- samples. This indicated that despite the extensive sample processing, which included internode harvesting, nucleus extraction, nucleus sorting, and RNA extraction, amplification, and sequencing, the results are in large reproducible in independent biological replicates.

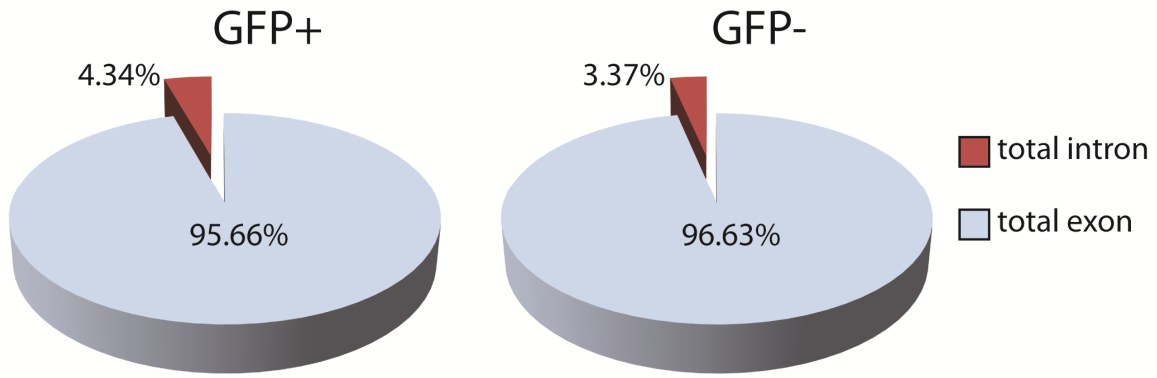

Figure 28: Read analysis. The reads produced from GFP+ (phloem) (A) and GFP- (rest of tissues) (B) samples were mapped to the *Arabidopsis* genome. Most reads (>95%) mapped to exons or exon-exon junctions. The rest mapped to introns.

4.7.2 Reads from APL and GFP are present in the phloem samples

To confirm a correct separation of the samples the distribution of reads mapping to the GFP and APL genes was checked in the produced datasets. The *APL:H4-GFP* transgenic line used for the sorting should express GFP only in cells where the *APL* promoter is active. The number of GFP-specific reads was, as expected, much higher in the phloem samples than in non-phloem samples (Figure 30). *APL*-specific reads showed a similar profile. Overall, an 8 to 10-fold enrichment comparing phloem and non-phloem samples was achieved. There were some reads of both transcripts in the GFP negative fraction (non-phloem tissues), indicating some cross-contamination or basal expression in that fraction (Figure 30). However, in total, the differences between samples indicated a successful separation of phloem and non-phloem samples.

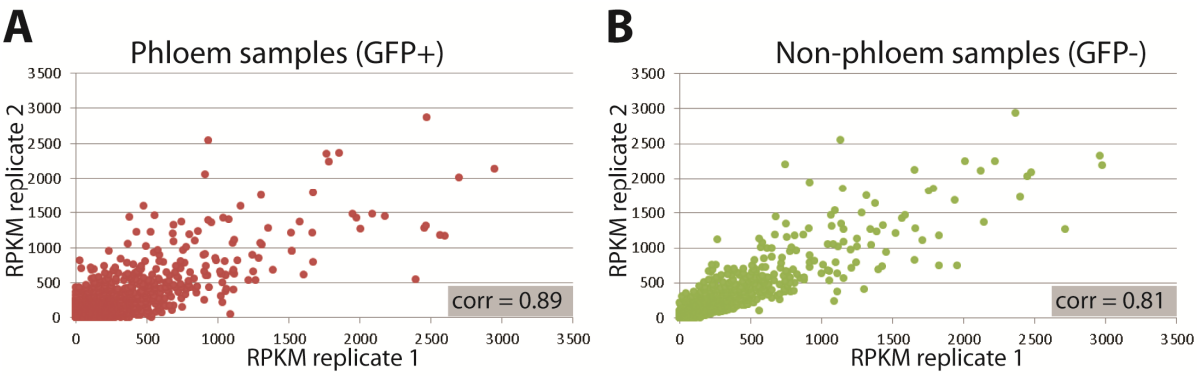

Figure 29: Correlation between replicates. Correlation between the two replicates of phloem transcriptomes (A) and the non-phloem transcriptomes (B).

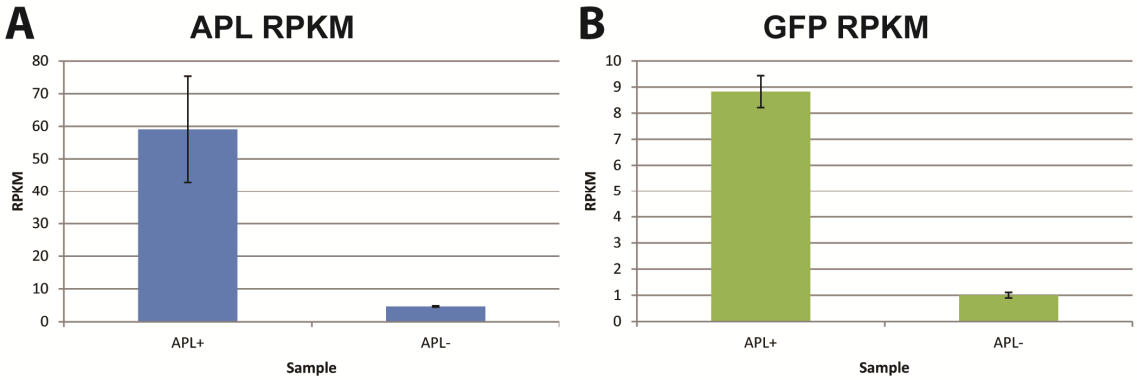

Figure 30: Distribution of APL and GFP-specific reads. APL and GFP-specific reads were predominantly detected in the phloem samples (APL+). A low number of reads was detected in the remaining tissues (APL-). Average values found in the two replicates are shown.

4.7.3 Statistical analysis of the datasets reveals a list of phloem-specific genes

To identify genes that are predominantly active in the phloem the values derived from the phloem samples of all genes in the genome were compared statistically with the values obtained for the rest of the tissues (GFP negative fraction). Genes for which no expression in the phloem samples was detected were excluded from the analysis. The values were analyzed statistically using the DESeq package for R (Anders and Huber, 2010), which is specifically designed for the analysis of RNA sequencing data. The analysis is based on tests for the negative binomial distribution, which is appropriate for the use of biological replicates. The Benjamini-Hochberg procedure was applied to adjust the p-values according to the false discovery rate (FDR). The analysis resulted into 69 genes that showed a significant (adjusted p-value < 0.05) enrichment in the phloem samples (Figure 31; Table 7, first 69 genes). Genes described to be predominantly active in the root phloem (Brady et al., 2007) are present in that group; however, the absence of *APL* in that group of genes indicated that the applied statistical analysis can produce false negatives. According to the expression behavior of *APL* (Figure 30) and the available information about its phloem specificity, the *APL* values were taken as a threshold for selecting a list of phloem genes. To the list described above genes with p-values lower than the *APL* p-value were added, resulting in a list of 132 genes (Table 7) that I considered as being predominantly active in the stem phloem. This list was compared with the phloem specific genes from the root described in other studies (Brady et al., 2007; Zhang et al., 2008) (Figure 32). Around one third of the generated list overlapped with the lists from the other studies, indicating the capacity of the established pipeline to identify phloem-specific genes.

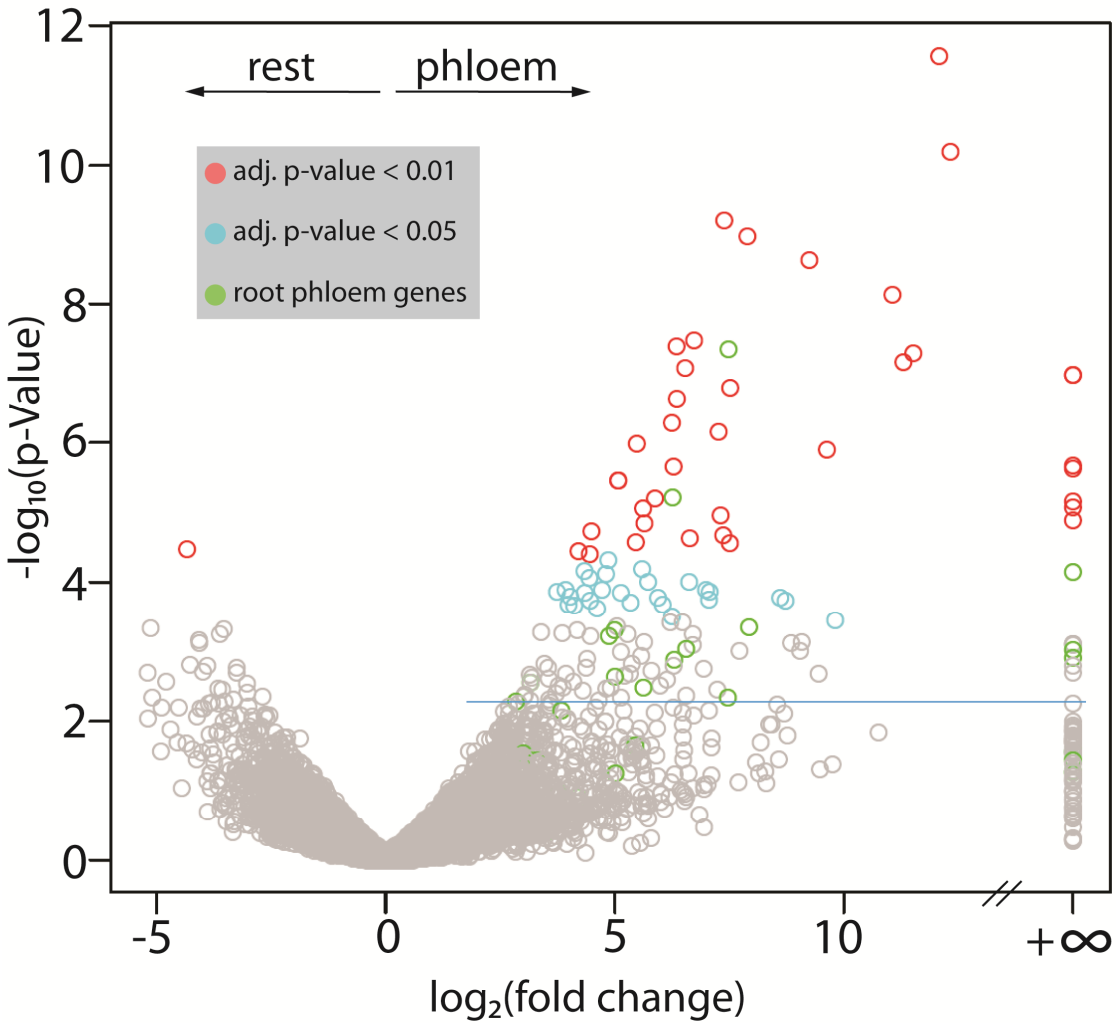

Figure 31: Global analysis of phloem sequencing data. The reads from 4 sequenced samples (GFP+, GFP-. 2 replicates) were analyzed with the package DESeq. Genes with significant enrichment are colored in red (adjusted p-value < 0.01) and blue (adjusted p-value < 0.05). Genes described by genevestigator as being specific to the root phloem appear in green. The line of genes on the right represents the genes that are only present in the phloem fractions. Blue line: *APL* threshold.

To see how described genes from the root phloem are distributed in the produced dataset, the 50 most specific genes from the root phloem were selected using the genevestigator platform (www.genevestigator.com) and colored in green in the significance plot (Figure 31). The genes appear in the plot to be higher expressed in the phloem than in the other tissues. When they are present they never showed a higher expression in the non-phloem tissues. Despite the correct tendency, most of the 50 genes were not classified as being significant. This could be due to the differences between the biological materials analyzed in each case. In all cases it was phloem, but the origin of the material (root and stem), the developmental stage, growing conditions, and processing varied.

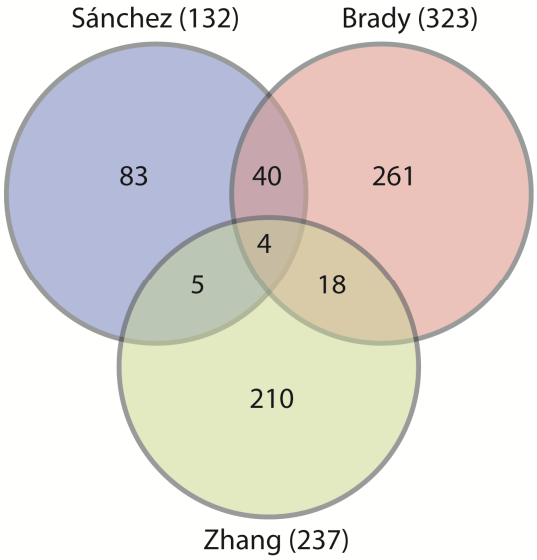

Figure 32: Overlap among phloem datasets. The phloem list of specific genes produced in this study (Sánchez) is compared with those produced in (Brady et al., 2007) and (Zhang et al., 2008).

In summary, the use of the established pipeline allowed the generation of a list of genes that are predominantly active in the stem phloem. This approach opens up the possibility to describe a complete set of tissue-specific transcriptomes of the *Arabidopsis* stem.

name_rank	foldChange	pval	padj	name
AT1G58007	4325.2021	2.64E-12	2.56E-08	NULL
AT5G45530	5137.9247	6.22E-11	3.02E-07	---
AT2G41300	167.74193	6.24E-10	2.02E-06	---
AT2G37950	238.60248	1.03E-09	2.51E-06	---
AT4G16015	607.25676	2.31E-09	0.0000045	NULL
AT5G39471	2137.9007	7.3E-09	0.0000118	NULL
AT5G40390	106.36816	3.3E-08	0.0000458	NULL
AT3G01670	81.451993	4.04E-08	0.000047	---
AT5G48690	179.26507	4.35E-08	0.000047	---
AT1G76220	2939.3076	5.03E-08	0.0000489	---
AT1G49930	2523.2962	6.8E-08	0.0000601	---
AT3G58720	92.987131	8.33E-08	0.0000674	NULL
AT1G79580	Inf	1.03E-07	0.0000713	SMB (SOMBRERO); transcription factor
AT4G20440	Inf	1.03E-07	0.0000713	smB (small nuc. ribonucleoprotein associated protein B)
AT5G14610	183.41711	1.58E-07	0.0001023	---
AT4G37180	81.882478	2.24E-07	0.0001363	---
AT1G14730	76.015418	5.13E-07	0.0002932	---

Table 7 (part one): Stem phloem genes. List of phloem specific genes in the primary stem of *Arabidopsis*, taking *APL* as threshold.

name_rank	foldChange	pval	padj	name
AT3G07800	154.46392	6.8E-07	0.0003674	---
AT3G03910	44.618312	1.01E-06	0.000515	GDH3 (GLUTAMATE DEHYDROGENASE 3)
AT5G22150	794.31614	1.26E-06	0.0006117	NULL
AT2G32870	Inf	2.08E-06	0.0009642	NULL
AT5G24920	78.012712	0.0000022	0.0009723	NULL
AT1G47603	Inf	0.0000023	0.0009729	NULL
AT4G24450	33.744765	3.45E-06	0.0013412	PWD (PHOSPHOGLUCAN, WATER DIKINASE)
AT5G26570	33.744765	3.45E-06	0.0013412	ATGWD3
AT3G07420	76.693891	6.02E-06	0.0022223	NS2; asparagine-tRNA ligase
AT5G11100	58.79184	6.17E-06	0.0022223	SYTD
AT1G75720	Inf	6.76E-06	0.0023458	---
AT3G57220	Inf	8.36E-06	0.0028034	---
AT4G37400	49.145198	8.65E-06	0.0028041	CYP81F3
AT1G13050	158.57403	0.000011	0.0034346	---
AT3G10840	Inf	0.0000126	0.0038416	---
AT1G31280	50.287362	0.0000141	0.004156	AGO2
AT1G67520	22.494011	0.0000181	0.0051669	NULL
AT3G25570	165.03374	0.0000206	0.0057296	NULL
AT1G34480	99.61768	0.0000227	0.0061269	---
AT5G01480	44.075576	0.000026	0.0068334	---
AT4G37540	182.85767	0.0000268	0.0068647	LBD39 (LOB DOMAIN-CONTAINING PROTEIN 39)
AT5G54660	18.533161	0.0000358	0.0087111	---
AT2G39850	21.940749	0.0000387	0.0091664	---
AT1G78320	29.119087	0.0000472	0.0109161	ATGSTU23
AT5G65280	48.544745	0.0000642	0.0145181	GCL1 (GCR2-LIKE 1)
AT3G20570	20.308277	0.000068	0.0150299	---
AT5G45320	Inf	0.000071	0.0153403	---
AT4G00900	28.035021	0.0000745	0.0157347	ECA2 (ER-TYPE CA2+-ATPASE 2)
AT5G02600	21.80891	0.0000868	0.0179572	---
AT5G55010	52.9115	0.0000965	0.0194856	---
AT4G25840	98.493025	0.0000982	0.0194856	GPP1 (glycerol-3-phosphatase 1)
AT4G10360	26.409023	0.0001273	0.024005	---
AT5G04690	127.50608	0.0001279	0.024005	NULL
AT4G00780	15.251237	0.0001284	0.024005	---
AT2G37925	134.47339	0.0001339	0.024373	NULL
AT1G12880	13.39845	0.0001376	0.024373	atnudt12
AT1G02630	20.345211	0.0001386	0.024373	NULL
AT4G27745	35.127575	0.0001404	0.024373	NULL
AT2G02020	16.329179	0.0001599	0.0270223	---
AT5G06850	61.48996	0.0001623	0.0270223	---
AT2G20515	391.26354	0.000164	0.0270223	---

Table 7 (continuation): Stem phloem genes. List of phloem specific genes in the primary stem of *Arabidopsis,* taking *APL* as threshold.

name_rank	foldChange	pval	padj	name
AT3G18670	133.51367	0.0001757	0.0284707	---
AT5G42010	424.92601	0.0001836	0.0289108	---
AT3G47090	22.088407	0.0001844	0.0289108	NULL
AT1G19270	40.567576	0.0001957	0.0301952	DA1
AT5G26940	66.204935	0.0002057	0.0311034	---
AT3G01680	15.909513	0.000208	0.0311034	---
AT2G16740	17.359631	0.0002142	0.0315514	UBC29 (ubiquitin-conjugating enzyme 29)
AT5G02260	24.567641	0.0002394	0.0347343	ATEXPA9 (ARABIDOPSIS THALIANA EXPANSIN A9)
AT3G55120	76.03273	0.0003093	0.0442169	TT5 (TRANSPARENT TESTA 5)
AT1G79480	900.67993	0.0003494	0.049225	NULL
AT5G61930	74.341669	0.000369	0.0512336	APO3 (ACCUMULATION OF PHOTOSYSTEM ONE 3)
AT1G75260	89.326133	0.000377	0.0516089	NULL
AT1G24575	33.061888	0.0004282	0.0578105	---
AT5G56720	244.13982	0.0004423	0.0588874	---
AT4G24250	31.89497	0.0004819	0.0615537	MLO13
AT1G68560	18.174992	0.0004876	0.0615537	XYL1 (ALPHA-XYLOSIDASE 1)
AT1G50600	10.495971	0.0005222	0.0650686	SCL5; transcription factor
AT1G10900	14.499547	0.0005368	0.066044	---
AT5G22870	104.43236	0.0005563	0.0665293	---
AT3G12890	38.803477	0.0005613	0.0665293	ASML2 (ACTIVATOR OF SPOMIN::LUC2)
AT1G29520	29.301556	0.0005921	0.0686359	---
AT5G04680	22.188021	0.0005932	0.0686359	NULL
AT3G13400	541.16293	0.0007274	0.0812524	sks13 (SKU5 Similar 13)
AT5G67460	49.941022	0.0007279	0.0812524	---
AT4G14830	461.66924	0.000744	0.0812524	NULL
AT3G21510	Inf	0.0007633	0.0824401	AHP1 (HISTIDINE-CONTAINING PHOSPHOTRANSMITTER 1)
AT4G05410	Inf	0.0007815	0.0831347	---
AT3G10310	Inf	0.0007869	0.0831347	---
AT3G21200	104.31545	0.0008031	0.0839382	---
AT4G12580	94.214618	0.000911	0.0942051	---
AT2G15310	Inf	0.0009338	0.0955456	ATARFB1A (ADP-ribosylation factor B1A)
AT1G16022	211.02496	0.0009585	0.0967863	NULL
AT1G10155	527.46049	0.0009659	0.0967863	NULL
AT1G06490	35.074763	0.0010147	0.1006411	ATGSL07 (glucan synthase-like 7)
AT5G50030	47.741736	0.0011359	0.1115232	---
AT2G14620	Inf	0.0012362	0.1201586	---
AT3G53230	21.070596	0.001258	0.1210644	---
AT2G34530	78.703198	0.0013001	0.1238889	---
AT5G11550	11.060561	0.0014727	0.1380724	---
AT3G12730	41.510221	0.0014773	0.1380724	---
AT3G21210	78.182638	0.0015639	0.1430674	---

Table 7 (continuation): Stem phloem genes. List of phloem specific genes in the primary stem of *Arabidopsis*, taking *APL* as threshold.

name_rank	foldChange	pval	padj	name
AT5G62940	Inf	0.0015896	0.1430674	---
AT4G32420	11.694069	0.0016865	0.1491322	---
AT1G47970	20.745928	0.0016877	0.1491322	---
AT2G44578	122.73996	0.0017215	0.1494054	NULL
AT5G38610	55.816399	0.0018929	0.1628191	---
AT2G33775	Inf	0.0020183	0.1676733	NULL
AT5G60440	40.298646	0.0020357	0.1676902	AGL62 (Agamous-like 62)
AT1G73040	15.344253	0.0020778	0.1681807	---
AT1G67790	698.11072	0.00209	0.1681807	---
AT2G27030	8.8487775	0.0020936	0.1681807	CAM5 (CALMODULIN 5)
AT5G13690	37.239196	0.0021887	0.1743765	---
AT1G13920	32.191609	0.0022548	0.1781822	---
AT5G22140	9.1123473	0.0023748	0.1861561	NULL
AT1G32580	11.813089	0.0024017	0.186756	---
AT3G11680	70.454818	0.0025043	0.1931891	NULL
AT3G14370	17.09593	0.0026625	0.2024449	WAG2; kinase/ protein serine/threonine kinase
AT3G58350	8.9396578	0.0027483	0.2054851	---
AT3G58350	8.9396578	0.0027483	0.2054851	NULL
AT1G73630	13.708194	0.0030243	0.2226958	---
AT3G16010	63.621543	0.0030993	0.2265057	---
AT5G14500	14.636442	0.0032233	0.2338059	---
AT4G32430	30.035256	0.0032736	0.235699	---
AT2G39830	49.547964	0.0033038	0.2361216	DAR2 (DA1-RELATED PROTEIN 2)
AT1G23530	28.173299	0.0033674	0.2371804	---
AT1G60030	150.7858	0.0035104	0.2437247	xanthine/uracil permease family protein
AT3G07170	19.748287	0.0036014	0.2482693	---
AT2G32390	13.179145	0.003976	0.2702578	ATGLR3.5 (GLUTAMATE RECEPTOR 3.5)
AT1G44100	8.2287723	0.0040709	0.2747849	AAP5
AT1G79030	94.206693	0.0043049	0.2877627	---
AT2G29140	8.102425	0.0044043	0.2912234	NULL
AT3G13590	176.95739	0.0045124	0.2963553	---
AT1G60740	35.185026	0.0045585	0.2973759	NULL
AT1G79430	11.850179	0.0047867	0.3081243	APL (ALTERED PHLOEM DEVELOPMENT)

Table 7 (continuation): Stem phloem genes. List of phloem specific genes in the primary stem of *Arabidopsis,* taking *APL* as threshold.

5 - Discussion

5.1 The *de novo* establishment of a stem cell niche

The transition from primary to secondary stem conformation involves the extension of vascular cell identities from discrete entities, the vascular bundles, to a continuous domain. In this work it was shown by using molecular markers that SS cells dedifferentiate during the transition to secondary stem conformation and produce a new stem cell niche in the interfascicular area. The establishment of vascular identity occurs already during the first division of SS cells, which is asymmetric. The developmental plasticity that is necessary for IC formation seems to be different to other processes such as lateral root formation. The dissection of this developmental process opens up possibilities for use as an informative model to address questions regarding cell fate acquisition.

According to histological analyses (Altamura et al., 2001) the SS is the origin of the IC at the base of the *Arabidopsis* inflorescence. However, *scr* and *shr* mutants that do not establish the SS (Fukaki et al., 1998) are still able to develop secondary vasculature (Sehr, 2010), indicating that SS identity is not required for IC formation. The analysis of the *SCR:YFP* marker line (Figure 10) further shows that the SS domain does not change during the transition from primary to secondary stem conformation. Before and after the transition, SS identity is restricted to a single cell layer in the innermost cell layer of the cortex composed of large oval cells. There is an apparent contradiction between the histological analyses suggesting the SS to be the origin of the IC and the presented observations showing that SS identity is maintained during the process and, furthermore, that it is not required to produce the IC. To clarify the contribution of the starch sheath to the process of IC formation, an inducible transgenic system (Figure 7) was used for tracking the SS cell progeny. Following two different approaches, natural IC formation at the base of the stem (Figure 8) and the NPA-induced formation of the IC were investigated (Figure 9). In both cases similar observations were made. In areas where the IC is not induced the SS remains as a single cell layer that does not divide (Figure 8-A; Figure 9-A). Where IC formation was induced, groups of clonally related cells were found in different conformations: from only two daughter cells (Figure 8-B; Figure 9-B), which presumably corresponded to the initial stages of IC formation when SS cells had just divided for the first time, to stacks of several cells with different identities (Figure 8-C; Figure 9-C), which presumably corresponded to a more developed IC. These results indicate that the produced cells are clonally connected with the SS cells, which, according to their morphology and their starch content (Fukaki et al., 1998), are differentiated cells. At the base of the stem, just above the uppermost rosette leaf (Figure 8-D), the secondary stem conformation is

clearly established, and this is already true for plants that are 2 cm tall (Sehr, 2010). However, the induced YFP signal is restricted to the SS. The plants used for tracking the IC formation at the base of the stem (Figure 8) were 5 cm tall at the moment of ethanol induction, and they therefore already carried the established IC at the base. The restriction of the YFP signal to the SS in the IC region at the base, just above the last rosette leaf (Figure 8-D), could indicate that the formation of the IC from the SS takes place in a discrete event and not in a continuous process of SS division; it could also mean that IC does not derive from the SS in all positions. That is in agreement with the observation that the SS maintains its identity in the transition from primary to secondary stem conformation (Figure 10). The fact that mutants lacking the SS (Fukaki et al., 1998) are still able to produce secondary growth (Sehr, 2010) points to the idea that such cells are not predetermined to develop the IC, as for example the pericycle cells during lateral root formation (Sugimoto et al., 2011), but that the reason for their selection as IC-precursor cells depends on the position they occupy.

The formation of the IC has classically been considered as a process involving dedifferentiation of cells, similar to somatic embryogenesis or lateral root formation (Birnbaum and Sanchez Alvarado, 2008; Malamy and Benfey, 1997). However, traditional beliefs that base such processes on dedifferentiation have become controversial, and other options like transdifferentiation or simply activation of existing meristematic cells are under debate (Sugimoto et al., 2011). A case of special interest in the context of this project is the formation of lateral roots since this process has a number of analogies with IC formation. In both cases, the processes are induced by auxins (Blakely et al., 1988; Little et al., 2002; Snow, 1935; Torrey, 1950) and a cylindrical cell layer (starch sheath or pericycle) is the origin of the new tissue or organ (Dubrovsky et al., 2000; Sehr et al., 2010). Recently, the classical view of lateral root formation as a process of dedifferentiation has been modified (Dastidar et al., 2012). Recent studies of the pericycle pointed out that it contains different cell types in terms of morphology, cell cycle and transcriptome (Beeckman et al., 2001; Himanen et al., 2004; Parizot et al., 2008). These discoveries suggested that the pericycle is an extended meristem and lateral root formation a process of meristem activation and subsequent differentiation (Casimiro et al., 2003). Such findings and debates re-open the question of whether IC formation is indeed a process of dedifferentiation. The analogies between both processes allow speculation about common mechanisms of control. However, *arf7* and *arf19* mutants impaired in lateral root formation (Okushima et al., 2007) are able to initiate secondary growth similarly to wild type plants (Eva Maria Sehr, unpublished). In the *alf4* mutant the first cell division from which the lateral root originates does not take place, as it is one of the mutants in

which lateral root formation is impaired at the beginning of the process. I therefore decided to investigate the formation of the IC in this mutant (Figure 19). My analyses showed that *alf4* mutants retain, despite their pleiotropic phenotype, the capacity to produce the IC. Therefore, we know that several mutants with defects at different stages of lateral root formation are able to produce the IC. This argues for independent mechanisms controlling lateral root and IC formation and suggests that individual processes of tissue or organ formation are not controlled by a general key mechanism. Clearly defining the origin of the IC was essential for identifying the establishment of cambium identity as a process of dedifferentiation. This conclusion is supported by the clonal connection between SS and IC cells, and by the differences in the required factors in comparison to lateral root initiation. These findings provide a new model for addressing questions regarding cell fate acquisition in plants.

5.2 Vascular gene expression in the vascular bundles

All plant meristems require tight regulation that permits a correct balance between cell division and cell differentiation, and at the same time allows the maintenance of the stem cell niche and the production of differentiated cells. The root and shoot apical meristems share similar control mechanisms (Sarkar et al., 2007). In the shoot apical meristem the transcription factor *WUS* controls non-cell-autonomously the stem cell population via the *CLV-WUS* pathway (Brand et al., 2000). In the root an equivalent system with *ACR4-CLV3-WOX5* controlling the root apical meristem is present. These two pathways are conserved, as demonstrated by the fact that both *CLE40* and *CLV3* and *WUS* and *WOX5* can replace each other, respectively (Hobe et al., 2003; Sarkar et al., 2007). A similar control mechanism, the *CLE41–PXY-WOX4* pathway, is present in the vascular stem cell niche. The signaling peptide CLE41, produced in the phloem, provides positional information and promotes cambium activity through the LRR-RLK PXY, which is expressed in the cambium, activates the transcription factor WOX4, and plays a key role in regulating the orientation of the cell divisions (Fisher and Turner, 2007). Since the spatial orientation of gene activity domains is crucial for the control of cambium activity, I considered it important to analyze the activity of their promoters in order to gain a general picture of the distribution of these genes during different developmental stages of the stem. This data provides insight into how those genes might interact in space and time and allows an interpretation of their mode of action. In the primary vascular bundles the expression domains of these genes is relatively stable, independently of the position along the stem and the mutant background studied. The *WOX4:YFP* reporter (Figure 12) is active not only in the cambium area but also in the primary

xylem cells close to the pith. This observation contradicts previous studies in which RNA in situ hibridizations (RISH) and GUS (β-glucuronidase) and fluorescence marker lines have been used to track *WOX4* expression (Agusti et al., 2011b; Hirakawa et al., 2010; Suer et al., 2011). It seems that the promoter used in the *WOX4:YFP* marker is also active in non-cambium areas. This would explain the fluorescence observed in the area close to the pith, as well as the patterns of *WOX4:YFP* in both the *pxy* background (Figure I11-C,F,I,L), in which YFP is detected even in the phloem area. This could correspond with xylem cells intermixing with the phloem, a characteristic of the *pxy* mutant (Fisher and Turner, 2007). The overlap between the *PXY* and *WOX4* domains in the cambium area is in agreement with the described mode of action of these genes (Hirakawa et al., 2010).

While *PXY* and *WOX4* were described to be cambium specific, *APL*, which is necessary for phloem development (Bonke et al., 2003), is active later on in vascular formation when the cambium cells have acquired a new fate and differentiated into phloem. The vascular bundles are produced early during stem development, immediately below the shoot apical meristem (Sanchez et al., 2012; Ye et al., 2002). In the studied developmental stages (from the base to the 3rd internode), the vascular bundles do not change substantially. There is a progressive enlargement of the *APL:CFP* domain towards the base, which is not the case for the cambium domain. This is probably a result of the fact that the cambium is a stem cell niche that maintains its size while the phloem grows. In *wox4* mutants the *APL:CFP* domain does not enlarge, probably due to the reduced cambium activity. The alterations of the phloem domain at the base of the *pxy* mutant might again be explained by the intermixing of xylem cells with the phloem in this mutant background (Fisher and Turner, 2007).

5.3 Vascular gene dynamics during IC formation

Analysis of the transcriptional markers for *PXY*, *WOX4*, and *APL* during the establishment of the IC allowed visualizing how vascular tissues identities are extended into interfascicular regions during the transition from primary to secondary stem conformation. The establishment of a continuous cylinder of vasculature in the *Arabidopsis* stem involves the *de novo* establishment of a stem cell niche, as indicated in the previous sections. The *pxy* mutants are able to produce vascular bundles but they present morphological alterations, presumably due to the abnormal division pattern of the fascicular cambium (Fisher and Turner, 2007). However, *pxy* is not able to induce vascular activity in the interfascicular areas. *pxy* did not show *PXY:YFP* or *WOX4:YFP* activity in the interfascicular region, indicating the absence of any cambium activity outside the vascular

bundles. Since all the machinery upstream of PXY should be active, it is interesting to observe that *PXY:YFP* is not active in the interfascicular areas at the base of the *pxy* stem. This absence could indicate the presence of a reinforcing feedback loop during the establishment of the IC, or it could also mean that IC formation depends on fascicular cambium activity, which is more disturbed in pxy than in wox4. As expected, *APL:YFP* activity was also completely absent. It seems that *PXY* is essential for the establishment of the IC. The fact that *pxy* mutants are able to produce vascular bundles suggests, at least partially, the presence of independent mechanisms controlling, respectively, the establishment of the procambium and the IC.

WOX4 promotes cambium activity (Hirakawa et al., 2010; Suer et al., 2011). In this study it was observed that in *wox4* mutants IC formation is delayed, and, based on the analysis of *PXY:YFP* and *WOX4:YFP* activities, that the base of the *wox4* stem resembles the transition zone of wild type plants. It seems that *wox4* mutants can initiate cambium activity in interfascicular areas but it is delayed in comparison with wild type or not maintained. Interestingly, *APL:CFP* activity in the interfascicular area at the base of the *wox4* stem indicates that this mutant not only produces the IC but, as some cells differentiate into phloem, can also complete vascular tissue formation.

To sum up, it seems that *PXY* is essential for the establishment of the IC, but not *WOX4*, which implies the existence of a pathway in which *PXY* acts independently of *WOX4*. However, *WOX4* appears to be crucial for normal IC development, since the *wox4* mutant is staked in the transition stage. Progressively more genes appear to be implicated in the control of cambium activity, such as recently the receptor like kinases *MOL1* and *RUL1* (Agusti et al., 2011b) or *XIP1* (Bryan et al., 2012). To gain a better understanding of the process of IC formation it will be important to elucidate their exact roles and interactions with known cambium regulators.

5.4 Asymmetric division of the SS cells

Vascular cell identity is established in the interfascicular areas during the transition from primary to secondary conformation of the stem. This identity can be visualized by different markers. Among the ones used in this study *PXY:YFP* is probably the most appropriate for detecting cambium identity. *PXY* is essential for the establishment of the IC, and it acts upstream of *WOX4*. It was discussed above that the IC is established *de novo* out of unrelated cell types. Therefore, a question that immediately springs up regards the timing of the acquisition of the vascular identity by the new cell lineage. By carefully analyzing the expression of *PXY* in the transition zone it was shown that already during the first division of the SS cells, two clearly distinct domains arise. The

proximal cell preferentially expresses *PXY* in contrast to the distal cell in which the *PXY:YFP* signal is reduced or absent. The differential expression of *PXY:YFP*, in addition to the maintenance of SS identity during IC formation, allow me to propose that during IC initiation the SS divides, giving rise to two daughter cells, the distal one maintaining SS identity and the proximal one acquiring IC identity. This observation reveals two crucial aspects of IC formation. The IC is established through an asymmetric cell division of the SS, and cambium cell identity is already established in the first daughter cell.

In multicellular organisms cells follow different fates during development. These fates are controlled by networks of genes that are tightly regulated in space and time (Levine and Davidson, 2005). Gene expression profiles from different tissues present in an organ can thereby give valuable information about gene networks controlling development (Birnbaum et al., 2003; Brady et al., 2007). The second part of this project aimed to establish a technique that allows the elucidation of transcriptional profiles from the *Arabidopsis* stem in a tissue-specific manner.

5.5 The challenge of isolating tissues

The first obstacle in extracting the transcriptomes of individual stem tissues is their degree of interconnection. Different possibilities of isolating tissues from the stem exist, including many based on morphological distinction and the dissection of the tissue of interest. Examples of these in plants are the isolation of the *Populus* cambium and cambium-derived tissues (Schrader et al., 2004) or the *Arabidopsis* epidermis (Suh et al., 2005). For tissues difficult to access the dissection can be assisted by laser capture micro-dissection (Agusti et al., 2011b). However, in all these cases the selection is based on morphological criteria. In the stem, tissues are tightly interconnected and partly show a similar cell structure. This is true, for example, for the cambium and the phloem, and makes it difficult to separate them based on morphology. Considering all these obstacles, the option of morphology-based isolation methods was discarded during the design of this project.

Flow cytometry was previously used for separating protoplasts or nuclei based on transgenic expression of fluorescent proteins (Galbraith et al., 2011). Flow cytometry applied to protoplasts has been used for almost 30 years (Millman and Lurquin, 1985). It requires the use of cellulases, hemicellulases, and pectinases (Galbraith, 1990) to release the cells from cell walls. The use of this method has been successfully applied in different plant species, including maize, tobacco, and *Arabidopsis* (Galbraith et al., 1999). In particular, young roots have been extensively studied using this technology. In fact, the transcriptome of all root tissues was described previously by applying

FACS (Birnbaum et al., 2003; Brady et al., 2007). Protoplast sorting was also applied on aerial tissues, as for example leaves (Gronlund et al., 2012) or the shoot apical meristem (Yadav et al., 2009). It also has been used for stems of small plants like pea seedlings (Long and Iino, 2001), or young rice stems (Bart et al., 2006), which needed enzymatic treatments of 4 hours to digest the cell walls. However, it was never successfully used in mature tissues like the *Arabidopsis* stem, a structure that contains secondary cell walls. Therefore it can be assumed that the hydrolysis of such structures to produce protoplasts would require even longer periods of enzymatic digestions, if they are not completely recalcitrant (Galbraith, 2007). The limitations of the isolation methods based on morphological criteria and the difficulties of digesting the cell walls in mature tissues like the stem made the use of Fluorescence Activated Nucleus Sorting (FANS) the procedure of choice for isolating tissue-specific stem material. This system has been used in different parts of the plant like the endosperm (Weinhofer et al., 2010), pollen (Borges et al., 2012), or leaves (Ascencio-Ibanez et al., 2008). These examples indicate that FANS can be a reliable method for isolating nuclei in a tissue-specific manner. A more recent method for isolating nuclei that is not based on flow cytometry is the INTACT method (Deal and Henikoff, 2010; Deal and Henikoff, 2011). This method is based on biotin labeling of a nuclear envelope protein in a cell type-specific manner. Subsequently, those nuclei are isolated by immunoprecipitation. This technique allows extensive washing of the bound nuclei. However, flow cytometry-based sorting allows the additional quantification of other parameters, such as the ploidy levels (see below), and can be upgraded to more complex experimental designs by adding more fluorescent markers and isolating double or triple-labeled subpopulations. All these benefits were the reasons we selected FANS as the method for isolating nuclei in this study.

5.6 Validating promoter specificities

Accessing the different tissues of the *Arabidopsis* primary stem (Figure 20) relied on the specificity of gene promoters. In several cases selected genes are fundamental for the differentiation or establishment of these tissues. The genes *LTP1, KNAT1, SCR, APL, XIP1, WOX4, PXY*, and *NST3* were selected based on existing literature as candidates for targeting the different tissues of interest (Table 4). In this approach, the pith and the phloem cap were excluded because no specific promoters are described for these two tissues. It would be necessary to use other approaches like LCM to determine tissue-specific genes for these tissues.

The activity of the selected promoters was visualized by stably transformed promoter-reporter transgenes in which the selected promoter drove the expression of a fluorescent protein that was

targeted to the ER in order to avoid passive diffusion of the reporter protein (Figure 21). Since the fluorescent protein is delivered to the nucleus the plant lines in which the promoters drove the expression of the H4-GFP fusion protein were not appropriate for determining the promoter activity domains. This made it difficult to analyze expression domains as the nuclei were not present in the same optical plane during confocal microscopy. This is especially problematic in tissues with large cells, such as mature stem tissues. The use of the promoter-reporter lines confirmed the expected expression domain for *LTP1, SCR, APL, PXY*, and *NST3*. However, the patterns of expression displayed by the KNAT1:CFP and *WOX4:YFP* reporters indicated that these promoters were not specific enough in the context of this project. Rather, the expected cambium-specific expression, *XIP1:CFP* showed activity in the phloem. These results underlined the importance of promoter validation. The subsequent transcriptome analyses are based on a proper separation of the different stem tissues. Therefore, non-tissue-specific activity of a promoter reduces the potential of the approach with respect to the elucidation of tissue-specific genes. *APL* and *XIP1* promoters were shown to be phloem-specific (Figure 21-D, E). The *APL* promoter was chosen for this project because its specificity was also demonstrated in previous studies (Bonke et al., 2003; Ollram, 2011). From the candidate promoters for the cambium, the *PXY* promoter was the most specific. In summary, the list of validated promoters represents a robust tool for driving transgene expression in various tissues of the *Arabidopsis* stem.

5.7 FANS allows tissue-specific RNA extraction

A tissue-specific transcriptional profiling depends on an accurate nucleus separation. For achieve this, different sorting gates were established in the FACSAriaIII cell sorter based on GFP activity and the intensity of DAPI staining, which is related to the ploidy level. These gates were established based on non-overlapping areas between negative (wild type) and positive (*35S:H4-GFP*) controls for GFP activity (Figure 22) and confirmed by testing the sorting accuracy under the fluorescence microscope (Figure 23). Overall, both approaches indicated separation efficiency close to 100%. This rate is much higher than the 50% efficiency described for FACS in other studies (Deal and Henikoff, 2010), probably due to the criteria applied for selecting the sorting gates or the use of different sorting equipment.

After the sequencing of APL+ and – fractions, a low level of GFP and APL-specific reads was present in the respective negative fractions (Figure 30). Different explanations are possible for these findings. A basal activity of the respective promoters in other tissues is one option. Another one is the presence of false negative nuclei whose RNA produce the reads in the negative

fractions. However, the definition of the gates and the validation under the microscope indicated that the selection of particles was successful (Figure 22, Figure 23). Another factor to consider is the presence of RNA molecules in the buffer used for sorting. The nuclei were washed twice before sorting; however, it is possible that the nuclei release RNA molecules into the buffer or that they break during the processing after the washing steps. Such molecules would be equally distributed in the buffer and they could be the origin of APL and GFP transcripts in the negative fractions. Independently of the origin of the basal levels in the negative fraction, the big difference in expression between positive and negative fractions indicates that the identification of tissue-specific genes is possible by following the established procedure.

5.8 Ploidy level profiles are different in various tissues

Variations in the number of genome copies (ploidy) can be found in different species (Bai et al., 2012), and even within a single organism. These variations can reflect differences in cell cycle, presenting 2C or 4C content depending on the phase of the cycle (De Veylder et al., 2002). Higher ploidy levels indicate that a cell underwent endoreduplication during which the M phase is aborted but the DNA duplication is performed.

The level of endoreduplication is positively correlated with cell size (Kondorosi et al., 2000; Melaragno et al., 1993). Furthermore, developmental processes like cell differentiation have been associated with higher ploidy levels (Li et al., 2012; Rewers and Sliwinska, 2012). The use of FANS allowed the determination of the ploidy profile in different tissues of the stem. Such information can provide an idea about the stage of the cell cycle or the level of differentiation in a particular tissue. Nuclei from NST3-expressing cells (xylem and interfascicular fibers) showed a ploidy profile shifted towards higher ploidy levels than the average (Figure 24-A, B). The cells from these tissues are relatively large, fitting the concept that higher ploidy levels and cell size is positively correlated (Melaragno et al., 1993). The secondary xylem cells undergo apoptosis to produce the conducting pipelines for water transport. Interestingly, high ploidy levels have been associated with apoptosis in plants (Schnittger et al., 2003). Therefore, the high ploidy levels in NST3 expressing cells could be linked to their larger size and/or the process of apoptosis. The ploidy distribution in phloem nuclei (APL+) is closer to the average (Figure 24-A, D). There is a higher percentage of 2C nuclei, perhaps indicating that in the developed phloem most cells are in the G1 phase of the cell cycle. Nuclei derived from WOX4-positive cells are mostly in the 4C stage. According to the analysis of the WOX4 promoter activity domain, cambium-derived nuclei are “contaminated” by nuclei from the xylem. The high level of 4C nuclei is probably not related

with an active process of endoreduplication because the percentages of 8C and 16C nuclei are similar to those in the control (Figure 24-A, F). The number of 4C nuclei was enhanced to the detriment of the 2C fraction, which, in the WOX4-positive cells, is drastically reduced. This distribution of ploidy levels suggests that in this case most cells are arrested in the S phase or the G2 phase of the cell cycle and did not enter M-phase. A possible developmental interpretation of this observation is that cambium cells are ready for cell division. Cyclins are involved in the control of the division and differentiation of meristematic cells (Andersen et al., 2008; Gaamouche et al., 2010). Interestingly, the overexpression of the cyclin CYCD3 increases the proportion of cells in G2 phase to the detriment of the cells in G1 phase, but this is not coupled with an activation of the M phase. CYCD3 is also associated with a retarded formation of xylem elements in the stem (Dewitte et al., 2003). Therefore, the elevated 4C ratio could reflect a "ready-to-go" stage of the cambium in the second internode.

In conclusion, the analyzed nuclei showed that different distributions of ploidy levels are present in different tissues of the stem. These differences are probably related to differences in the cell cycle control in these tissues. The use of ploidy profiles in combination with transcriptional information for cyclins and other regulators of the cell cycle could be a valuable source of information for addressing questions regarding cell-cycle control, DNA content, or degree of differentiation.

5.9 Nuclear mRNA for describing the transcriptome state of the cell

The process of nucleus isolation was adapted to the stem to avoid alterations in the transcriptional state during the isolation process. The processing that preceded the disruption of the material was performed in a span of minutes, during which time the plant material was kept on ice. While some low-temperature responsive genes are downregulated within minutes (Horvath et al., 1993), their upregulation takes place over a span of hours and new transcripts are detected only after hours of cold treatment (Hajela et al., 1990; Nordin et al., 1993), indicating that the fast regulation is probably due to posttranslational mechanisms (Horvath et al., 1993). Therefore, the appearance of cold-response transcripts should not be a problem in this case because the handling time was too short.

mRNA processing and transport from the nucleus to the cytoplasm and the time the mRNA spends in each compartment may generate doubt about the degree to which the nucleus-derived mRNA reflects the transcriptional profile of the whole cell. This concern was addressed by comparing

mRNA extracted from nuclei and from whole cells. I observed similar correlation rates between the results from nucleus-derived replicates and between the nucleus and whole cell samples. This indicates that differences between both methods are found due to the differences between biological replicates. The percentage of reads mapped to introns was slightly higher in the nucleus-derived samples (DAPI and phloem) than in the whole cell-derived samples (STEM), indicating that nucleus samples contain more immature RNA molecules. However, the number of reads mapped to exons in nucleus-derived samples was always higher that 96% (Figure 26, Figure 28). This suggests that the intron reads do not affect transcript quantification and that the nuclear mRNA can be taken as an approximation for the transcriptional profile of the whole cell. These findings are in agreement with other studies showing that mRNA from nuclei is informative for gene expression analysis (Barthelson et al., 2007; Deal and Henikoff, 2010; Jacob et al., 2007).

5.10 A group of genes predominantly active in the phloem was deciphered

In this study the transcriptome of the phloem was analyzed as a proof of principle for the whole approach. The phloem was selected for this purpose because it is one of the internal tissues of the stem, has a close connection to the cambium, and is partially surrounded by other tissues with secondary cell walls (Figure 27-A). These properties hamper the use of tissue separation methods that are based on morphological characteristics or during which protoplasting is necessary (Agusti et al., 2011b; Birnbaum et al., 2003; Brady et al., 2007; Suh et al., 2005). The established workflow should represent the scheme to follow for other stem tissues. The initial selection of the *APL* promoter as phloem-specific was based on the literature (Bonke et al., 2003; Ollram, 2011). In addition, its activity was tested by a transcriptional marker line (Figure 21-E) that allowed visualizing the domain of the *APL* promoter activity. This analysis confirmed its phloem specificity. The use of the *APL* promoter to drive the expression of the H4-GFP fusion protein made the isolation of phloem nuclei possible (Figure 27-C, D). The RNA extracted from the nuclei was amplified in order to generate the amount of RNA necessary for deep sequencing analyses. The amplification resulted in a bias toward the 3´ end of the genes. However, this bias is the same for all genes and therefore relative levels can be compared (Mortazavi et al., 2008; Phillips and Eberwine, 1996). The use of RNA-seq instead of microarrays for analyzing the transcriptome provides a higher sensitivity because quantification is based directly on RNA reads and not extrapolated from signal intensity (Tang et al., 2010). In contrast to microarrays that give

information only about the probes spotted to the array, the use of RNA-seq produces expression values for all the genes present in the genome.

The produced reads were mapped to the genome and analyzed statistically using the package DEseq for R. This package was developed especially for analysis of RNA-seq data (Anders and Huber, 2010). It is adequate for experiments with biological replicates in which a higher variability than in technical replicates is expected. The analysis provided a list of 69 genes that are predominantly active in the phloem (Figure 31). The absence of *APL* from that list argues that the statistical analysis produced some false negatives. The consideration that *APL* is a transcription factor with a modest level of expression, along with its certain presence in the phloem, were the criteria for selecting *APL* as a threshold for selecting additional genes that might have been false negatives in the previous analysis. The 132 genes with lower p-value than *APL* were classified as phloem-specific (Figure 31; Table 7). One third of those genes (Figure 32) were also present among genes described as specific to the root phloem tissue (Brady et al., 2007; Zhang et al., 2008). This overlap underlines the power of the approach for identifying tissue-specific genes. The identification of many genes that did not appear in the root analysis may be due to the investigation of different organs (roots and stems) or the different developmental stages. To see how described phloem-specific genes are distributed in my dataset, the genevestigator (www.genevestigator.com) was used for selecting the 50 most expressed genes in the root phloem. These genes are colored green in the plot (Figure 31, green dots). Despite the different organ of origin, the different developmental stage, and the different processing of the plant material, when they were present, they were always active in the stem phloem.

In summary, the observations presented here provide a better understanding of the process of IC initiation. The description of the origin of the IC, of the expression dynamics of cambium-related genes during the process, or of the time when the new identity is acquired are examples for this. However, our understanding of the mechanisms controlling growth and development of the plant stem is still limited (Sanchez et al., 2012), and crucial aspects remain to be addressed in the future. This holds true, for instance, for the nature of the signals inducing the change of the cell fate in such a specific manner or the genes or proteins that are the targets of these signals. To open the door to a deeper understanding of the machinery controlling these processes, it is necessary to analyze specific tissues and cells separately. Consequently, in the second part I addressed the technical challenge of isolating individual stem tissues. The established system for characterizing the transcriptional profile of individual *Arabidopsis* stem tissues was validated by investigating the

phloem. The phloem transcriptome was presented, opening potential avenues for investigating phloem specification and physiology. In addition, the proposed technique opens up the possibility of producing a transcriptional atlas of the stem at tissue-specific resolution which in combination with detailed information about developmental processes such as IC formation, will promote the role of the stem as a model for addressing questions regarding cell fate acquisition and plant growth.

6 - References

Agusti, J., Herold, S., Schwarz, M., Sanchez, P., Ljung, K., Dun, E. A., Brewer, P. B., Beveridge, C. A., Sieberer, T., Sehr, E. M. et al. (2011a). Strigolactone signaling is required for auxin-dependent stimulation of secondary growth in plants. *Proc Natl Acad Sci USA* **108**, 20242-20247.

Agusti, J., Lichtenberger, R., Schwarz, M., Nehlin, L. and Greb, T. (2011b). Characterization of Transcriptome Remodeling during Cambium Formation Identifies MOL1 and RUL1 as Opposing Regulators of Secondary Growth. *PLoS Genet* **7**, e1001312.

Aida, M., Ishida, T. and Tasaka, M. (1999). Shoot apical meristem and cotyledon formation during Arabidopsis embryogenesis: interaction among the CUP-SHAPED COTYLEDON and SHOOT MERISTEMLESS genes. *Development* **126**, 1563-70.

Albert, M. and Peters, A. H. (2009). Genetic and epigenetic control of early mouse development. *Curr Opin Genet Dev* **19**, 113-21.

Altamura, M. M., Possenti, M., Matteucci, A., Baima, S., Ruberti, I. and Morelli, G. (2001). Development of the vascular system in the inflorescence stem of Arabidopsis. *New Phytologist* **151**, 381-389.

Anders, S. and Huber, W. (2010). Differential expression analysis for sequence count data. *Genome Biol* **11**, R106.

Andersen, S. U., Buechel, S., Zhao, Z., Ljung, K., Novak, O., Busch, W., Schuster, C. and Lohmann, J. U. (2008). Requirement of B2-type cyclin-dependent kinases for meristem integrity in Arabidopsis thaliana. *Plant Cell* **20**, 88-100.

Artavanis-Tsakonas, S., Rand, M. D. and Lake, R. J. (1999). Notch signaling: cell fate control and signal integration in development. *Science* **284**, 770-6.

Ascencio-Ibanez, J. T., Sozzani, R., Lee, T. J., Chu, T. M., Wolfinger, R. D., Cella, R. and Hanley-Bowdoin, L. (2008). Global analysis of Arabidopsis gene expression uncovers a complex array of changes impacting pathogen response and cell cycle during geminivirus infection. *Plant Physiol* **148**, 436-54.

Bai, C., Alverson, W. S., Follansbee, A. and Waller, D. M. (2012). New reports of nuclear DNA content for 407 vascular plant taxa from the United States. *Ann Bot*.

Bart, R., Chern, M., Park, C. J., Bartley, L. and Ronald, P. C. (2006). A novel system for gene silencing using siRNAs in rice leaf and stem-derived protoplasts. *Plant Methods* **2**, 13.

Barthelson, R. A., Lambert, G. M., Vanier, C., Lynch, R. M. and Galbraith, D. W. (2007). Comparison of the contributions of the nuclear and cytoplasmic compartments to global gene expression in human cells. *BMC Genomics* **8**, 340.

Beeckman, T., Burssens, S. and Inze, D. (2001). The peri-cell-cycle in Arabidopsis. *J Exp Bot* **52**, 403-11.

Benjamini, Y. and Hochberg, Y. (1995). Controlling the false discovery rate: a practical and powerful approach to multiple testing. *J. R. Stat. Soc. B* **57**, 289–300.

Benjamins, R., Quint, A., Weijers, D., Hooykaas, P. and Offringa, R. (2001). The PINOID protein kinase regulates organ development in Arabidopsis by enhancing polar auxin transport. *Development* **128**, 4057-67.

Birnbaum, K., Shasha, D. E., Wang, J. Y., Jung, J. W., Lambert, G. M., Galbraith, D. W. and Benfey, P. N. (2003). A gene expression map of the Arabidopsis root. *Science* **302**, 1956-60.

Birnbaum, K. D. and Sanchez Alvarado, A. (2008). Slicing across kingdoms: regeneration in plants and animals. *Cell* **132**, 697-710.

Blakely, L. M., Blakely, R. M., Colowit, P. M. and Elliot, D. S. (1988). Experimental studies on lateral root formation in Radish seedlings roots. *Plant Phys* **87**, 414-419.

Boevink, P., Oparka, K., Santa Cruz, S., Martin, B., Betteridge, A. and Hawes, C. (1998). Stacks on tracks: the plant Golgi apparatus traffics on an actin/ER network. *Plant J* **15**, 441-7.

Bonke, M., Thitamadee, S., Mähönen, A. P., Hauser, M. T. and Helariutta, Y. (2003). APL regulates vascular tissue identity in Arabidopsis. *Nature* **426**, 181-186.

Borges, F., Gardner, R., Lopes, T., Calarco, J. P., Boavida, L. C., Slotkin, R. K., Martienssen, R. A. and Becker, J. D. (2012). FACS-based purification of Arabidopsis microspores, sperm cells and vegetative nuclei. *Plant Methods* **8**, 44.

Brady, S. M., Orlando, D. A., Lee, J. Y., Wang, J. Y., Koch, J., Dinneny, J. R., Mace, D., Ohler, U. and Benfey, P. N. (2007). A high-resolution root spatiotemporal map reveals dominant expression patterns. *Science* **318**, 801-6.

Brand, U., Fletcher, J. C., Hobe, M., Meyerowitz, E. M. and Simon, R. (2000). Dependence of stem cell fate in Arabidopsis on a feedback loop regulated by CLV3 activity. *Science* **289**, 617-9.

Brandenberger, R., Wei, H., Zhang, S., Lei, S., Murage, J., Fisk, G. J., Li, Y., Xu, C., Fang, R., Guegler, K. et al. (2004). Transcriptome characterization elucidates signaling networks that control human ES cell growth and differentiation. *Nat Biotechnol* **22**, 707-16.

Bryan, A. C., Obaidi, A., Wierzba, M. and Tax, F. E. (2012). XYLEM INTERMIXED WITH PHLOEM1, a leucine-rich repeat receptor-like kinase required for stem growth and vascular development in Arabidopsis thaliana. *Planta* **235**, 111-22.

Buss, L. W. (1982). Somatic cell parasitism and the evolution of somatic tissue compatibility. *Proc Natl Acad Sci U S A* **79**, 5337-41.

Busse, J. S. and Evert, R. F. (1999). Vascular differentiation and transition in the seedling of Arabidopsis thaliana (Brassicaceae). *International Journal of Plant Sciences* **160**, 241-251.

Casimiro, I., Beeckman, T., Graham, N., Bhalerao, R., Zhang, H., Casero, P., Sandberg, G. and Bennett, M. J. (2003). Dissecting Arabidopsis lateral root development. *Trends Plant Sci* **8**, 165-71.

Celenza, J. L., Jr., Grisafi, P. L. and Fink, G. R. (1995). A pathway for lateral root formation in Arabidopsis thaliana. *Genes Dev* **9**, 2131-42.

Chaffey, N., Cholewa, E., Regan, S. and Sundberg, B. (2002). Secondary xylem development in Arabidopsis: a model for wood formation. *Physiologia plantarum* **114**, 594-600.

Ciais, P., Tans, P. P., Trolier, M., White, J. W. and Francey, R. J. (1995). A Large Northern Hemisphere Terrestrial CO2 Sink Indicated by the 13C/12C Ratio of Atmospheric CO2. *Science* **269**, 1098-102.

Clark, S. E., Williams, R. W. and Meyerowitz, E. M. (1997). The CLAVATA1 gene encodes a putative receptor kinase that controls shoot and floral meristem size in Arabidopsis. *Cell* **89**, 575-85.

Clough, S. J. and Bent, A. F. (1998). Floral dip: a simplified method for Agrobacterium-mediated transformation of Arabidopsis thaliana. *Plant J* **16**, 735-43.

Coleman, A. W., Maguire, M. J. and Coleman, J. R. (1981). Mithramycin- and 4'-6-diamidino-2-phenylindole (DAPI)-DNA staining for fluorescence microspectrophotometric measurement of DNA in nuclei, plastids, and virus particles. *J Histochem Cytochem* **29**, 959-68.

Costa, S. and Shaw, P. (2007). 'Open minded' cells: how cells can change fate. *Trends Cell Biol* **17**, 101-6.

Dastidar, M. G., Jouannet, V. and Maizel, A. (2012). Root branching: mechanisms, robustness, and plasticity. *Wiley Interdisciplinary Reviews: Developmental Biology* **1**, 329-343.

De Smet, I., Vassileva, V., De Rybel, B., Levesque, M. P., Grunewald, W., Van Damme, D., Van Noorden, G., Naudts, M., Van Isterdael, G., De Clercq, R. et al. (2008). Receptor-like kinase ACR4 restricts formative cell divisions in the Arabidopsis root. *Science* **322**, 594-7.

De Veylder, L., Beeckman, T., Beemster, G. T., de Almeida Engler, J., Ormenese, S., Maes, S., Naudts, M., Van Der Schueren, E., Jacqmard, A., Engler, G. et al. (2002). Control of proliferation, endoreduplication and differentiation by the Arabidopsis E2Fa-DPa transcription factor. *EMBO J* **21**, 1360-8.

Deal, R. B. and Henikoff, S. (2010). A simple method for gene expression and chromatin profiling of individual cell types within a tissue. *Dev Cell* **18**, 1030-40.

Deal, R. B. and Henikoff, S. (2011). The INTACT method for cell type-specific gene expression and chromatin profiling in Arabidopsis thaliana. *Nat Protoc* **6**, 56-68.

Dewitte, W., Riou-Khamlichi, C., Scofield, S., Healy, J. M., Jacqmard, A., Kilby, N. J. and Murray, J. A. (2003). Altered cell cycle distribution, hyperplasia, and inhibited differentiation in Arabidopsis caused by the D-type cyclin CYCD3. *Plant Cell* **15**, 79-92.

DiDonato, R. J., Arbuckle, E., Buker, S., Sheets, J., Tobar, J., Totong, R., Grisafi, P., Fink, G. R. and Celenza, J. L. (2004). Arabidopsis ALF4 encodes a nuclear-localized protein required for lateral root formation. *Plant J* **37**, 340-53.

Dolan, L., Janmaat, K., Willemsen, V., Linstead, P., Poethig, S., Roberts, K. and Scheres, B. (1993). Cellular organisation of the Arabidopsis thaliana root. *Development* **119**, 71-84.

Douglas, S. J., Chuck, G., Dengler, R. E., Pelecanda, L. and Riggs, C. D. (2002). KNAT1 and ERECTA regulate inflorescence architecture in Arabidopsis. *Plant Cell* **14**, 547-58.

Dubrovsky, J. G., Doerner, P. W., Colon-Carmona, A. and Rost, T. L. (2000). Pericycle cell proliferation and lateral root initiation in Arabidopsis. *Plant Physiol* **124**, 1648-57.

Eriksson, S., Stransfeld, L., Adamski, N. M., Breuninger, H. and Lenhard, M. (2010). KLUH/CYP78A5-dependent growth signaling coordinates floral organ growth in Arabidopsis. *Curr Biol* **20**, 527-32.

Espina, V., Heiby, M., Pierobon, M. and Liotta, L. A. (2007). Laser capture microdissection technology. *Expert Rev Mol Diagn* **7**, 647-57.

Fisher, K. and Turner, S. (2007). PXY, a Receptor-like Kinase Essential for Maintaining Polarity during Plant Vascular-Tissue Development. *Curr Biol* **17**, 1061-6.

Friedman, W. E., Moore, R. C. and Purugganan, M. D. (2004). The evolution of plant development. *Am J Bot* **91**, 1726-41.

Fukaki, H., Wysocka-Diller, J., Kato, T., Fujisawa, H., Benfey, P. N. and Tasaka, M. (1998). Genetic evidence that the endodermis is essential for shoot gravitropism in Arabidopsis thaliana. *Plant Journal* **14**, 425-430.

Gaamouche, T., Manes, C. L., Kwiatkowska, D., Berckmans, B., Koumproglou, R., Maes, S., Beeckman, T., Vernoux, T., Doonan, J. H., Traas, J. et al. (2010). Cyclin-dependent kinase activity maintains the shoot apical meristem cells in an undifferentiated state. *Plant J* **64**, 26-37.

Galbraith, D. W. (1990). Isolation and flow cytometric characterization of plant protoplasts. *Methods Cell Biol* **33**, 527-47.

Galbraith, D. W. (2007). Protoplast analysis using flow cytometry and sorting. In *Flow Cytometry with Plant Cells*, (ed. J. Dolezel J. Greilhuber and J. Suda), pp. 231-250. Weinheim, Germany: Wiley-VCH.

Galbraith, D. W., Harkins, K. R., Maddox, J. M., Ayres, N. M., Sharma, D. P. and Firoozabady, E. (1983). Rapid flow cytometric analysis of the cell cycle in intact plant tissues. *Science* **220**, 1049-51.

Galbraith, D. W., Herzenberg, L. A. and Anderson, M. T. (1999). Flow cytometric analysis of transgene expression in higher plants: green fluorescent protein. *Methods Enzymol* **302**, 296-315.

Galbraith, D. W., Janda, J. and Lambert, G. M. (2011). Multiparametric analysis, sorting, and transcriptional profiling of plant protoplasts and nuclei according to cell type. *Methods Mol Biol* **699**, 407-29.

Gerrienne, P., Gensel, P. G., Strullu-Derrien, C., Lardeux, H., Steemans, P. and Prestianni, C. (2011). A simple type of wood in two Early Devonian plants. *Science* **333**, 837.

Gordon, S. P., Chickarmane, V. S., Ohno, C. and Meyerowitz, E. M. (2009). Multiple feedback loops through cytokinin signaling control stem cell number within the Arabidopsis shoot meristem. *Proc Natl Acad Sci U S A* **106**, 16529-34.

Gronlund, J. T., Eyres, A., Kumar, S., Buchanan-Wollaston, V. and Gifford, M. L. (2012). Cell specific analysis of Arabidopsis leaves using fluorescence activated cell sorting. *J Vis Exp*.

Grosberg, R. K. and Strathmann, R. R. (2007). The Evolution of Multicellularity: A Minor Major Transition? *Annu. Rev. Ecol. Evol. Syst.* **38**, 37.

Haenni, S., Ji, Z., Hoque, M., Rust, N., Sharpe, H., Eberhard, R., Browne, C., Hengartner, M. O., Mellor, J., Tian, B. et al. (2012). Analysis of C. elegans intestinal gene expression and polyadenylation by fluorescence-activated nuclei sorting and 3'-end-seq. *Nucleic Acids Res* **40**, 6304-18.

Hajela, R. K., Horvath, D. P., Gilmour, S. J. and Thomashow, M. F. (1990). Molecular Cloning and Expression of cor (Cold-Regulated) Genes in Arabidopsis thaliana. *Plant Physiol* **93**, 1246-52.

Haseloff, J., Siemering, K. R., Prasher, D. C. and Hodge, S. (1997). Removal of a cryptic intron and subcellular localization of green fluorescent protein are required to mark transgenic Arabidopsis plants brightly. *Proc Natl Acad Sci U S A* **94**, 2122-7.

Hellens, R. P., Edwards, E. A., Leyland, N. R., Bean, S. and Mullineaux, P. M. (2000). pGreen: a versatile and flexible binary Ti vector for Agrobacterium-mediated plant transformation. *Plant Mol Biol* **42**, 819-32.

Himanen, K., Vuylsteke, M., Vanneste, S., Vercruysse, S., Boucheron, E., Alard, P., Chriqui, D., Van Montagu, M., Inze, D. and Beeckman, T. (2004). Transcript profiling of early lateral root initiation. *Proc Natl Acad Sci U S A* **101**, 5146-51.

Hirakawa, Y., Kondo, Y. and Fukuda, H. (2010). TDIF peptide signaling regulates vascular stem cell proliferation via the WOX4 homeobox gene in Arabidopsis. *Plant Cell* **22**, 2618-29.

Hobe, M., Muller, R., Grunewald, M., Brand, U. and Simon, R. (2003). Loss of CLE40, a protein functionally equivalent to the stem cell restricting signal CLV3, enhances root waving in Arabidopsis. *Dev Genes Evol* **213**, 371-81.

Hofgen, R. and Willmitzer, L. (1988). Storage of competent cells for Agrobacterium transformation. *Nucleic Acids Res* **16**, 9877.

Horvath, D. P., McLarney, B. K. and Thomashow, M. F. (1993). Regulation of Arabidopsis thaliana L. (Heyn) cor78 in response to low temperature. *Plant Physiol* **103**, 1047-53.

Ibanes, M., Fabregas, N., Chory, J. and Cano-Delgado, A. I. (2009). Brassinosteroid signaling and auxin transport are required to establish the periodic pattern of Arabidopsis shoot vascular bundles. *Proc Natl Acad Sci U S A* **106**, 13630-5.

Jacob, Y., Mongkolsiriwatana, C., Veley, K. M., Kim, S. Y. and Michaels, S. D. (2007). The nuclear pore protein AtTPR is required for RNA homeostasis, flowering time, and auxin signaling. *Plant Physiol* **144**, 1383-90.

Jacqmard, A., Detry, N., Dewitte, W., Van Onckelen, H. and Bernier, G. (2002). In situ localisation of cytokinins in the shoot apical meristem of Sinapis alba at floral transition. *Planta* **214**, 970-3.

Jeong, S., Trotochaud, A. E. and Clark, S. E. (1999). The Arabidopsis CLAVATA2 gene encodes a receptor-like protein required for the stability of the CLAVATA1 receptor-like kinase. *Plant Cell* **11**, 1925-34.

Jurgens, G. (2001). Apical-basal pattern formation in Arabidopsis embryogenesis. *EMBO J* **20**, 3609-16.

Ko, J. H. and Han, K. H. (2004). Arabidopsis whole-transcriptome profiling defines the features of coordinated regulations that occur during secondary growth. *Plant Molecular Biology* **55**, 433-453.

Ko, J. H., Han, K. H., Park, S. and Yang, J. (2004). Plant body weight-induced secondary growth in Arabidopsis and its transcription phenotype revealed by whole-transcriptome profiling. *Plant Physiology* **135**, 1069-1083.

Kondorosi, E., Roudier, F. and Gendreau, E. (2000). Plant cell-size control: growing by ploidy? *Curr Opin Plant Biol* **3**, 488-92.

Laux, T. (2003). The stem cell concept in plants: a matter of debate. *Cell* **113**, 281-3.

Laux, T., Mayer, K. F., Berger, J. and Jurgens, G. (1996). The WUSCHEL gene is required for shoot and floral meristem integrity in Arabidopsis. *Development* **122**, 87-96.

Lenhard, M. and Laux, T. (2003). Stem cell homeostasis in the Arabidopsis shoot meristem is regulated by intercellular movement of CLAVATA3 and its sequestration by CLAVATA1. *Development* **130**, 3163-73.

Levine, M. and Davidson, E. H. (2005). Gene regulatory networks for development. *Proc Natl Acad Sci U S A* **102**, 4936-42.

Li, X., Yu, E., Fan, C., Zhang, C., Fu, T. and Zhou, Y. (2012). Developmental, cytological and transcriptional analysis of autotetraploid Arabidopsis. *Planta* **236**, 579-96.

Little, C. H. A., MacDonald, J. E. and Olsson, O. (2002). Involvement of indole-3-acetic acid in fascicular and interfascicular cambial growth and interfascicular extraxylary fiber differentiation in Arabidopsis thaliana inflorescence stems. *International Journal of Plant Sciences* **163**, 519-529.

Long, C. and Iino, M. (2001). Light-dependent osmoregulation in pea stem protoplasts. photoreceptors, tissue specificity, ion relationships, and physiological implications. *Plant Physiol* **125**, 1854-69.

Makanae, A. and Satoh, A. (2012). Early regulation of axolotl limb regeneration. *Anat Rec (Hoboken)* **295**, 1566-74.

Malamy, J. E. and Benfey, P. N. (1997). Organization and cell differentiation in lateral roots of Arabidopsis thaliana. *Development* **124**, 33-44.

Mayer, K. F., Schoof, H., Haecker, A., Lenhard, M., Jurgens, G. and Laux, T. (1998). Role of WUSCHEL in regulating stem cell fate in the Arabidopsis shoot meristem. *Cell* **95**, 805-15.

McCarroll, S. A., Murphy, C. T., Zou, S., Pletcher, S. D., Chin, C. S., Jan, Y. N., Kenyon, C., Bargmann, C. I. and Li, H. (2004). Comparing genomic expression patterns across species identifies shared transcriptional profile in aging. *Nat Genet* **36**, 197-204.

McSteen, P. and Leyser, O. (2005). Shoot branching. *Annu Rev Plant Biol* **56**, 353-74.

Melaragno, J. E., Mehrotra, B. and Coleman, A. W. (1993). Relationship between Endopolyploidy and Cell Size in Epidermal Tissue of Arabidopsis. *Plant Cell* **5**, 1661-1668.

Melzer, S., Lens, F., Gennen, J., Vanneste, S., Rohde, A. and Beeckman, T. (2008). Flowering-time genes modulate meristem determinacy and growth form in Arabidopsis thaliana. *Nature Genetics* **40**, 1489-1492.

Michod, R. E. (1996). Cooperation and conflict in the evolution of individuality. II. Conflict mediation. *Proc Biol Sci* **263**, 813-22.

Millman, R. A. and Lurquin, P. F. (1985). Study of plant protoplast-bacterial spheroplast and cell interactions by flow cytometry. *J Plant Physiol* **117**, 431-40.

Mitalipov, S. M., Yeoman, R. R., Kuo, H. C. and Wolf, D. P. (2002). Monozygotic twinning in rhesus monkeys by manipulation of in vitro-derived embryos. *Biol Reprod* **66**, 1449-55.

Mitsuda, N., Iwase, A., Yamamoto, H., Yoshida, M., Seki, M., Shinozaki, K. and Ohme-Takagi, M. (2007). NAC transcription factors, NST1 and NST3, are key regulators of the formation of secondary walls in woody tissues of Arabidopsis. *Plant Cell* **19**, 270-280.

Miyashima, S., Sebastian, J., Lee, J. Y. and Helariutta, Y. (2012). Stem cell function during plant vascular development. *EMBO J*.

Miyawaki, A., Llopis, J., Heim, R., McCaffery, J. M., Adams, J. A., Ikura, M. and Tsien, R. Y. (1997). Fluorescent indicators for Ca2+ based on green fluorescent proteins and calmodulin. *Nature* **388**, 882-7.

Morozova, O., Hirst, M. and Marra, M. A. (2009). Applications of new sequencing technologies for transcriptome analysis. *Annu Rev Genomics Hum Genet* **10**, 135-51.

Mortazavi, A., Williams, B. A., McCue, K., Schaeffer, L. and Wold, B. (2008). Mapping and quantifying mammalian transcriptomes by RNA-Seq. *Nat Methods* **5**, 621-8.

Muday, G. K. and DeLong, A. (2001). Polar auxin transport: controlling where and how much. *Trends Plant Sci* **6**, 535-42.

Müller, R., Bleckmann, A. and Simon, R. (2008). The Receptor Kinase CORYNE of Arabidopsis Transmits the Stem Cell-Limiting Signal CLAVATA3 Independently of CLAVATA1. *Plant Cell*, tpc.107.057547.

Nakajima, K., Sena, G., Nawy, T. and Benfey, P. N. (2001). Intercellular movement of the putative transcription factor SHR in root patterning. *Nature* **413**, 307-11.

Nawrath, C. (2006). Unraveling the complex network of cuticular structure and function. *Curr Opin Plant Biol* **9**, 281-7.

Nordin, K., Vahala, T. and Palva, E. T. (1993). Differential expression of two related, low-temperature-induced genes in Arabidopsis thaliana (L.) Heynh. *Plant Mol Biol* **21**, 641-53.

Odell, J. T., Nagy, F. and Chua, N. H. (1985). Identification of DNA sequences required for activity of the cauliflower mosaic virus 35S promoter. *Nature* **313**, 810-2.

Ogawa, M., Shinohara, H., Sakagami, Y. and Matsubayashi, Y. (2008). Arabidopsis CLV3 peptide directly binds CLV1 ectodomain. *Science* **319**, 294.

Okushima, Y., Fukaki, H., Onoda, M., Theologis, A. and Tasaka, M. (2007). ARF7 and ARF19 regulate lateral root formation via direct activation of LBD/ASL genes in Arabidopsis. *Plant Cell* **19**, 118-30.

Ollram, K. (2011). The Identification of Potential Factors Involved in the Transcriptional Regulation of the Phloem-Specific Gene ALTERED PHLOEM DEVELOPMENT (APL) and the Analysis of its Role during Embryogenesis in Arabidopsis thaliana. *PhD Thesis - University of Vienna*, 121.

Parizot, B., Laplaze, L., Ricaud, L., Boucheron-Dubuisson, E., Bayle, V., Bonke, M., De Smet, I., Poethig, S. R., Helariutta, Y., Haseloff, J. et al. (2008). Diarch symmetry of the vascular bundle in Arabidopsis root encompasses the pericycle and is reflected in distich lateral root initiation. *Plant Physiol* **146**, 140-8.

Phillips, J. and Eberwine, J. H. (1996). Antisense RNA Amplification: A Linear Amplification Method for Analyzing the mRNA Population from Single Living Cells. *Methods* **10**, 283-8.

Rewers, M. and Sliwinska, E. (2012). Endoreduplication intensity as a marker of seed developmental stage in the Fabaceae. *Cytometry A*.

Rhodes, D. R., Yu, J., Shanker, K., Deshpande, N., Varambally, R., Ghosh, D., Barrette, T., Pandey, A. and Chinnaiyan, A. M. (2004). Large-scale meta-analysis of cancer microarray data identifies common transcriptional profiles of neoplastic transformation and progression. *Proc Natl Acad Sci U S A* **101**, 9309-14.

Roslan, H. A., Salter, M. G., Wood, C. D., White, M. R., Croft, K. P., Robson, F., Coupland, G., Doonan, J., Laufs, P., Tomsett, A. B. et al. (2001). Characterization of the ethanol-inducible alc gene-expression system in Arabidopsis thaliana. *Plant J* **28**, 225-35.

Rowe, N. and Speck, T. (2005). Plant growth forms: an ecological and evolutionary perspective. *New Phytol* **166**, 61-72.

Rubery, P. H. (1990). Phytotropins: receptors and endogenous ligands. *Symp Soc Exp Biol* **44**, 119-46.

Ruegger, M., Dewey, E., Hobbie, L., Brown, D., Bernasconi, P., Turner, J., Muday, G. and Estelle, M. (1997). Reduced naphthylphthalamic acid binding in the tir3 mutant of Arabidopsis is associated with a reduction in polar auxin transport and diverse morphological defects. *Plant Cell* **9**, 745-57.

Ruonala, R., Rinne, P. L., Kangasjarvi, J. and van der Schoot, C. (2008). CENL1 expression in the rib meristem affects stem elongation and the transition to dormancy in Populus. *Plant Cell* **20**, 59-74.

Sambrook, J. and Russell, D. W. (2006). Isolation of High-molecular-weight DNA from Mammalian Cells Using Proteinase K and Phenol. *CSH Protoc* **2006**.

Sanchez, P., Nehlin, L. and Greb, T. (2012). From thin to thick – major transitions during stem development. *Trends Plant Sci* **17**, 113-121.

Sarkar, A. K., Luijten, M., Miyashima, S., Lenhard, M., Hashimoto, T., Nakajima, K., Scheres, B., Heidstra, R. and Laux, T. (2007). Conserved factors regulate signalling in Arabidopsis thaliana shoot and root stem cell organizers. *Nature* **446**, 811-4.

Schena, M., Shalon, D., Davis, R. W. and Brown, P. O. (1995). Quantitative monitoring of gene expression patterns with a complementary DNA microarray. *Science* **270**, 467-70.

Schnittger, A., Weinl, C., Bouyer, D., Schobinger, U. and Hulskamp, M. (2003). Misexpression of the cyclin-dependent kinase inhibitor ICK1/KRP1 in single-celled Arabidopsis trichomes reduces endoreduplication and cell size and induces cell death. *Plant Cell* **15**, 303-15.

Schopf, J. W. (1993). Microfossils of the Early Archean Apex chert: new evidence of the antiquity of life. *Science* **260**, 640-6.

Schrader, J., Nilsson, J., Mellerowicz, E., Berglund, A., Nilsson, P., Hertzberg, M. and Sandberg, G. (2004). A high-resolution transcript profile across the wood-forming meristem of poplar identifies potential regulators of cambial stem cell identity. *Plant Cell* **16**, 2278-2292.

Sehr, E. M. (2010). Molecular control of secondary growth initiation in the Arabidopsis stem. *PhD Thesis - University of Vienna*.

Sehr, E. M., Agusti, J., Lehner, R., Farmer, E. E., Schwarz, M. and Greb, T. (2010). Analysis of secondary growth in the Arabidopsis shoot reveals a positive role of jasmonate signalling in cambium formation. *Plant J* **63**, 811-22.

Sgorbati, S., Levi, M., Sparvoli, E., Trezzi, F. and Lucchini, G. (1986). Cytometry and flow cytometry of 4',6-diamidino-2-phenylindole(DAPI)-stained suspensions of nuclei released from tissues of plants. *Physiol Plant* **68**, 471-476.

Shah, K., Gadella, T. W., Jr., van Erp, H., Hecht, V. and de Vries, S. C. (2001). Subcellular localization and oligomerization of the Arabidopsis thaliana somatic embryogenesis receptor kinase 1 protein. *J Mol Biol* **309**, 641-55.

Snow, R. (1935). Activation of cambial growth by pure hormones. *New Phytologist* **34**, 347-360.

Southern, E. M. (1975). Detection of specific sequences among DNA fragments separated by gel electrophoresis. *J Mol Biol* **98**, 503-17.

Spicer, R. and Groover, A. (2010). Evolution of development of vascular cambia and secondary growth. *New Phytol* **186**, 577-92.

Stahl, Y., Wink, R. H., Ingram, G. C. and Simon, R. (2009). A signaling module controlling the stem cell niche in Arabidopsis root meristems. *Curr Biol* **19**, 909-14.

Su, Y. H. and Zhang, X. S. (2009). Auxin gradients trigger de novo formation of stem cells during somatic embryogenesis. *Plant Signal Behav* **4**, 574-6.

Suer, S., Agusti, J., Sanchez, P., Schwarz, M. and Greb, T. (2011). WOX4 Imparts Auxin Responsiveness to Cambium Cells in Arabidopsis *Plant Cell* **23**, 3247-59.

Sugimoto, K., Gordon, S. P. and Meyerowitz, E. M. (2011). Regeneration in plants and animals: dedifferentiation, transdifferentiation, or just differentiation? *Trends Cell Biol* **21**, 212-8.

Suh, M. C., Samuels, A. L., Jetter, R., Kunst, L., Pollard, M., Ohlrogge, J. and Beisson, F. (2005). Cuticular lipid composition, surface structure, and gene expression in Arabidopsis stem epidermis. *Plant Physiol* **139**, 1649-65.

Sundberg, B., Tuominen, H. and Little, C. (1994). Effects of the Indole-3-Acetic Acid (IAA) Transport Inhibitors N-1-Naphthylphthalamic Acid and Morphactin on Endogenous IAA Dynamics in Relation to Compression Wood Formation in 1-Year-Old Pinus sylvestris (L.) Shoots. *Plant Physiol* **106**, 469-476.

Sussex, I. M. (1989). Developmental programming of the shoot meristem. *Cell* **56**, 225-9.

Takacs, E. M., Li, J., Du, C., Ponnala, L., Janick-Buckner, D., Yu, J., Muehlbauer, G. J., Schnable, P. S., Timmermans, M. C., Sun, Q. et al. (2012). Ontogeny of the maize shoot apical meristem. *Plant Cell* **24**, 3219-34.

Tang, F., Barbacioru, C., Nordman, E., Li, B., Xu, N., Bashkirov, V. I., Lao, K. and Surani, M. A. (2010). RNA-Seq analysis to capture the transcriptome landscape of a single cell. *Nat Protoc* **5**, 516-35.

Taub, R. (2004). Liver regeneration: from myth to mechanism. *Nat Rev Mol Cell Biol* **5**, 836-47.

Thoma, S., Hecht, U., Kippers, A., Botella, J., De Vries, S. and Somerville, C. (1994). Tissue-specific expression of a gene encoding a cell wall-localized lipid transfer protein from Arabidopsis. *Plant Physiol* **105**, 35-45.

Tomitani, A., Knoll, A. H., Cavanaugh, C. M. and Ohno, T. (2006). The evolutionary diversification of cyanobacteria: molecular-phylogenetic and paleontological perspectives. *Proc Natl Acad Sci U S A* **103**, 5442-7.

Torrey, J. G. (1950). The induction of lateral roots by indoleacetic acid and root decapitation. *Am J Bot* **37**, 257-264.

Turner, S. and Sieburth, L. E. (2003). Vascular patterning. *Arabidopsis Book* **2**, 73.

Wagers, A. J., Christensen, J. L. and Weissman, I. L. (2002). Cell fate determination from stem cells. *Gene Ther* **9**, 606-12.

Wang, H., Avci, U., Nakashima, J., Hahn, M. G., Chen, F. and Dixon, R. A. (2010). Mutation of WRKY transcription factors initiates pith secondary wall formation and increases stem biomass in dicotyledonous plants. *Proc Natl Acad Sci U S A* **107**, 22338-43.

Wang, Z., Gerstein, M. and Snyder, M. (2009). RNA-Seq: a revolutionary tool for transcriptomics. *Nat Rev Genet* **10**, 57-63.

Weigel, D. and Glazebrook, J. (2002). Arabidopsis: A laboratory manual.

Weinhofer, I., Hehenberger, E., Roszak, P., Hennig, L. and Kohler, C. (2010). H3K27me3 profiling of the endosperm implies exclusion of polycomb group protein targeting by DNA methylation. *PLoS Genet* **6**.

Wysocka-Diller, J. W., Helariutta, Y., Fukaki, H., Malamy, J. E. and Benfey, P. N. (2000). Molecular analysis of SCARECROW function reveals a radial patterning mechanism common to root and shoot. *Development* **127**, 595-603.

Yadav, R. K., Girke, T., Pasala, S., Xie, M. and Reddy, G. V. (2009). Gene expression map of the Arabidopsis shoot apical meristem stem cell niche. *Proc Natl Acad Sci U S A* **106**, 4941-6.

Ye, Z. H., Freshour, G., Hahn, M. G., Burk, D. H. and Zhong, R. (2002). Vascular development in Arabidopsis. *International Review of Cytology* **220**, 225-256.

Zhang, C., Barthelson, R. A., Lambert, G. M. and Galbraith, D. W. (2008). Global characterization of cell-specific gene expression through fluorescence-activated sorting of nuclei. *Plant Physiol* **147**, 30-40.

Zhong, R., Lee, C. and Ye, Z. H. (2010). Global analysis of direct targets of secondary wall NAC master switches in Arabidopsis. *Mol Plant* **3**, 1087-103.

Acknowledgments

This work was performed in the Gregor Mendel Institute GmbH. (Vienna) and supported by Austrian Science Fund (FWF) Grant P23781-B16.

I would like to thank Thomas Greb for giving me the opportunity to do my PhD in his lab and for his advice and patience during the last years. Thanks also to my PhD Committee Karel Riha and Wim Soppe for their guidance and counsel.

I want to thank the current and former members of the Greb lab for their collaboration and ideas that were fundamental for this thesis, especially Eva Sehr who started with the analysis of the interfascicular cambium formation, and also the two summer students, Marcelina Bilicka and Valentina Zehetbauer, who worked with me in 2008 and 2009, repectively.

I want to thank all the groups of the GMI and the VBC that provided advice and material for this project.

In the personal aspect, I want to thank the Spanish crowd that „adopted“ me when I arrived at the Vienna Biocenter: Sabina, Jesús, Sara, Andrea and specially Javier for the shared kilometers and hours.

To all the nice people I found in Vienna during these years who made my stay here a very nice experience: Lale, Cécile, Hansjörg, Georg, Thomas, Itziar, Tamara, Wolfgang, Lisa, Julia, Robert and many others.

In particular I want to thank Alexis whose endless support made it possible to finish this work.

To all the people I left back in Spain, but who supported me even from a distance, in particular Eduardo, Silvia, Javier, Dani and Carmen.

Y por último a mis padres, Esther y Valentín, a quienes va dedicada esta tesis, porque de ellos aprendí las cosas importantes, porque si he llegado hasta aquí es gracias a ellos.

Curriculum vitae

Pablo Sánchez

Nationality	Spanish
Date of birth	2nd November 1982
Place of birth	Gijón, Spain

Education

2008 - Present	**PhD. Student in Molecular Biology**. University of Vienna (Austria). Thesis: "Cell fate regulation in the *Arabidopsis thaliana* stem: analysis of interfascicular cambium formation and development of a method for tissue-specific transcriptome analysis". Supervisor: Dr. Thomas Greb.
2007	CAP (equivalent to the English PGCE, **Postgraduate Certificate in Education**). University of Oviedo (Spain).
2000 – 2007	**MSc. degree in Biology**. University of Oviedo (Spain). Thesis: "Methylation of genomic DNA and cellular plasticity: morphogenic competence in *Pinus radiata* D. Don. embryos". Supervised by Dr. M. Jesús Cañal. *Epiphysage* Research Group. Organisms and Systems Biology Department.

Career

2008 - Present	**Gregor Mendel Institute** (Vienna, Austria). a basic research institute of the Austrian Academy of Sciences for Molecular Plant Biology. Research in Molecular Biology as PhD. student in the group of Dr. Thomas Greb.
2007	**Leiden University** (The Netherlands). Plant Secondary Metabolomics Department. Six months guess researcher in the Prof. Verpoorte group as *Leonardo da Vinci* grant-holder (European Commission programme).
2005 - 2007	**University of Oviedo** (Spain). Organisms and Systems Biology Department. Epiphysage Research Group. Coord. by Prof. R. Rodríguez and Dr. M. Jesús Cañal. Colaborator with a grant from the Spanish Ministry of Education and Science.
2005	**SERIDA** (Asturias, Spain). Two months practice at the "Regional Service for Agriculture and Food Research".

Publications

Sanchez, P., Nehlin, L. and Greb, T. (2012). From thin to thick – major transitions during stem development. Trends Plant Sci 17, 113-121.

Agusti, J., Herold, S., Schwarz, M., **Sanchez, P.**, Ljung, K., Dun, E. A., Brewer, P. B., Beveridge, C. A., Sieberer, T., Sehr, E. M. et al. (2011). Strigolactone signaling is required for auxin-dependent stimulation of secondary growth in plants. Proc Natl Acad Sci USA 108, 20242-20247.

Suer, S., Agusti, J., **Sanchez, P.**, Schwarz, M. and Greb, T. (2011). *WOX4* Imparts Auxin Responsiveness to Cambium Cells in *Arabidopsis*. Plant Cell 23, 3247-59.

Rodríguez, R., Valledor, L., **Sánchez, P.**, Fraga, M. F., Berdasco, M., Hasbún, R., Rodríguez, J. L., Pacheco, J. C., García, I., Uribe, M. M. et al. (2007) Propagation of Selected Pinus Genotypes Regardless of Age. In: S. Mohan Jain and H. Häggman (eds.) Protocols for Micropropagation of Woody Trees and Fruits. Dordrecht (NL): Springer; pp.137-146. ISBN 978-1-4020-6352-7.

Popular Science:
Pablo Sanchez (2012) "*El sueño de un viaje a la epigenetica*". In: D. Sampedro Ruiz (Coord.) *Un breve viaje por la ciencia*. Logrono (Spain); pp.39-43. ISBN: 978-84-96487-69-7

Awards

2010 Ensaya'10 popular science award in biotechnology (University La Rioja, Spain).
2007 *Leonardo da Vinci* Grant. 6 months (European Commission).
2006 - 2007 Collaboration Grant at U. of Oviedo (Spanish Ministry of Education and Science).
2005 Best Project award in Health Biology section (10 people team), Faculty of Biology. University of Oviedo (Spain).

Languages

Spanish: Mother tongue (C2).
English: Advanced level (C1).
French: Medium level (A2).
German: Medium level (A2).